

Gifford & Partners

Additional Modelling - Mersey Gateway

Technical Notes

Date: December 2005

Project Ref: R/3411/4

Report No: R.1241



Gifford & Partners

Additional Modelling - Mersey Gateway

Technical Note A: Residual Modelling - Stage I

Date: December 2005

Project Ref: R/3411/4

Report No: R.1241a



Gifford & Partners

Additional Modelling - Mersey Gateway Technical Note A: Residual Modelling - Stage I

Date: December 2005

Project Ref: R/3411/4

Report No: R.1241a

© ABP Marine Environmental Research Ltd

Version	Details of Change	Authorised By	Date
1	Draft for Comment	J M Harris	9/12/2005
2	Final	J M Harris	20/12/2005

Document Authorisation		Signature	Date
Project Manager:	J M Harris	<i>John Harris</i>	20/12/2005
Quality Manager:	R H Swift	<i>Richard Swift</i>	10/01/2006
Project Director:	W S Cooper	<i>W. Cooper</i>	10-1-06

ABP Marine Environmental Research Ltd
Suite B, Waterside House
Town Quay
SOUTHAMPTON
Hampshire
SO14 2AQ



Tel: +44(0)23 8071 1840
Fax: +44(0)23 8071 1841
Web: www.abpmer.co.uk
Email: enquires@abpmer.co.uk



INVESTOR IN PEOPLE

Summary

This technical note describes Stage I of the residual modelling undertaken as part of the additional modelling studies carried out for Phase II of the Mersey Gateway Project. Under Stage I several pier shapes (square and rectangular) were modelled without any sediment included to look at the effect of pier shape on residual flows. From these runs the impact of an elongated pier shape on the flow residuals was determined.

This report is one of a series of five Technical Notes (R1241a to R.1241e):

- Technical Note A: Residual Modelling - Stage I;
- Technical Note B: Residual Modelling - Stage II;
- Technical Note C: Flat Bed Morphological Modelling;
- Technical Note D: Real Hydrograph Modelling; and
- Technical Note E: Phase Differences.

An idealized model has been used to make an assessment of two pier layouts (one representative of the proposed bridge towers and the other representative of an elongated structure) on the residual flow for typical flow conditions and an extreme fluvial condition. From these tests the key conclusions drawn are:

- Under normal flow conditions for the channel configuration used the residuals close to the structures are small in magnitude. The largest directional change in the velocity is as the flow approaches the tower with flows bifurcating around the structure, before gradually returning to the original baseline directions and magnitude.
- The model results show both acceleration of the flow around the structure and deceleration behind it due to the blockage effect. Under normal conditions (spring-neap-spring tidal cycle) the velocity residuals are low in magnitude and typically less than 0.08m/s. Away from the structure within the north channel the residuals increase to about 0.25m/s.
- The elongated structure shows the widest extent of change, although the extent of the change is limited to about 100m radius centred on the structure. This also demonstrates why the proposed bridge towers have little impact, as the size of the structures relative to the flow and their impact relative to each other is outside their respective spheres of influence.
- Under a different channel configuration it would be expected that the elongated structure could lead to significantly different residual patterns depending on the angle of approach of the flow to the obstacle. However, this is not a problem for the proposed bridge tower as it offers the same profile to the flow regardless of the angle of approach.

- Based on the modelling undertaken to date it has been demonstrated that the impact of the proposed bridge towers will have little impact on the tidal flow and the corresponding residuals. In turn this suggests that any impact on the morphological response of the system will be secondary to any changes happening naturally. An assessment of the response of the upper estuary under a different channel configuration has already been undertaken for the Route 3A preferred option and has demonstrated that whilst the overall pattern of change is different the extent and magnitude of the change is of a similar order to that predicted using the 2002 bathymetry. Therefore, it is suggested that for different channel configurations, whilst the spatial pattern of change may vary, particularly local to the structures, the overall magnitude and extent of change remains similar.



Additional Modelling - Mersey Gateway Technical Note A: Residual Modelling - Stage I

Contents

	Page
Summary	i
1. Introduction	1
2. Results	1
3. Conclusion.....	2

Figures

1.	Tidal curve at downstream boundary showing tidal residual averaging periods	5
2.	Model extent	5
3a.	Tidal residuals around short structure in north channel over a spring-neap-spring cycle under extreme fluvial flows	6
3b.	Tidal residuals around long structure in north channel over a spring-neap-spring cycle under extreme fluvial flows	6
3c.	Tidal residuals around short structure in north channel integrated over several spring tides under extreme fluvial flows	7
3d.	Tidal residuals around long structure in north channel integrated over several spring tides under extreme fluvial flows	7
3e.	Tidal residuals around short structure in north channel integrated over several neap tides under extreme fluvial flows	8
3f.	Tidal residuals around long structure in north channel integrated over several neap tides under extreme fluvial flows	8
4a.	Tidal residuals around short structure in north channel over a spring-neap-spring cycle under extreme fluvial flows	9
4b.	Tidal residuals around long structure in north channel over a spring-neap-spring cycle under extreme fluvial flows	9
4c.	Tidal residuals around short structure in north channel integrated over several spring tides under extreme fluvial flows	10
4d.	Tidal residuals around long structure in north channel integrated over several spring tides under extreme fluvial flows	10
4e.	Tidal residuals around short structure in north channel integrated over several neap tides under extreme fluvial flows	11
4f.	Tidal residuals around long structure in north channel integrated over several neap tides under extreme fluvial flows	11

1. Introduction

Tidal residuals represent the net pattern of the flow field integrated over a tidal period. For example, in the present study several periods have been used to integrate the flow field over, a spring-neap-spring tidal cycle covering a 15 days period, a spring tide and a neap tide period. Sediment transport paths can be inferred indirectly from measurements/predictions of flow intensity profiles during entire tidal cycles. Therefore, changes in tidal residuals can be used to indicate likely changes in sediment transport paths.

Two scenarios have been run initially. The first scenario represents a typical spring-neap-spring cycle with representative mean daily flows, whilst the second represents the same spring-neap-spring tidal cycle with mean daily flows that represent an extreme fluvial event over the weir at Westy.

Figure 1 shows the spring-neap-spring tidal cycle used on the downstream boundary.

2. Results

The extent of the model grid used is shown in Figure 2.

The model scenarios undertaken have been carried out for a structure representative of the proposed bridge towers (1 model cell – termed short) and also for an elongated structure represented by 5 model cells (termed long). Residuals have been calculated for three different periods as described above and shown in Figure 1.

Scenario 1 is representative of a typical spring-neap-spring cycle with typical fluvial flows representative of January. Scenario 2 uses the same spring-neap-spring tidal cycle but with extreme fluvial flows measured at Westy weir. Overall, the results of the two scenario runs show similar patterns in the flow residuals although with greater magnitude for the extreme event. The black vectors represent the baseline case, whilst the red vectors represent the particular scenario.

Figures 3a to 3f show the results for scenario 1. Other than the variation in magnitude of the residuals for the different periods of integration, there is no marked difference in pattern. The residuals determined by integrating the velocity over several spring tides have the greatest magnitude, whilst the residuals corresponding to a neap tide show the lowest values (as expected). The elongated structure (shown as blank cells) shows the widest extent of change, although the extent of the change is limited to about 100m radius centred on the structure. This also demonstrates why the proposed towers have little impact, as the size of the structures relative to the flow and their impact relative to each other is outside their respective spheres of influence.

Figures 4a to 4f show the results for scenario 2. The modelling results for the extreme fluvial event show a similar pattern of change compared to those of the normal spring-neap-spring cycle although the magnitude of the change is greater.

Based on the residual pattern the greatest changes in the channel will occur on the intertidal bank side of the structures as the strongest residuals are predicted at this position. For the elongated tower structure the vectors show the obstacle to cause alignment of the vectors along its bank side flank. The greatest directional change in the velocity is as the flow approaches the tower with flows bifurcating around the structure, before gradually returning to the original baseline directions and magnitude.

The model results show both acceleration of the flow around the structure and deceleration behind it due to the blockage effect. Under normal conditions (spring-neap-spring tidal cycle) the velocity residuals are low in magnitude and typically less than 0.08m/s. Away from the structure within the north channel the residuals increase to about 0.25m/s.

Under a different channel configuration it would be expected that the elongated structure could lead to significantly different residual patterns depending on the angle of approach of the flow to the obstacle. However, this is not a problem for the proposed bridge tower as it offers the same profile to the flow regardless of the angle of approach.

3. Conclusion

An idealized model has been used to make an assessment of two pier layouts (one representative of the proposed bridge towers and the other representative of an elongated structure) on the residual flow for typical flow conditions and an extreme fluvial condition.

- Under normal flow conditions for the channel configuration used the residuals close to the structures are small in magnitude. The largest directional change in the velocity is as the flow approaches the tower with flows bifurcating around the structure, before gradually returning to the original baseline directions and magnitude.
- The model results show both acceleration of the flow around the structure and deceleration behind it due to the blockage effect. Under normal conditions (spring-neap-spring tidal cycle) the velocity residuals are low in magnitude and typically less than 0.08m/s. Away from the structure within the north channel the residuals increase to about 0.25m/s.

- The elongated structure shows the widest extent of change, although the extent of the change is limited to about 100m radius centred on the structure. This also demonstrates why the proposed bridge towers have little impact, as the size of the structures relative to the flow and their impact relative to each other is outside their respective spheres of influence.
- Under a different channel configuration it would be expected that the elongated structure could lead to significantly different residual patterns depending on the angle of approach of the flow to the obstacle. However, this is not a problem for the proposed bridge tower as it offers the same profile to the flow regardless of the angle of approach.
- Based on the modelling undertaken to date it has been demonstrated that the impact of the proposed bridge towers will have little impact on the tidal flow and the corresponding residuals. In turn this suggests that any impact on the morphological response of the system will be secondary to any changes happening naturally. An assessment of the response of the upper estuary under a different channel configuration has already been undertaken for the Route 3A preferred option and has demonstrated that whilst the overall pattern of change is different the extent and magnitude of the change is of a similar order to that predicted using the 2002 bathymetry. Therefore, it is suggested that for different channel configurations, whilst the spatial pattern of change may vary, particularly local to the structures, the overall magnitude and extent of change remains similar.

Figures

Figure 1. Tidal curve at downstream boundary showing tidal residual averaging periods

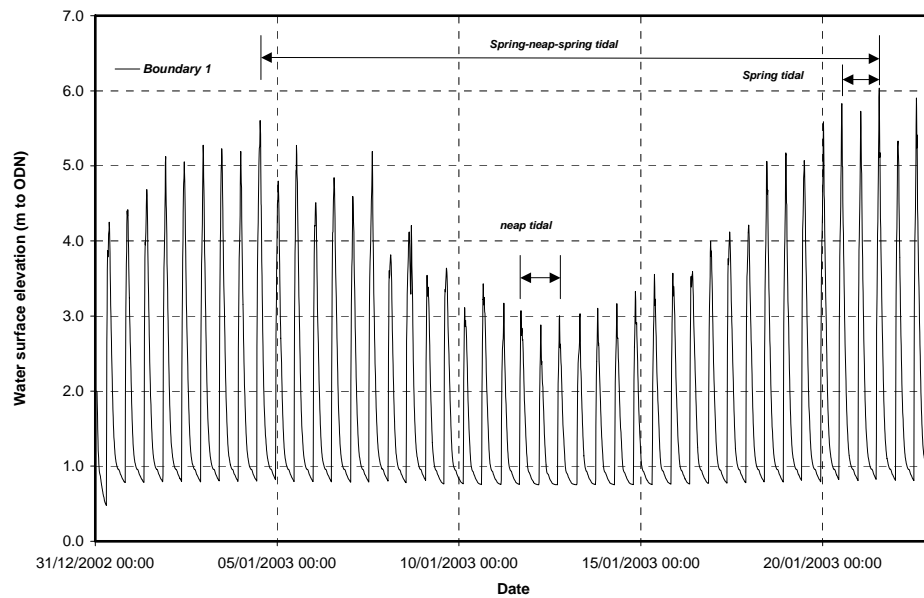


Figure 2. Model extent

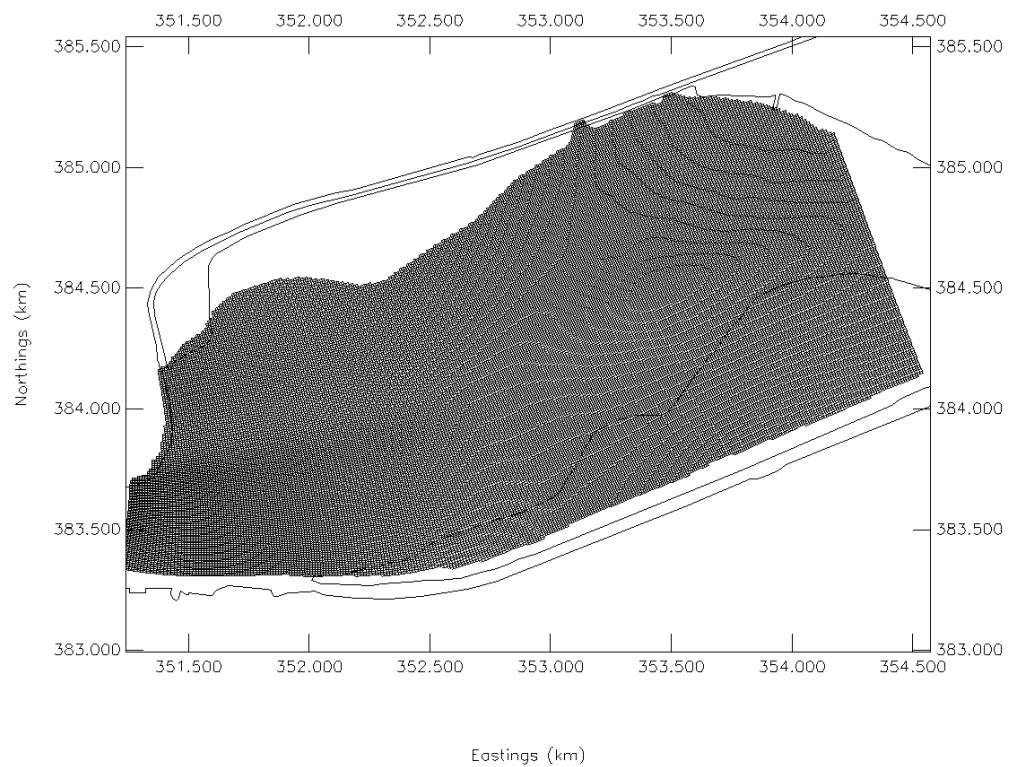


Figure 3a. Tidal residuals around short structure in north channel over a spring-neap-spring cycle under extreme fluvial flows

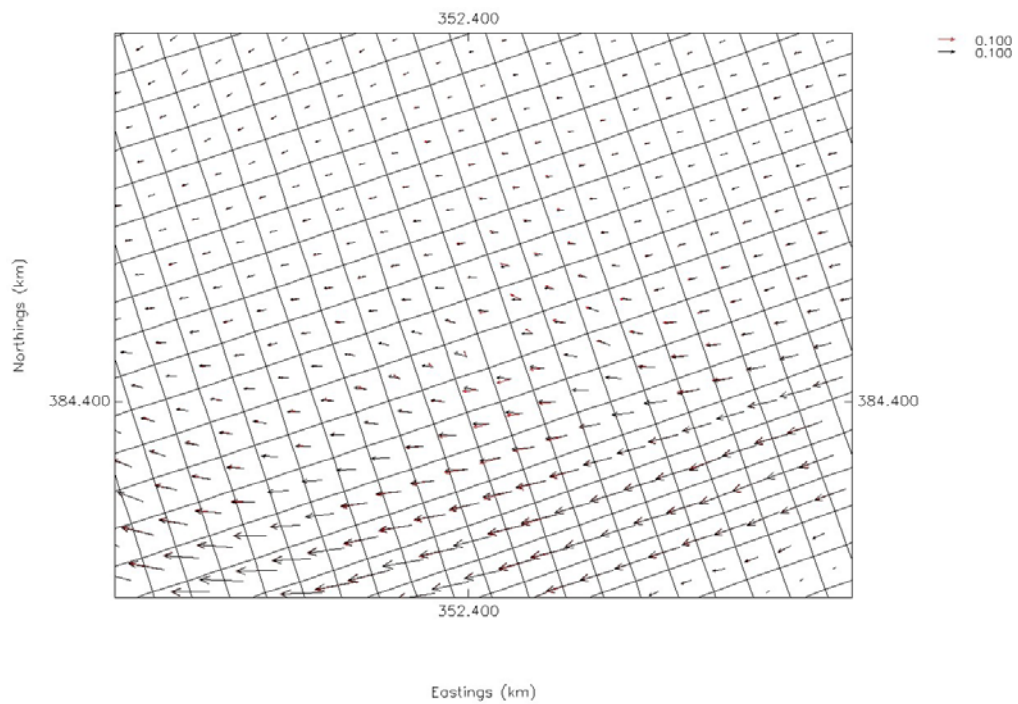


Figure 3b. Tidal residuals around long structure in north channel over a spring-neap-spring cycle under extreme fluvial flows

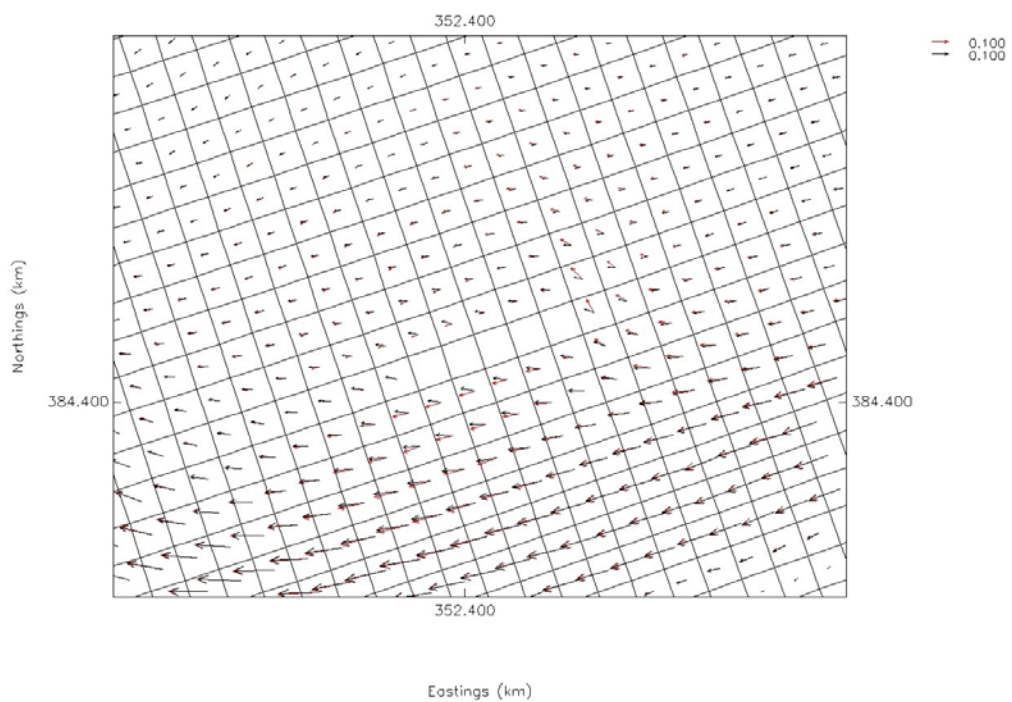


Figure 3c. Tidal residuals around short structure in north channel integrated over several spring tides under extreme fluvial flows

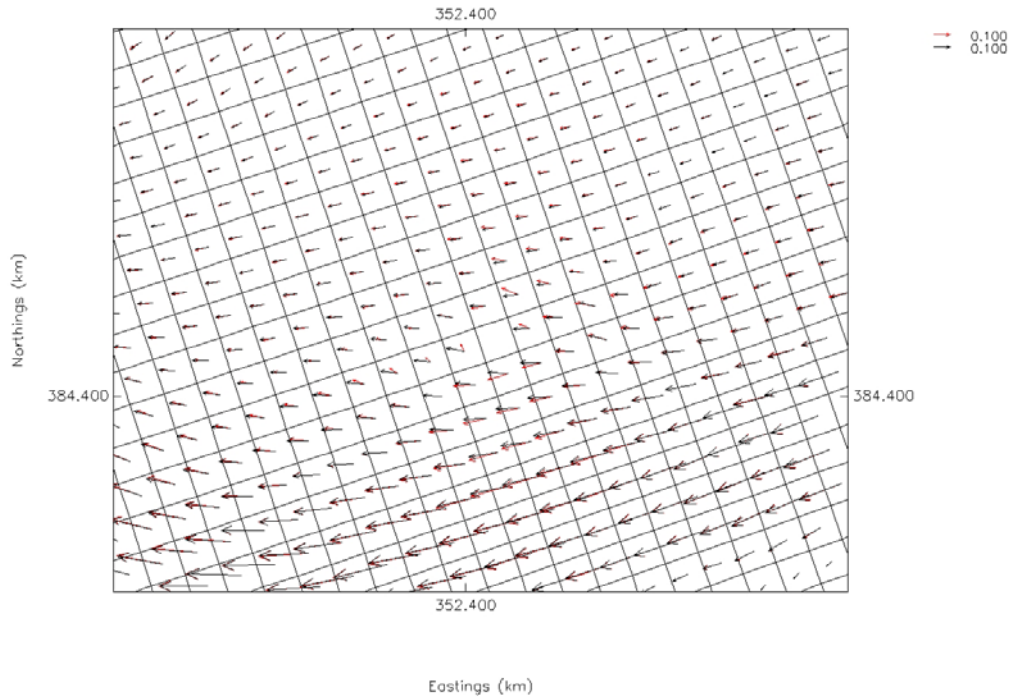


Figure 3d. Tidal residuals around long structure in north channel integrated over several spring tides under extreme fluvial flows

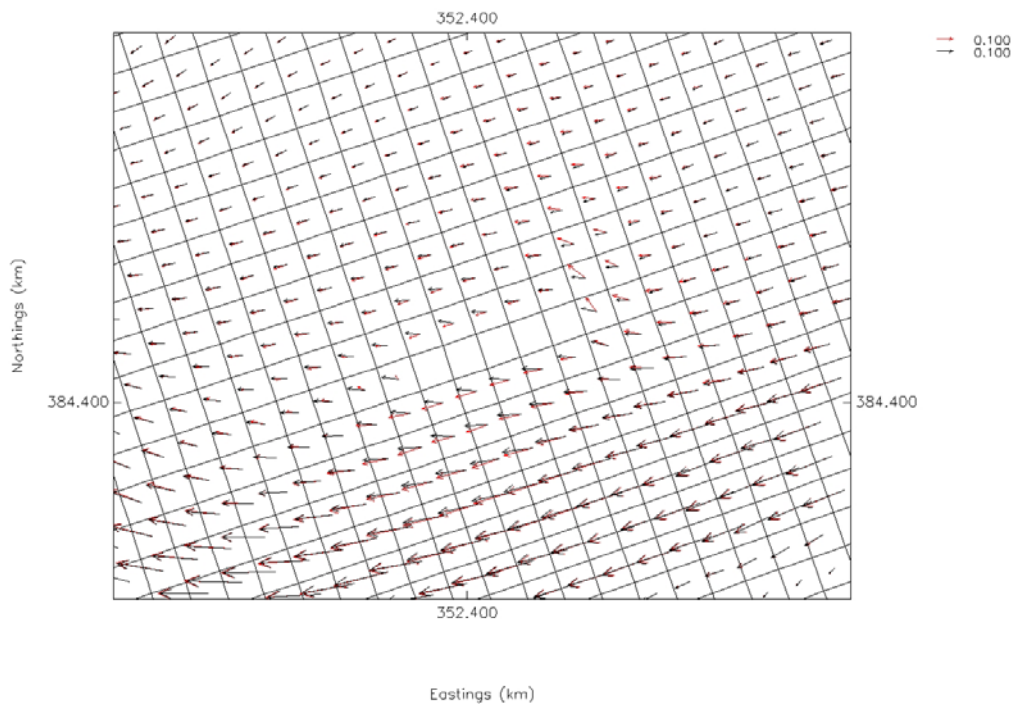


Figure 3e. Tidal residuals around short structure in north channel integrated over several neap tides under extreme fluvial flows

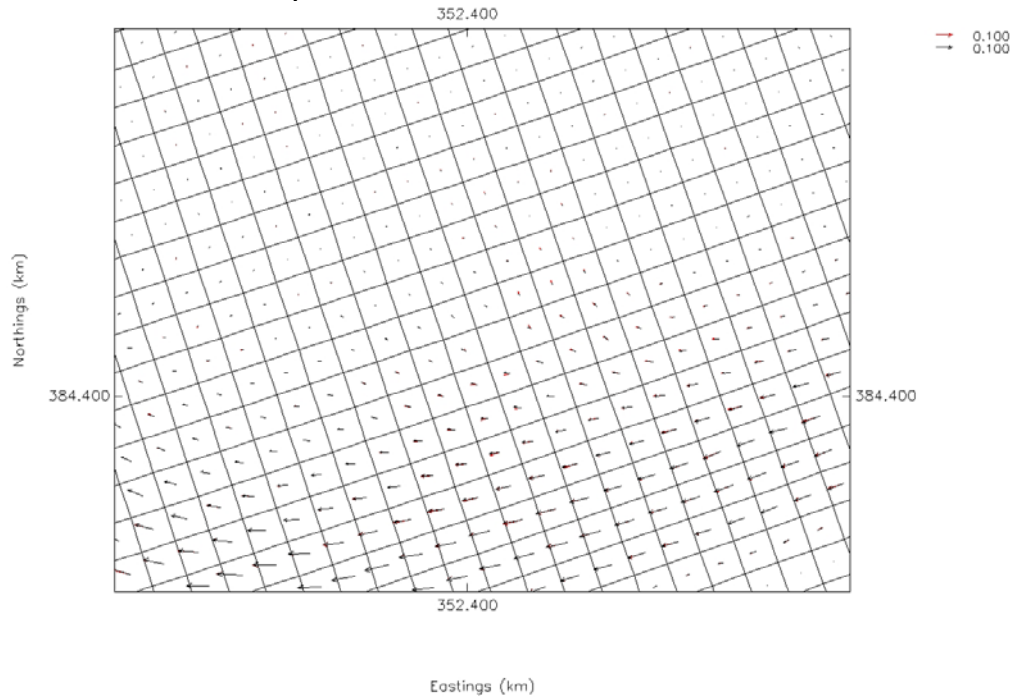


Figure 3f. Tidal residuals around long structure in north channel integrated over several neap tides under extreme fluvial flows

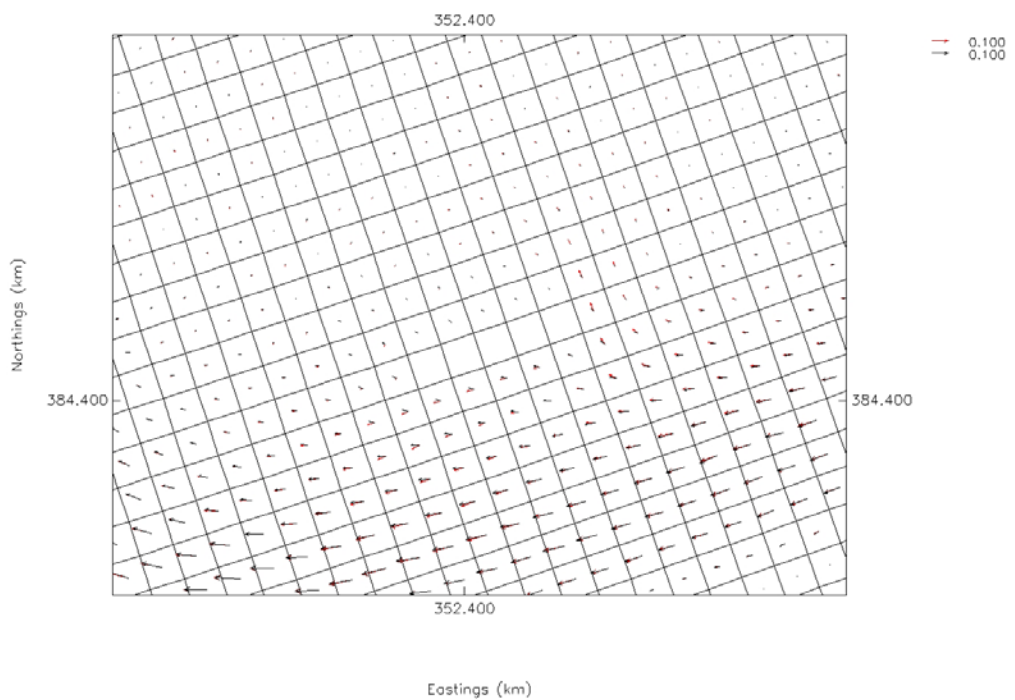


Figure 4a. Tidal residuals around short structure in north channel over a spring-neap-spring cycle under extreme fluvial flows

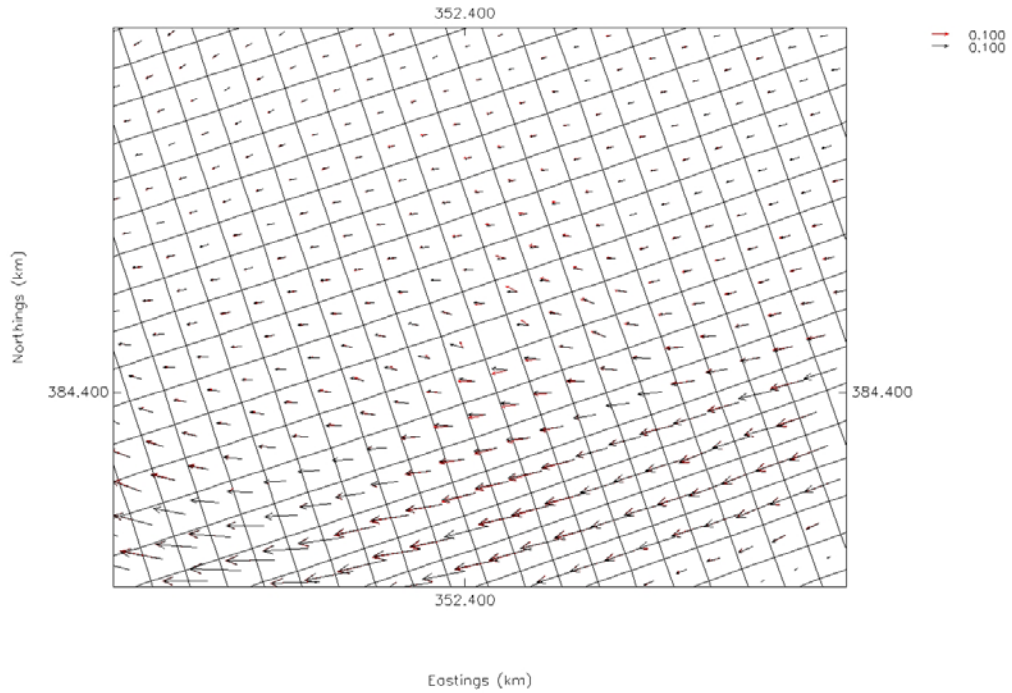


Figure 4b. Tidal residuals around long structure in north channel over a spring-neap-spring cycle under extreme fluvial flows

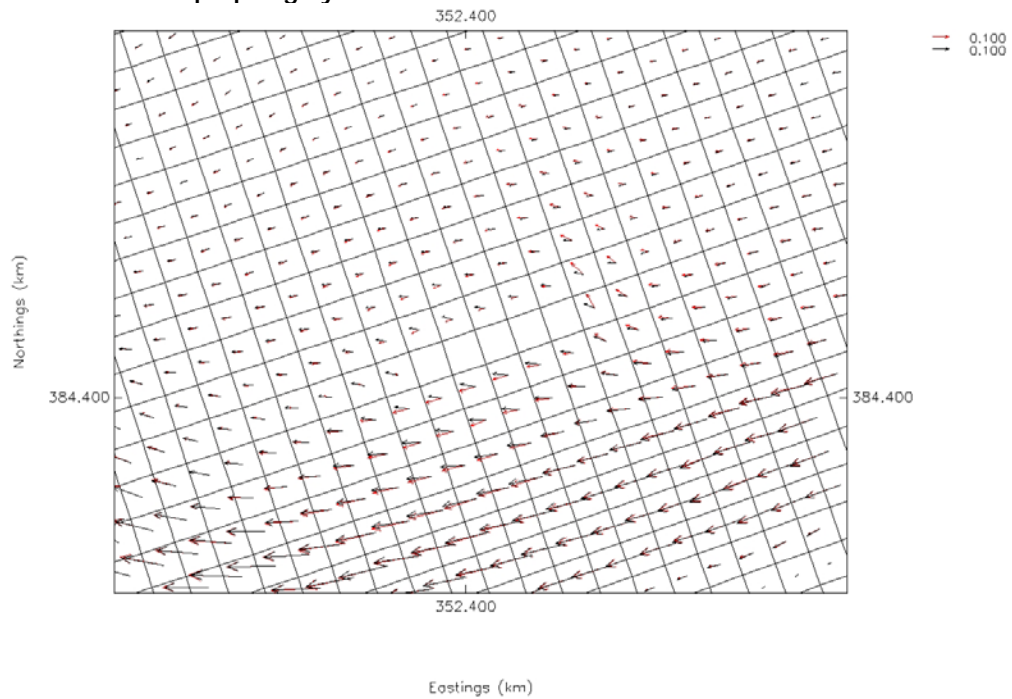


Figure 4c. Tidal residuals around short structure in north channel integrated over several spring tides under extreme fluvial flows

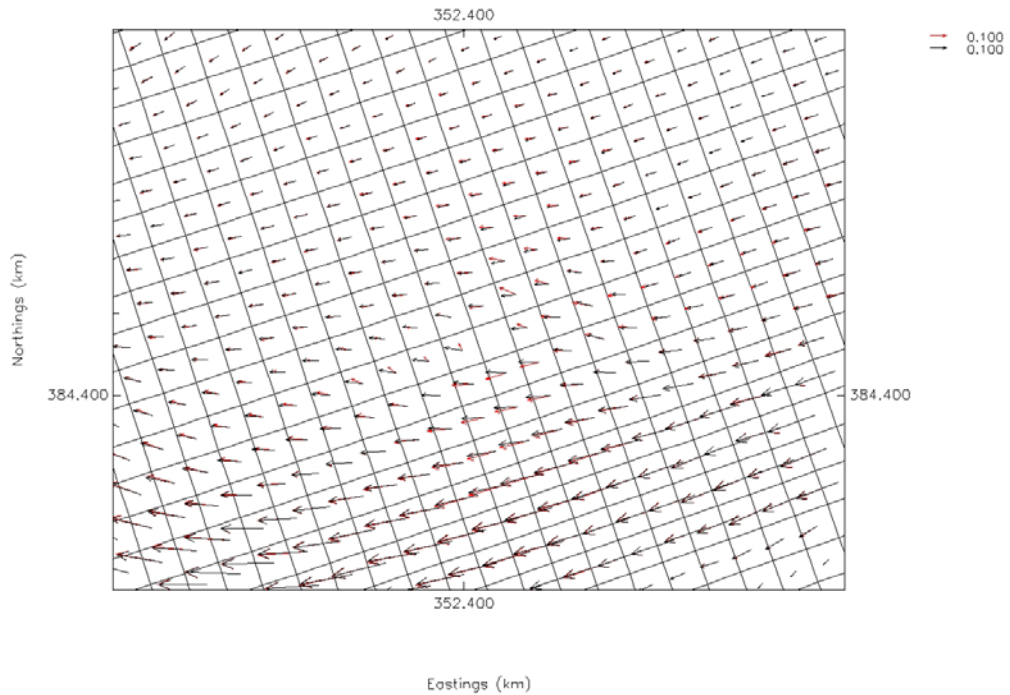


Figure 4d. Tidal residuals around long structure in north channel integrated over several spring tides under extreme fluvial flows

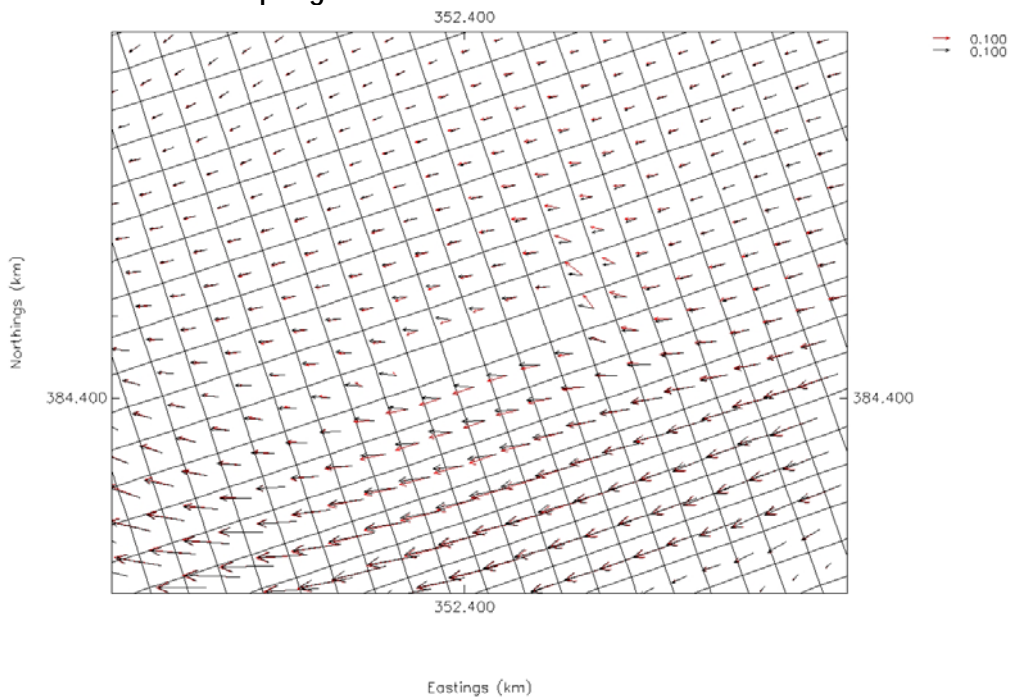


Figure 4e. Tidal residuals around short structure in north channel integrated over several neap tides under extreme fluvial flows

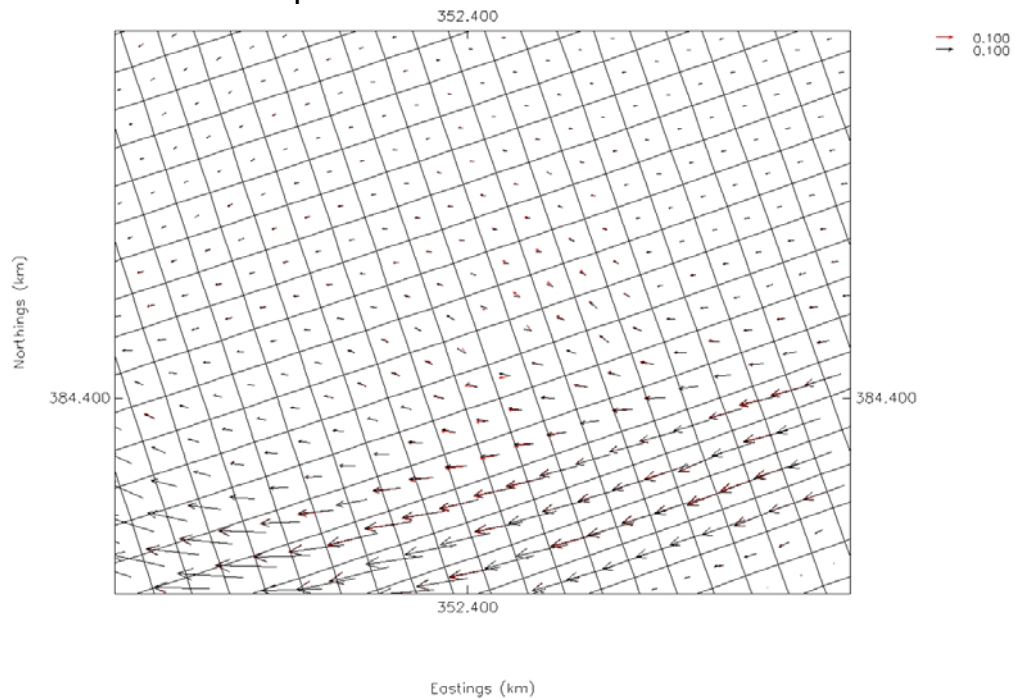
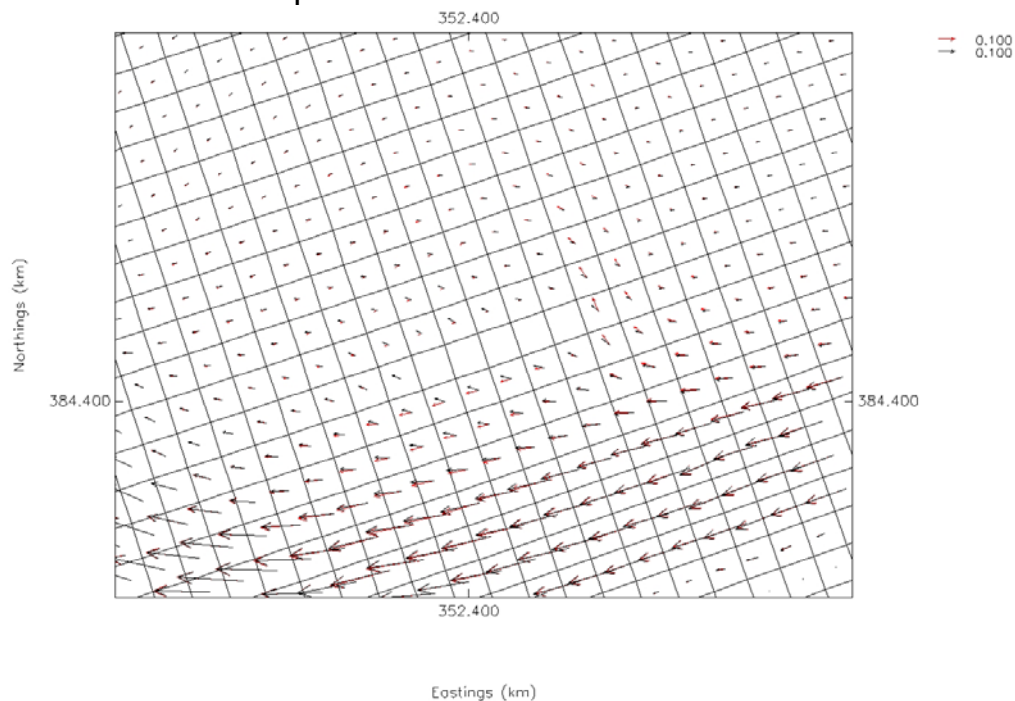


Figure 4f. Tidal residuals around long structure in north channel integrated over several neap tides under extreme fluvial flows





ABP Marine Environmental Research Ltd
Suite B, Waterside House
Town Quay
Southampton
Hampshire SO14 2AQ

Tel: +44 (0)23 8071 1840
Fax: +44 (0)23 8071 1841
Email: enquiries@abpmer.co.uk

www.abpmer.co.uk



Gifford & Partners

Additional Modelling - Mersey Gateway

Technical Note B: Residual Modelling - Stage II

Date: December 2005

Project Ref: R/3411/4

Report No: R.1241b



Gifford & Partners

Additional Modelling - Mersey Gateway Technical Note B: Residual Modelling - Stage II

Date: December 2005

Project Ref: R/3411/4

Report No: R.1241b

© ABP Marine Environmental Research Ltd

Version	Details of Change	Authorised By	Date
1	Draft for Comment	J M Harris	9/12/2005
2	Final	J M Harris	20/12/2005

Document Authorisation		Signature	Date
Project Manager:	J M Harris	<i>John Harris</i>	20/12/2005
Quality Manager:	R H Swift	<i>Richard Swift</i>	10/01/2006
Project Director:	W S Cooper	<i>W S Cooper</i>	10-1-06

ABP Marine Environmental Research Ltd
Suite B, Waterside House
Town Quay
SOUTHAMPTON
Hampshire
SO14 2AQ



Tel: +44(0)23 8071 1840
Fax: +44(0)23 8071 1841
Web: www.abpmer.co.uk
Email: enquires@abpmer.co.uk



INVESTOR IN PEOPLE

Summary

This technical note describes Stage II of the residual modelling undertaken as part of the additional modelling studies carried out for Phase II of the Mersey Gateway Project. Under Stage I several pier shapes (square and rectangular) were modelled without any sediment included to look at the effect of pier shape on residual flows. From these runs the impact of an elongated pier shape on the flow residuals was determined.

This report is one of a series of five Technical Notes (R1241a to R.1241e):

- Technical Note A: Residual Modelling - Stage I;
- Technical Note B: Residual Modelling - Stage II;
- Technical Note C: Flat Bed Morphological Modelling;
- Technical Note D: Real Hydrograph Modelling; and
- Technical Note E: Phase Differences.

An idealized model has been used to make an assessment of scouring around the bridge towers using a morphological model and to investigate the impact on the residual flow over typical tidal conditions as well as the impact of a channel passing through the proposed alignment of the bridge crossing. The key conclusions are:

- The largest directional change in the velocity is as the flow approaches the tower with flows bifurcating around the structure, before gradually returning to the original baseline directions and magnitude.
- The model results show both acceleration of the flow around the structure and deceleration behind it due to the blockage effect. Under normal conditions (spring-neap-spring tidal cycle) the velocity residuals are low in magnitude and typically less than 0.10m/s. Away from the structure within the north channel the residuals increase to about 0.25 - 0.30m/s.
- The modelling shows that the bedload transport is generally significantly less than the suspended transport (up to 100 times smaller, approximately) demonstrating the high energy in the system. In addition, over a normal tidal cycle the flooding tide is the most significant in terms of sediment transport.
- The modelling is limited by the period of the simulation and the forcing applied. Therefore, the results provide information on the short-term response of the system but limit what can be inferred over the longer-term. In the short-term the system moves towards a new stable equilibrium.
- The imposed scour holes are too deep to be sustained by the model, but this may be a limitation in the numerical model and its ability to fully represent the 3-dimensional nature of the scouring process. However, this could also be as a result of Equation 1 overestimating the equilibrium scour depth as this is for steady state conditions rather

than for tidal flows. This could be investigated using a fully 3D Computational Fluid Dynamics (CFD) model. This will have limited benefit at this stage as it is the long-term response on the system that is of greatest import and a CFD model will only provide short-term information on the system response.

- The impact of having a channel passing through all three bridge tower positions is limited by the strength of cross-estuary flows. This is not unexpected as the principal axis of the tidal flow is directed along the length of the estuary.

Additional Modelling - Mersey Gateway Technical Note B: Residual Modelling - Stage II

Contents

	Page
Summary	i
1. Introduction	1
2. Scour Hole - Methodology	1
2.1 Impact of Scour Holes	1
2.2 Results	3
3. Imposed Channel - Methodology	4
3.1 Impact of Imposed Channel Along Bridge Alignment	4
3.2 Results	4
4. Conclusions	5
5. References	6

Tables

1. Predicted equilibrium scour depth under steady currents	2
2. Angle of repose for different soils (from Hoffmans & Verheij, 1997)	2
3. Predicted scour width at the various tower positions for different angles of repose for fine sand under steady flow conditions	3

Figures

1.	Tidal curve at downstream boundary showing tidal residual averaging periods	8
2.	Model extents	8
3.	Scour hole width for southern tower, for angle of repose of 27°	9
4.	Modified bathymetry showing scour holes around bridge towers	9
5a.	Plot showing differences in sediment thickness between the scheme and the baseline case over a spring-neap period. Plotted using a finer scale	10
5b.	Plot showing differences in sediment thickness between the scheme and the baseline case over a spring-neap period. Plotted using a coarser scale	10
6.	A 3-dimensional image of the differences in sediment thickness between the scheme and the baseline case over a spring-neap period. Note negative values represent deposition and positive values erosion	11
7a.	Plot showing differences in sediment thickness between the scheme and the baseline case over a second spring-neap period. Plotted using a finer scale.....	12
7b.	Plot showing differences in sediment thickness between the scheme and the baseline case over a second spring-neap period. Plotted using a coarser scale.....	12
7c.	Plot showing differences in sediment thickness between the last time-step for the two spring-neap period runs for the scheme.....	13
8a.	Plot showing tidal residuals over a spring-neap period for the scheme (red) and the baseline case (black).....	14
8b.	Plot showing a close up of the tidal residuals around the north bridge tower over a spring-neap period for the scheme (red) and the baseline case (black)	14
8c.	Plot showing a close up of the tidal residuals around the south bridge tower over a spring-neap period for the scheme (red) and the baseline case (black)	15
9a.	Plot showing depth-averaged suspended sediment transport vectors around low water on a spring tide for the scheme (red) and the baseline case (black).....	16
9b.	Plot showing depth-averaged suspended sediment transport vectors around peak flood on a spring tide for the scheme (red) and the baseline case (black)	16
9c.	Plot showing depth-averaged suspended sediment transport vectors around high water on a spring tide for the scheme (red) and the baseline case (black)	17
9d.	Plot showing depth-averaged suspended sediment transport vectors around peak ebb on a spring tide for the scheme (red) and the baseline case (black).....	17

10a.	Plot showing bedload sediment transport vectors around low water on a spring tide for the scheme (red) and the baseline case (black)	18
10b.	Plot showing bedload sediment transport vectors around peak flood on a spring tide for the scheme (red) and the baseline case (black)	18
10c.	Plot showing bedload sediment transport vectors around high water on a spring tide for the scheme (red) and the baseline case (black)	19
10d.	Plot showing bedload sediment transport vectors around peak ebb on a spring tide for the scheme (red) and the baseline case (black)	19
11.	Three-dimensional image of initial channel bathymetry	20
12.	Three-dimensional image showing differences in sediment thickness between the scheme and the baseline case. Note negative values represent deposition and positive values erosion	20
13a.	Plot showing differences in sediment thickness between the scheme and the baseline case over a spring-neap period. Plotted using a finer scale	21
13b.	Plot showing differences in sediment thickness between the scheme and the baseline case over a spring-neap period. Plotted using a coarser scale	21
14a.	Plot showing the tidal residuals for the baseline case and scheme	22
14b.	Plot showing the tidal residuals for the baseline case and scheme in close up around the north bridge tower	22

1. Introduction

This technical note describes Stage II of the residual modelling undertaken as part of the additional modelling studies carried out for Phase II of the Mersey Gateway Project. Under Stage I several pier shapes (square and rectangular) were modelled without any sediment included to look at the effect of pier shape on residual flows. From these runs the impact of an elongated pier shape on the flow residuals was determined.

For Stage II two further scenarios have been investigated using only the square pier shape. These two scenarios represent the morphological change and impact on tidal residuals as a result of imposing scour holes around the three bridge towers and the impact of having a channel running along the alignment of the three bridge towers, respectively.

Tidal residuals represent the net pattern of the flow field integrated over a tidal period. For example, in the present study several periods have been used to integrate the flow field over, a spring-neap-spring tidal cycle covering a 15 days period, a spring tide and a neap tide period (Figure 1). Sediment transport paths can be inferred indirectly from measurements/predictions of flow intensity profiles during entire tidal cycles. Therefore, changes in tidal residuals can be used to indicate likely changes in sediment transport paths.

Figure 1 shows the spring-neap-spring tidal cycle used on the downstream boundary. The extents of the model grid used are shown in Figure 2.

2. Scour Hole - Methodology

2.1 Impact of Scour Holes

The scour formula of Breusers *et al.* (1977) has been applied to estimate scour depth under steady currents (Eqn.1). This formula allows for a correction for scour in shallow water.

$$S_c = 1.5K_i D \tanh\left(\frac{h_0}{D}\right) \quad (1)$$

in which:

D	= Pile diameter (m)
h_0	= Flow depth (m)
K_i	= Correction factor
S_c	= Equilibrium scour depth under steady flow

For the three tower positions the equilibrium scour depth has been calculated as given in Table 1.

Table 1. Predicted equilibrium scour depth under steady currents

Bridge Tower Position	Equilibrium Scour Depth Sc (m)
South	3.5
Middle	0.8
North	3.4

The plan-view extent of the scour hole formed around a bridge pier is a function of the magnitude of the vortices formed, the depth of scour and the sediment characteristics. Around a monopile structure the upstream scour slope is, typically, equal to the angle of repose for the sediment (Table 2), whilst the average downstream slope is generally less steep and is often taken to be half the upstream slope angle. However, under tidal conditions where the flow direction is reversing with the flooding and ebbing tide then the shape and dimensions of the scour hole are also likely to change within the tidal cycle and may take on a more symmetrical conical shape.

Table 2. Angle of repose for different soils (from Hoffmans & Verheij, 1997)

Sediment Type	Soil Type	Angle of Repose ϕ (°)
Coarse sand	Compact	45
	Firm	38
	Loose	32
Medium sand	Compact	40
	Firm	34
	Loose	30
Fine sand	Compact	30-34
	Firm	28-30
	Loose	26-28

Under steady flow conditions the dimensions of the scour hole are approximated for the 10m diameter bridge towers as shown in Figure 3 for the southern most tower. The approach assumes a loosely compacted, fine sand with an assumed angle of repose, ϕ , of 27°. The total width of scour is some 43.2m, approximately. Table 3 presents the results for all three tower positions together with scour hole widths for assumed angles of repose, corresponding to 26° and 34°.

Table 3. Predicted scour width at the various tower positions for different angles of repose for fine sand under steady flow conditions

Angle of Repose	Area	Upstream	Downstream	Total
		Scour Width (m)		
$\phi = 27^\circ$	South tower	17.8	25.4	43.2
	Middle tower	12.6	14.4	27.0
	North tower	17.6	25.0	42.6
$\phi = 26^\circ$	South tower	18.1	26.0	44.1
	Middle tower	12.7	14.5	27.2
	North tower	17.9	25.5	43.4
$\phi = 34^\circ$	South tower	16.1	22.3	38.4
	Middle tower	12.2	13.6	25.9
	North tower	16.0	22.0	37.9

Using the predicted scour depths and assumed shape and extents of the scour holes based on an assumed angle of repose, ϕ , of 27° the bathymetry in the model has been adjusted (Figure 4). Using this modified bathymetry the model has then been run over a spring-neap period using a coupled hydrodynamic and morphological model with the bridge structures represented as solid objects. This run has then been compared with the results of a baseline simulation with no scour holes or structures run over an identical time-period.

2.2 Results

Figure 5 shows the difference in sediment thickness between the scheme and the baseline simulation. Figure 5a shows the results using a finer scaling to look at the smaller changes in deposition and erosion of the sediment, whilst Figure 5b uses a coarser scale to allow the larger scale changes to be seen more clearly. Both figures are plotted together with the baseline tidal residuals. From the model results the scour holes are infilled over the period of the simulation, which would imply both that the holes were over-deepened and also that they are secondary to the wider-scale changes. However, this may indicate more a limitation in the model not being capable of reproducing the 3-dimensional nature of the scouring process and the turbulence effects around the structure. The infilling is clearly visible in a 3-dimensional image of the differences (Figure 6). Within the northern channel the modelling shows the channel deepening to the south of the north bridge tower. At the middle tower, changes in sedimentation are not significant, primarily because the tower position is currently on top of a bank, which will only be flooded on spring tides.

Figure 7 shows the difference in sediment thickness between the scheme and the baseline case after a second spring-neap period. The predicted changes are similar to those over the first period and in fact the differences in sediment thickness between the last time-step of the first spring-neap period and those of the second spring-neap period are not significant (Figure 7c). This is partly as a response to driving the model

with the same signal over the two spring-neap periods. The model appears to be approaching a new equilibrium state. Figure 8 shows the tidal residuals averaged over the spring-neap-spring cycle shown in Figure 1. In general, changes in the residual pattern as a result of the placing of the bridge towers within the flow are confined to the immediate area local to the structures. Figure 8b shows the tidal residuals around the north tower showing some directional change between the baseline and scheme vectors close to the structures. Around the south tower (Figure 8c) the changes in the residual pattern are minimal.

Figures 9 and 10 show the depth-averaged suspended transport vectors and the bedload transport vectors, respectively. The plots show results for both the baseline and the scheme at different tidal states over a spring tide. From the figures it is clear that the greatest movement of sediment happens on the flooding tide and that suspended sediment transport is the dominant process. Note the difference in scale between the suspended sediment plots and those for the bedload transport (a factor of 100 greater). As with the tidal residuals, there is some change in magnitude and direction of the vectors local to the structures.

3. Imposed Channel - Methodology

3.1 Impact of Imposed Channel Along Bridge Alignment

A channel, which passed along the alignment of the proposed Route3A crossing, was imposed upon the 2002 bathymetry. The resulting bathymetry is shown in Figure 11. The purpose of this layout was to expose all three bridge towers to the flow through a typical spring-neap cycle. Under the existing 2002 bathymetry the central bridge tower is only exposed to flow on spring tides when the intertidal banks are flooded.

3.2 Results

Figure 12 shows a 3-dimensional image of the differences in sediment thickness between the scheme and the baseline over the spring-neap-spring period (see Figure 1). The largest changes occur around the northern most tower with deposition upstream and downstream of the structure and erosion along the sides. A similar effect occurs local to the southern most tower, whilst in the vicinity of the central tower the model predicts mostly accretion of sediment. Despite the channel passing through the alignment of the piers the dominant flow is still along the estuary rather than across the estuary. This is not unexpected as the principal axis of the tidal flow is directed along the length of the estuary. Figure 13 shows the difference in sediment thickness between the baseline and the scheme at two scales, a finer scale (Figure 13a) and a coarser scale (Figure 13b). This allows both the smaller-scale changes to be observed whilst also allowing any significant larger scale changes to be seen.

A comparison of the tidal residuals for the baseline and the scheme are shown in Figure 14. The changes are confined to the regions local to the structures as seen in the previous scenario (Figure 14a). Local to the structures the changes in the pattern of the residuals (magnitude and direction) is small and appears to be less than observed in the scour hole scenario (Figure 14b). This just demonstrates the effect that the variability in channel positions relative to the structures has on the changes in residual flow pattern.

4. Conclusions

An idealized model has been used to make an assessment of scouring around the bridge towers using a morphological model and to investigate the impact on the residual flow over typical tidal conditions as well as the impact of a channel passing through the proposed alignment of the bridge crossing. The key conclusions are:

- The largest directional change in the velocity is as the flow approaches the tower with flows bifurcating around the structure, before gradually returning to the original baseline directions and magnitude.
- The model results show both acceleration of the flow around the structure and deceleration behind it due to the blockage effect. Under normal conditions (spring-neap-spring tidal cycle) the velocity residuals are low in magnitude and typically less than 0.10m/s. Away from the structure within the north channel the residuals increase to about 0.25 - 0.30m/s.
- The modelling shows that the bedload transport is generally significantly less than the suspended transport (up to 100 times smaller, approximately) demonstrating the high energy in the system. In addition, over a normal tidal cycle the flooding tide is the most significant in terms of sediment transport.
- The modelling is limited by the period of the simulation and the forcing applied. Therefore, the results provide information on the short-term response of the system but limit what can be inferred over the longer-term. In the short-term the system moves towards a new stable equilibrium.
- The imposed scour holes are too deep to be sustained by the model, but this may be a limitation in the numerical model and its ability to fully represent the 3-dimensional nature of the scouring process. However, this could also be as a result of Equation 1 overestimating the equilibrium scour depth as this is for steady state conditions rather than for tidal flows. This could be investigated using a fully 3D Computational Fluid Dynamics (CFD) model. This will have limited benefit at this stage as it is the long-term response on the system that is of greatest import and a CFD model will only provide short-term information on the system response.

- The impact of having a channel passing through all three bridge tower positions is limited by the strength of cross-estuary flows. This is not unexpected as the principal axis of the tidal flow is directed along the length of the estuary.

5. References

Breusers, H.N.C., Nicollet, G. & Shen, H.W., 1977. Local scour around cylindrical piers. *Jr. Hydraulic Res., IAHR*, 15 (3), pp 211-252.

Hoffmans G.J.C.M. & Verheij H.J., 1997. *Scour Manual*. AA Balkema, Rotterdam.

Figures

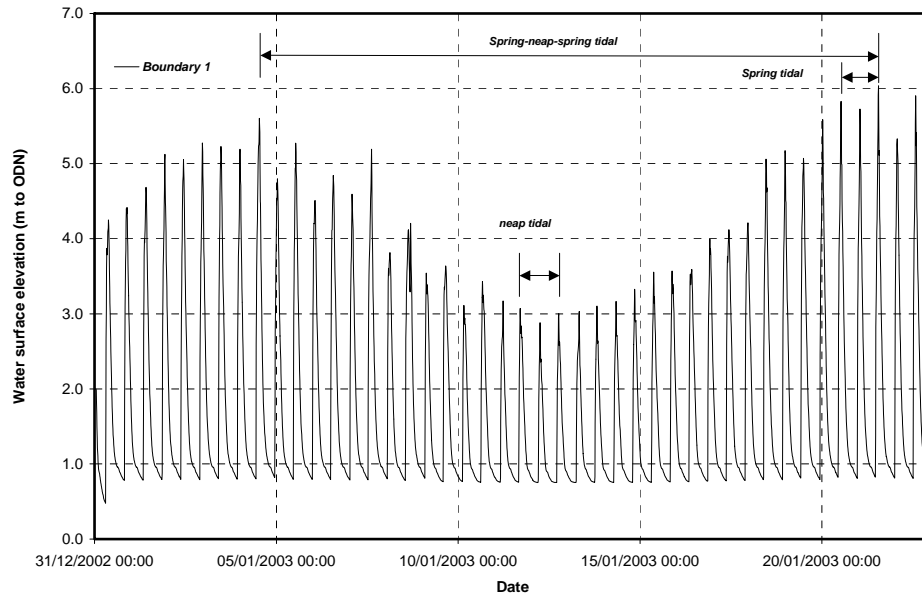


Figure 1. Tidal curve at downstream boundary showing tidal residual averaging periods

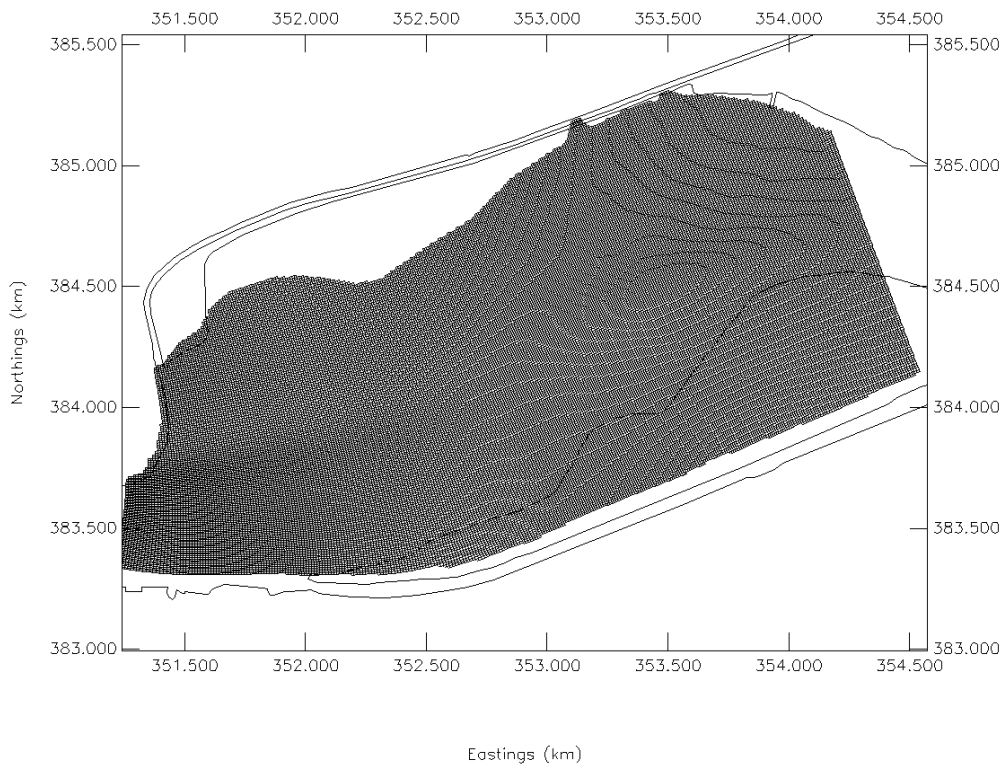


Figure 2. Model extents

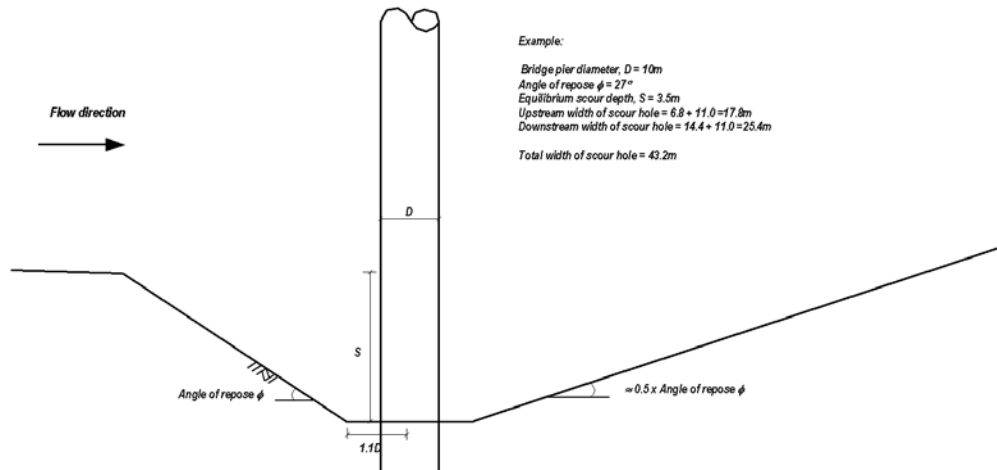


Figure 3. Scour hole width for southern tower, for angle of repose of 27°

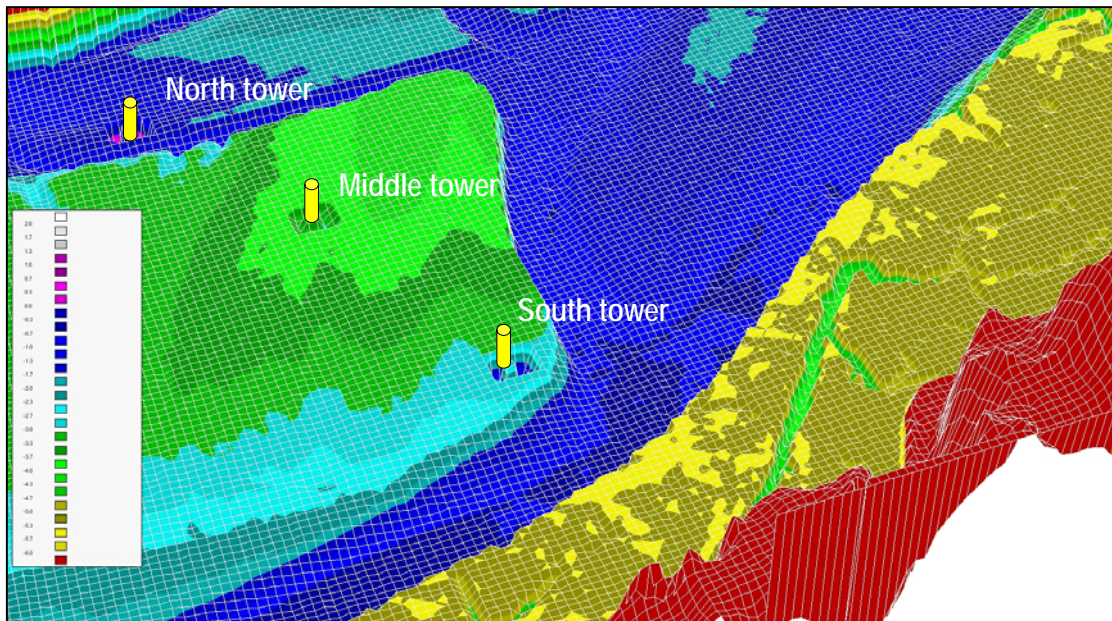


Figure 4. Modified bathymetry showing scour holes around bridge towers

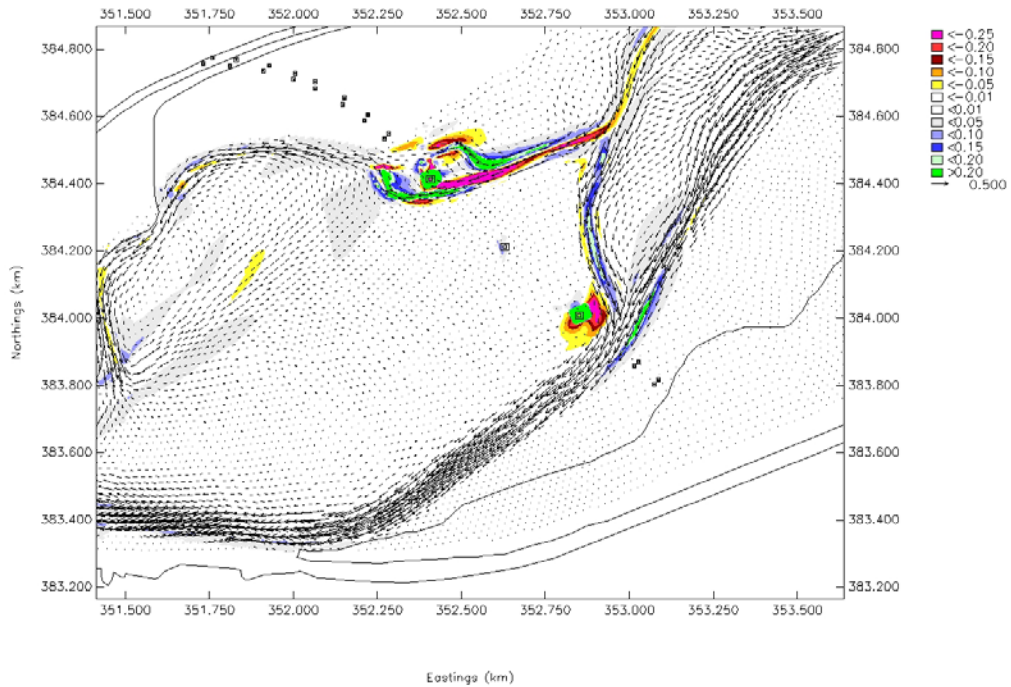


Figure 5a. Plot showing differences in sediment thickness between the scheme and the baseline case over a spring-neap period. Plotted using a finer scale

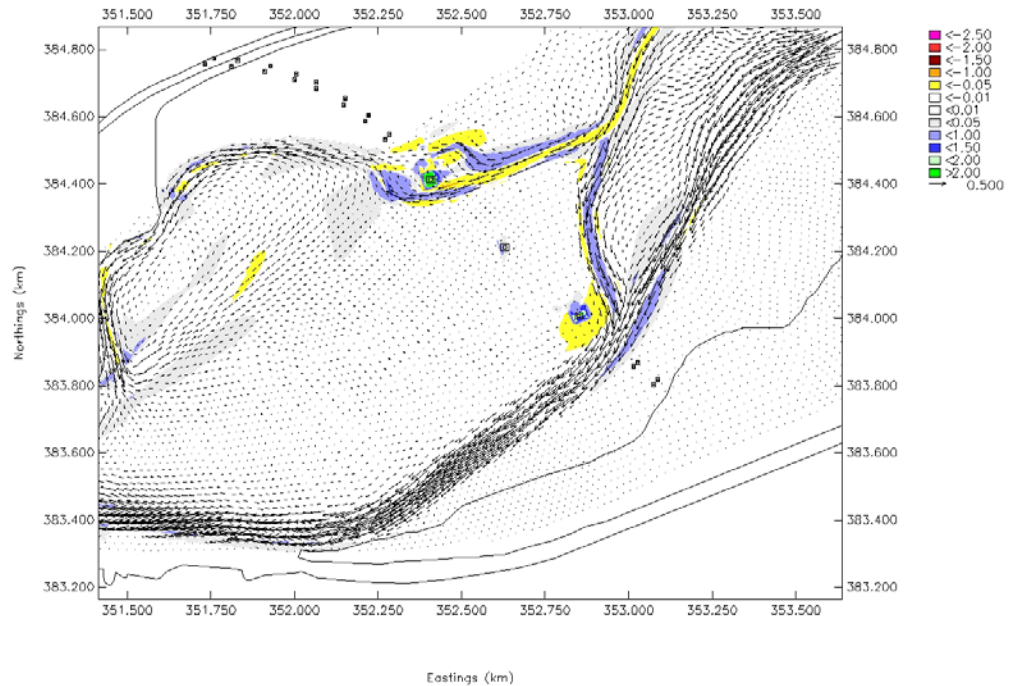


Figure 5b. Plot showing differences in sediment thickness between the scheme and the baseline case over a spring-neap period. Plotted using a coarser scale

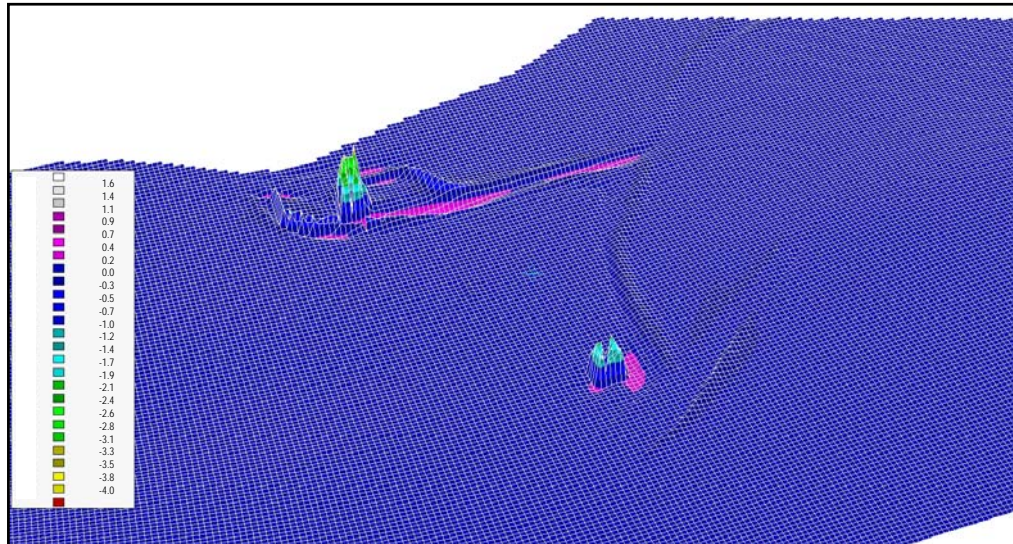


Figure 6. A 3-dimensional image of the differences in sediment thickness between the scheme and the baseline case over a spring-neap period. Note negative values represent deposition and positive values erosion

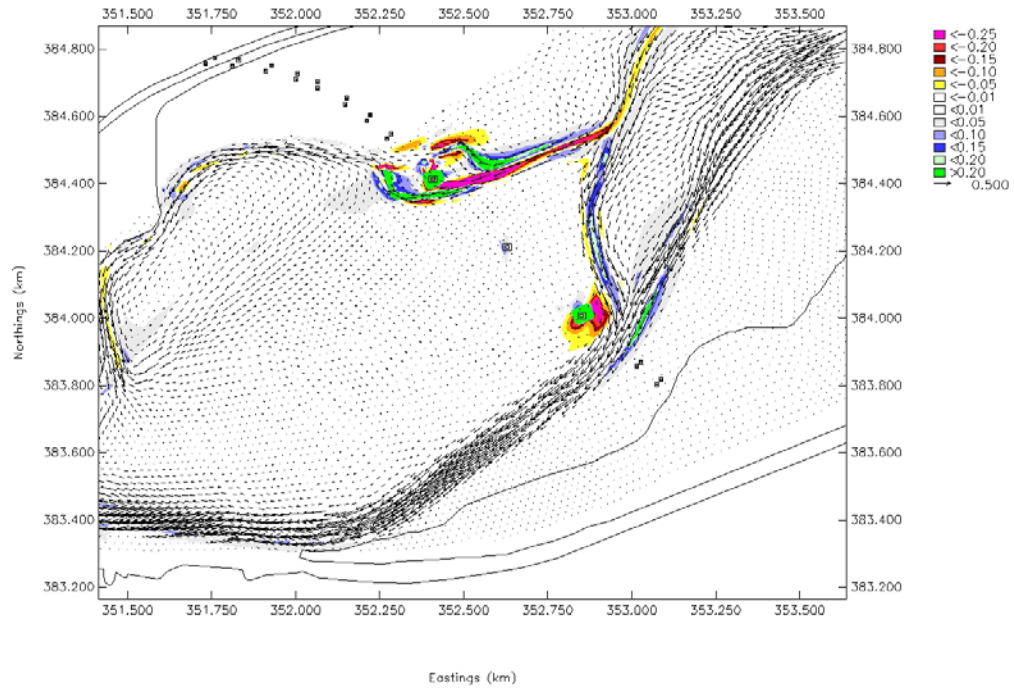


Figure 7a. Plot showing differences in sediment thickness between the scheme and the baseline case over a second spring-neap period. Plotted using a finer scale.

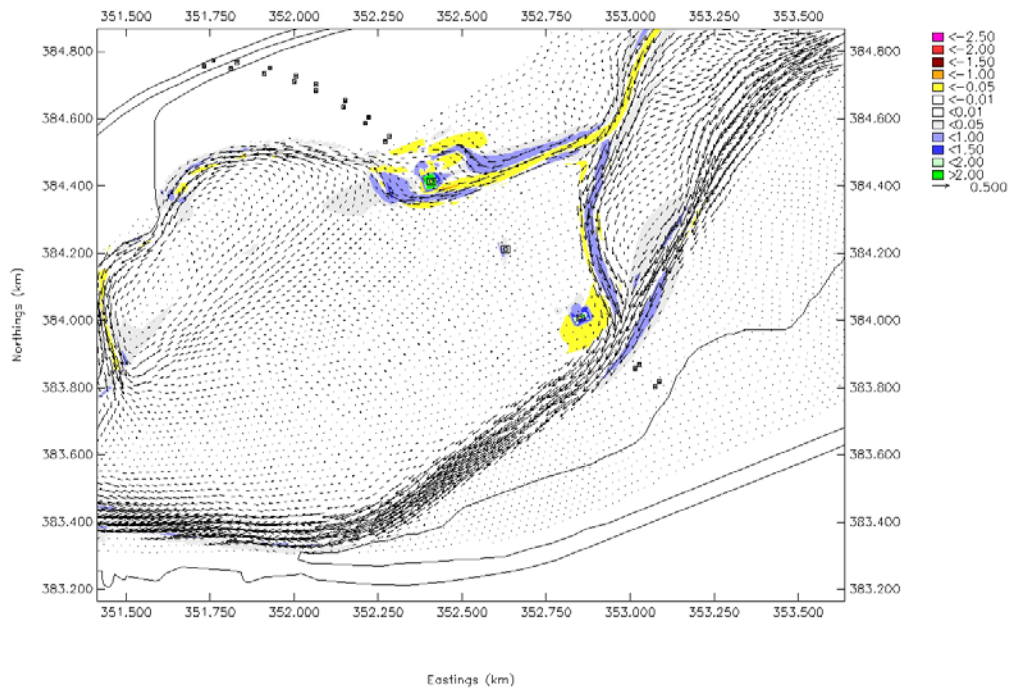


Figure 7b. Plot showing differences in sediment thickness between the scheme and the baseline case over a second spring-neap period. Plotted using a coarser scale

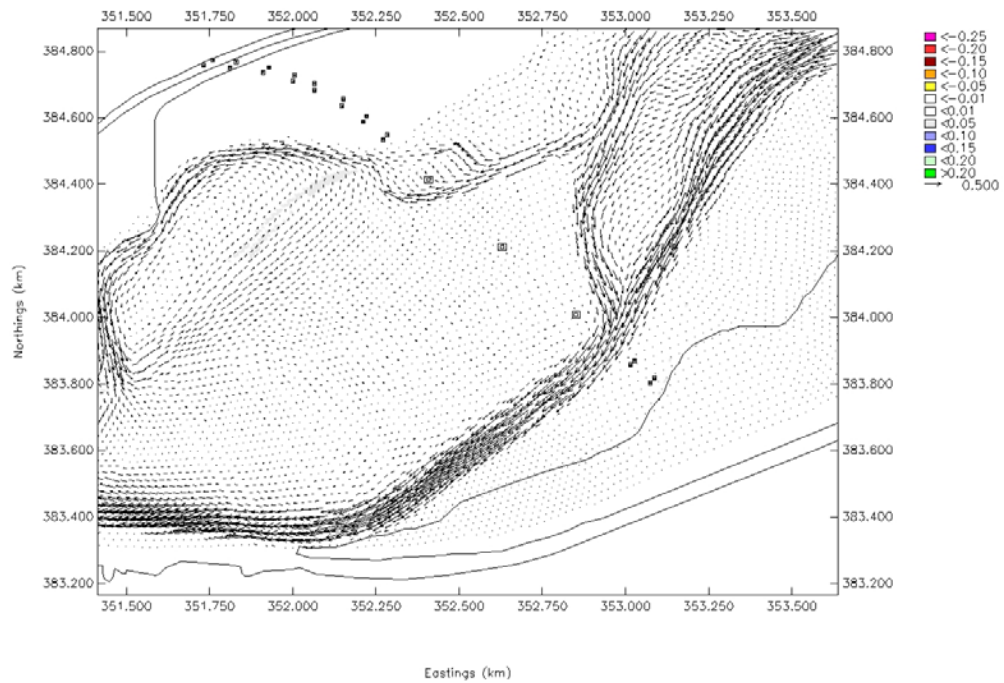


Figure 7c. Plot showing differences in sediment thickness between the last time-step for the two spring-neap period runs for the scheme

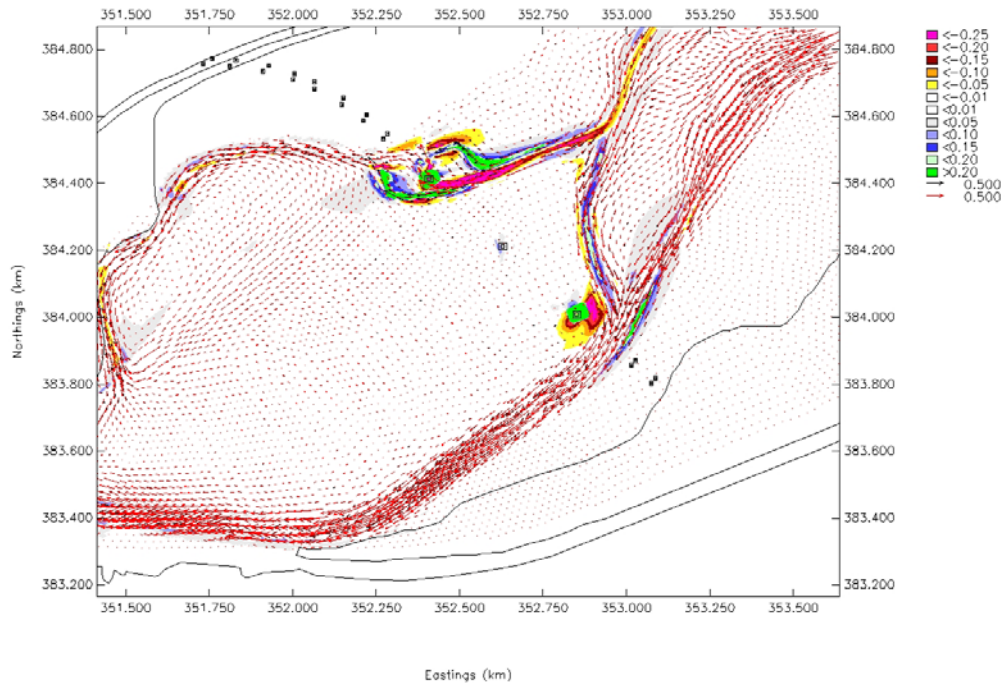


Figure 8a. Plot showing tidal residuals over a spring-neap period for the scheme (red) and the baseline case (black)

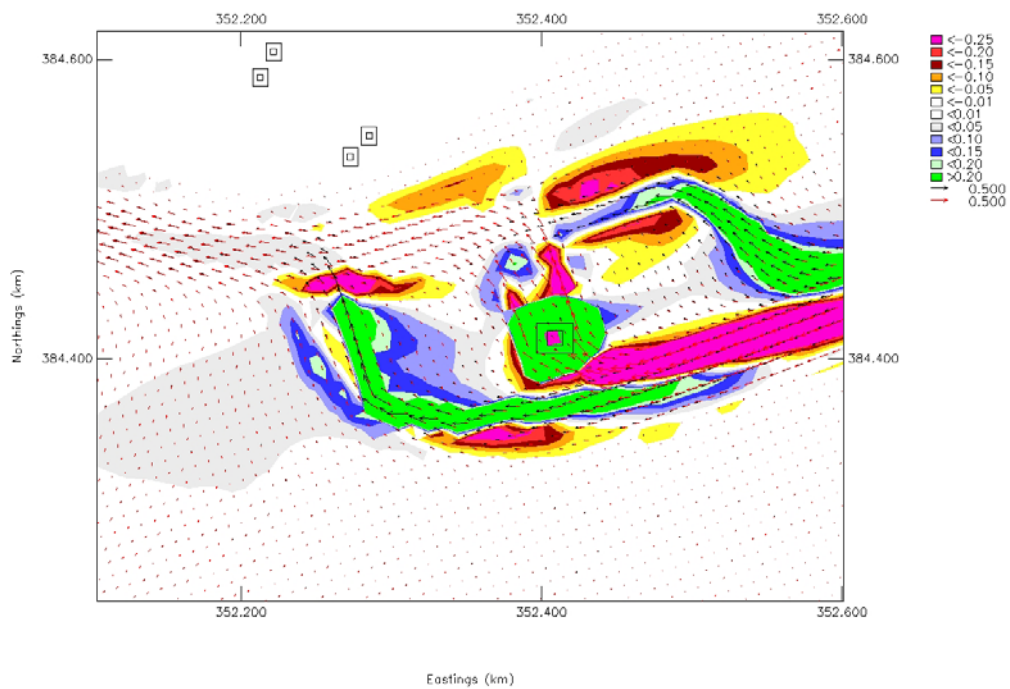


Figure 8b. Plot showing a close up of the tidal residuals around the north bridge tower over a spring-neap period for the scheme (red) and the baseline case (black)

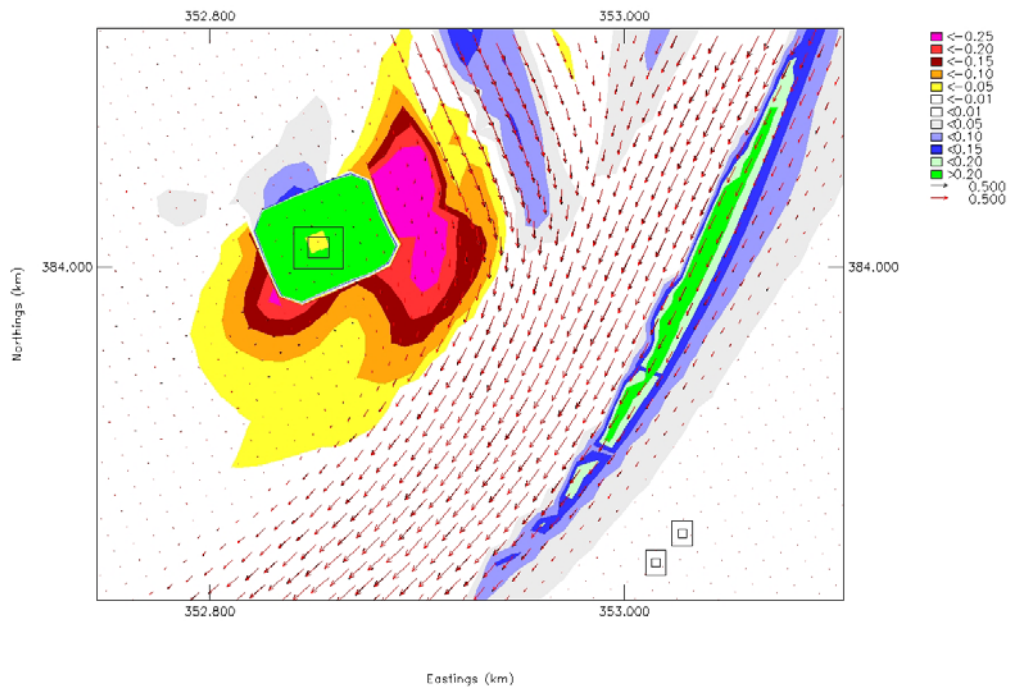


Figure 8c. Plot showing a close up of the tidal residuals around the south bridge tower over a spring-neap period for the scheme (red) and the baseline case (black)

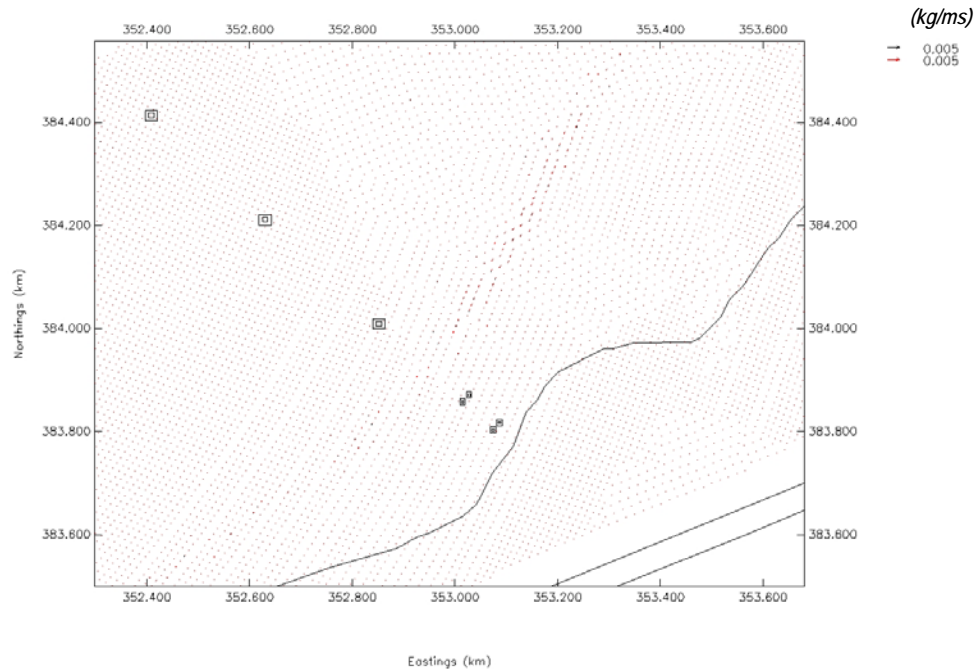


Figure 9a. Plot showing depth-averaged suspended sediment transport vectors around low water on a spring tide for the scheme (red) and the baseline case (black)

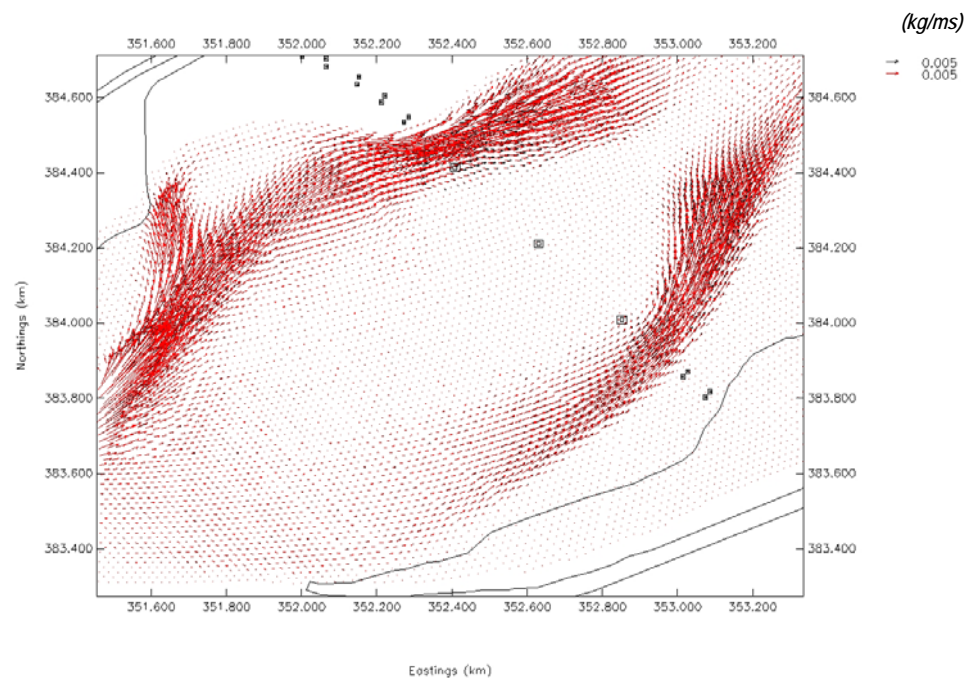


Figure 9b. Plot showing depth-averaged suspended sediment transport vectors around peak flood on a spring tide for the scheme (red) and the baseline case (black)

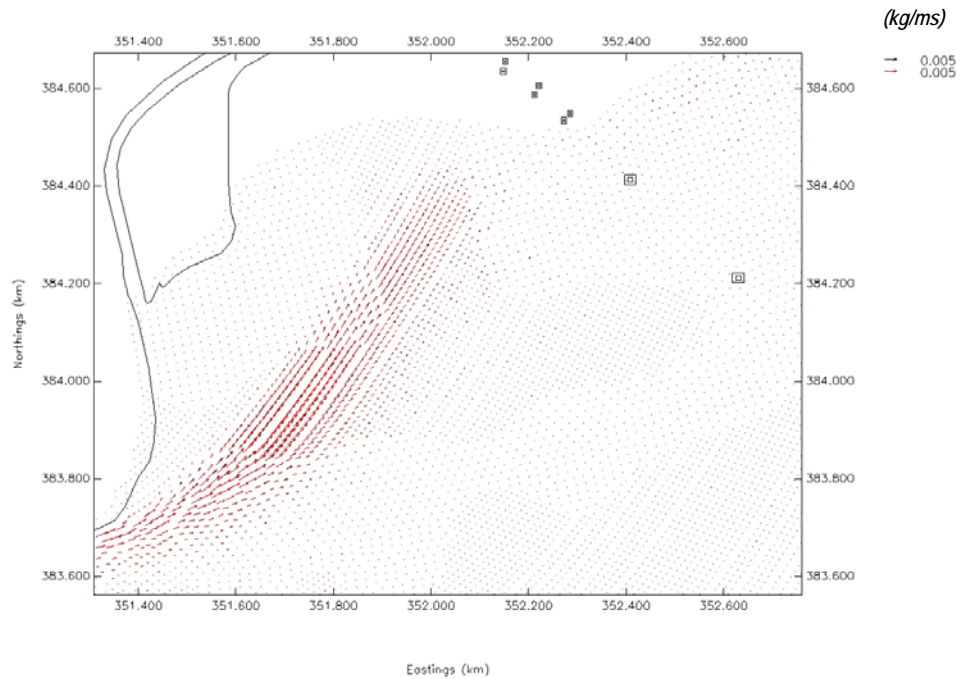


Figure 9c. Plot showing depth-averaged suspended sediment transport vectors around high water on a spring tide for the scheme (red) and the baseline case (black)

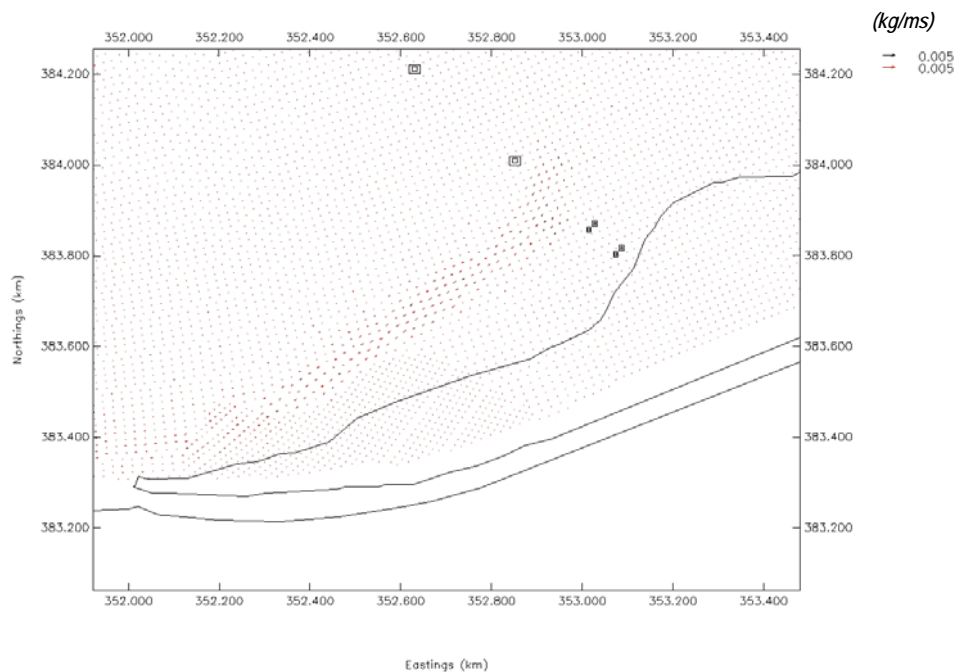


Figure 9d. Plot showing depth-averaged suspended sediment transport vectors around peak ebb on a spring tide for the scheme (red) and the baseline case (black)

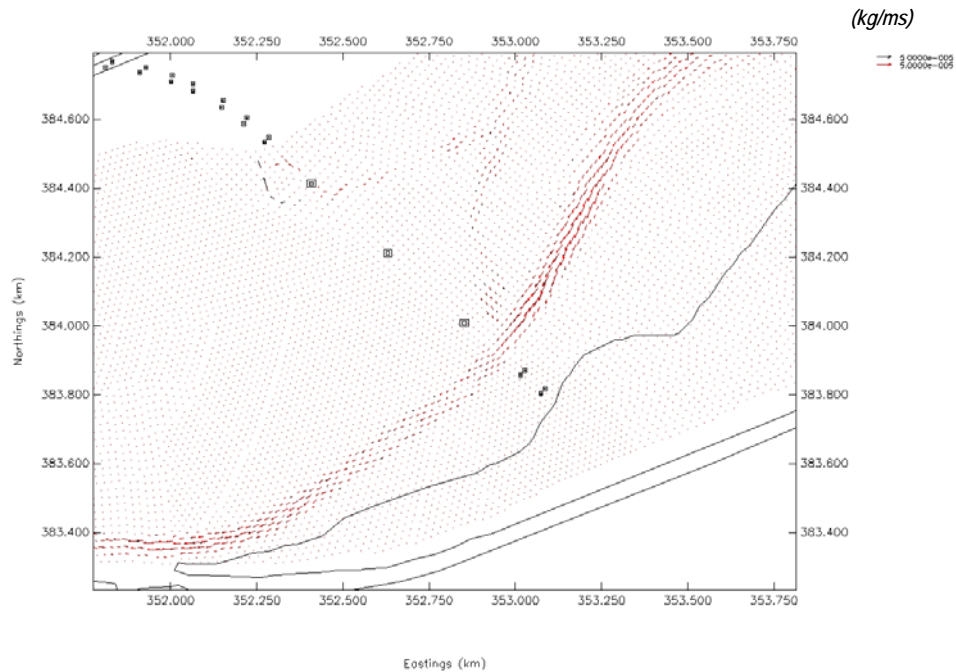


Figure 10a. Plot showing bedload sediment transport vectors around low water on a spring tide for the scheme (red) and the baseline case (black)

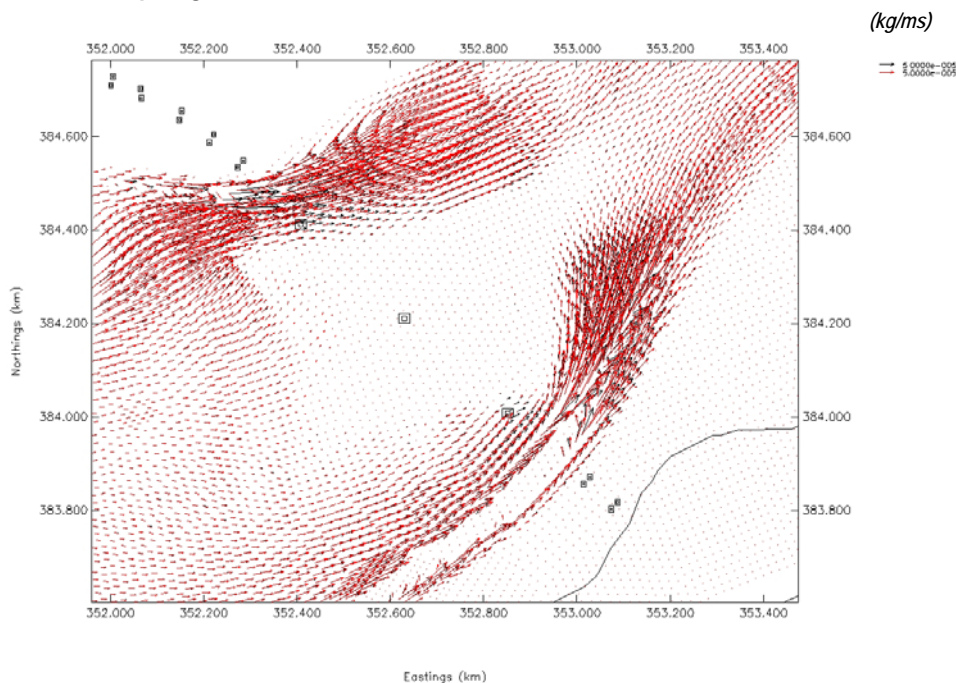


Figure 10b. Plot showing bedload sediment transport vectors around peak flood on a spring tide for the scheme (red) and the baseline case (black)

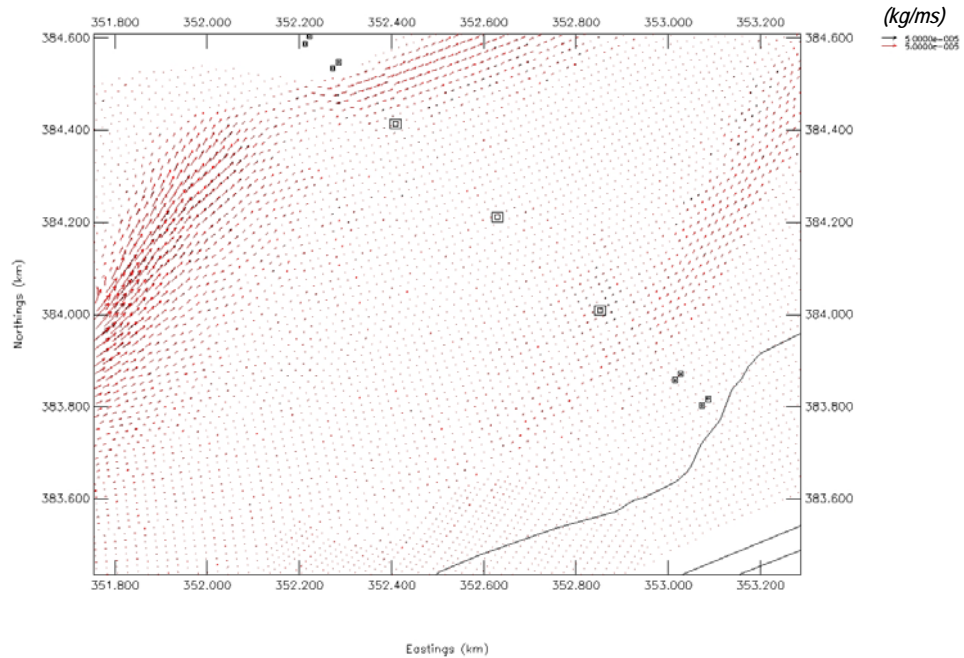


Figure 10c. Plot showing bedload sediment transport vectors around high water on a spring tide for the scheme (red) and the baseline case (black)

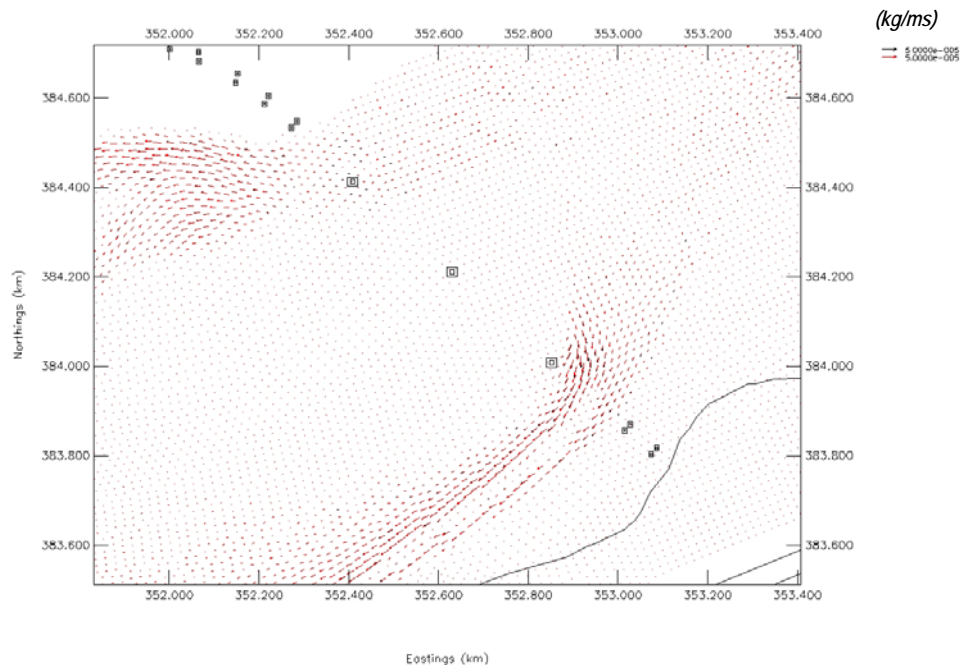


Figure 10d. Plot showing bedload sediment transport vectors around peak ebb on a spring tide for the scheme (red) and the baseline case (black)

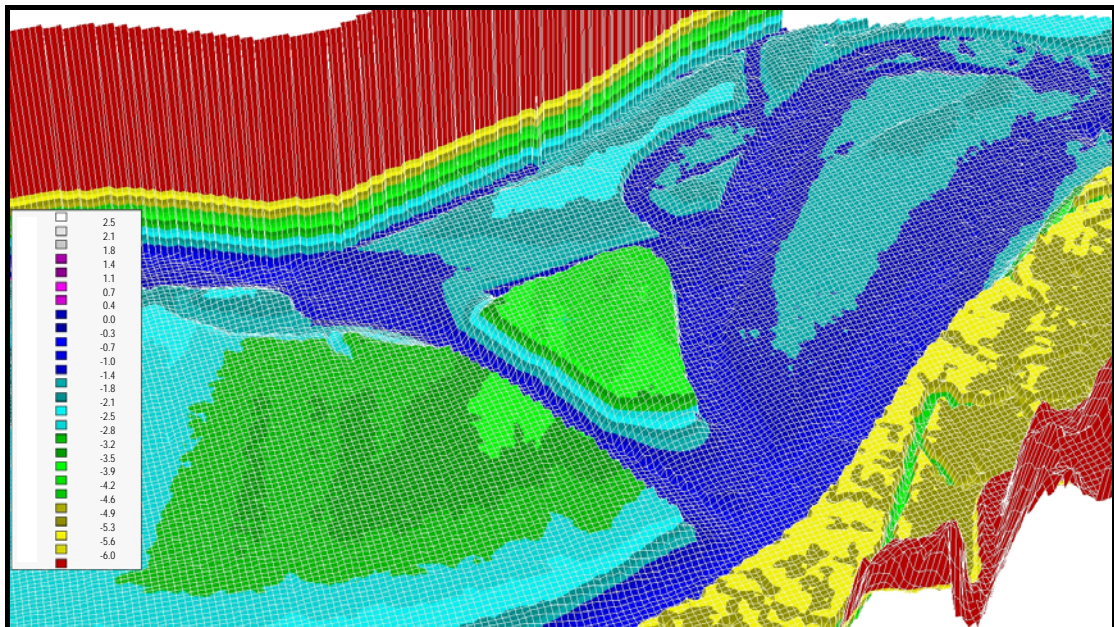


Figure 11. Three-dimensional image of initial channel bathymetry

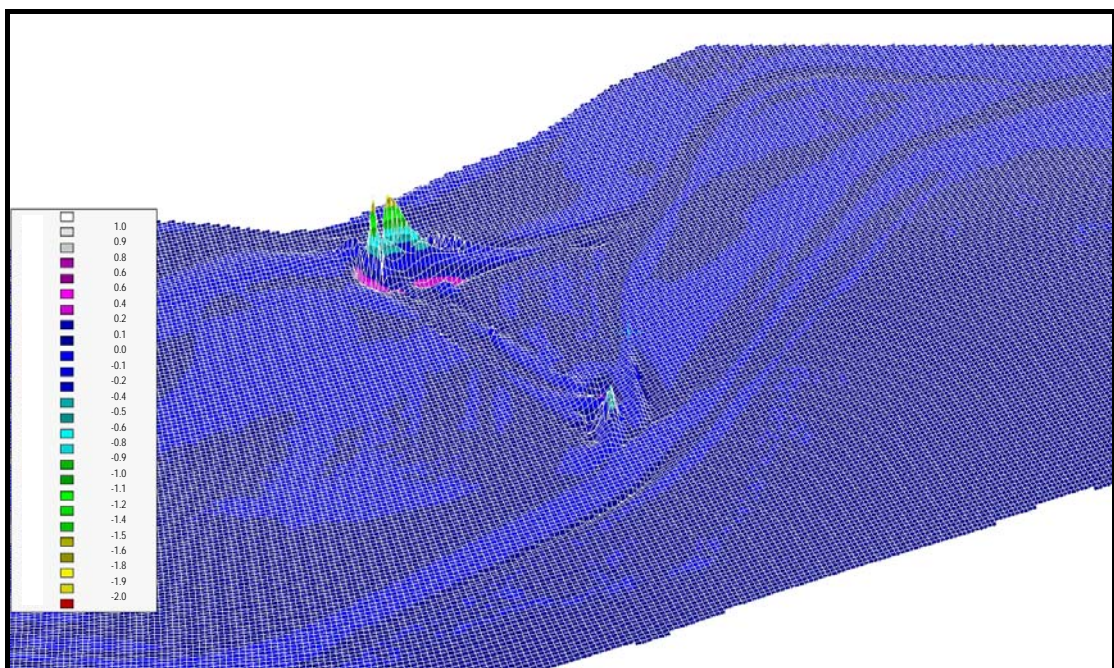


Figure 12. Three-dimensional image showing differences in sediment thickness between the scheme and the baseline case. Note negative values represent deposition and positive values erosion

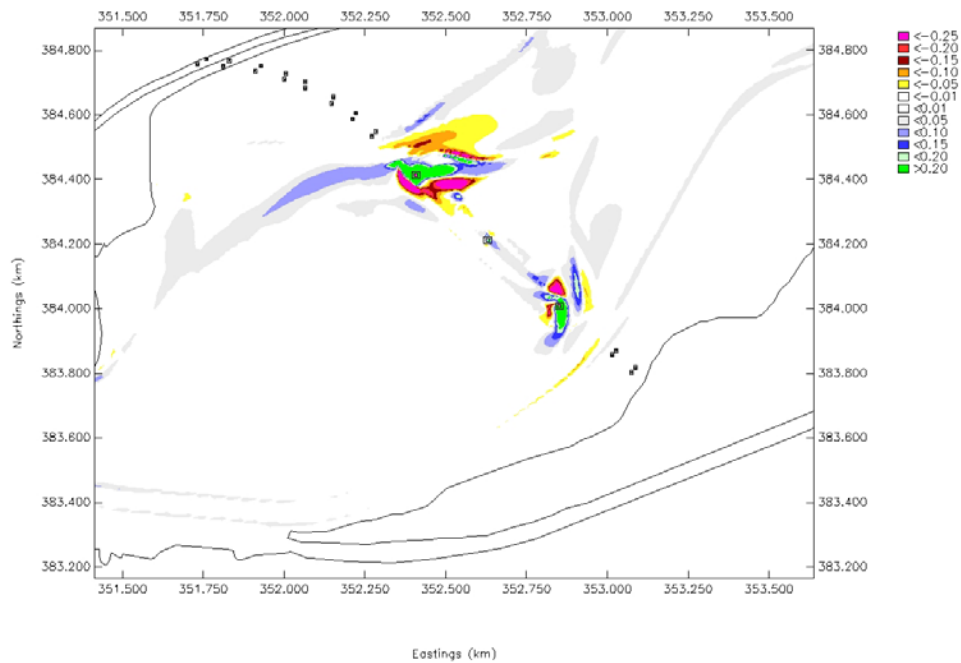


Figure 13a. Plot showing differences in sediment thickness between the scheme and the baseline case over a spring-neap period. Plotted using a finer scale

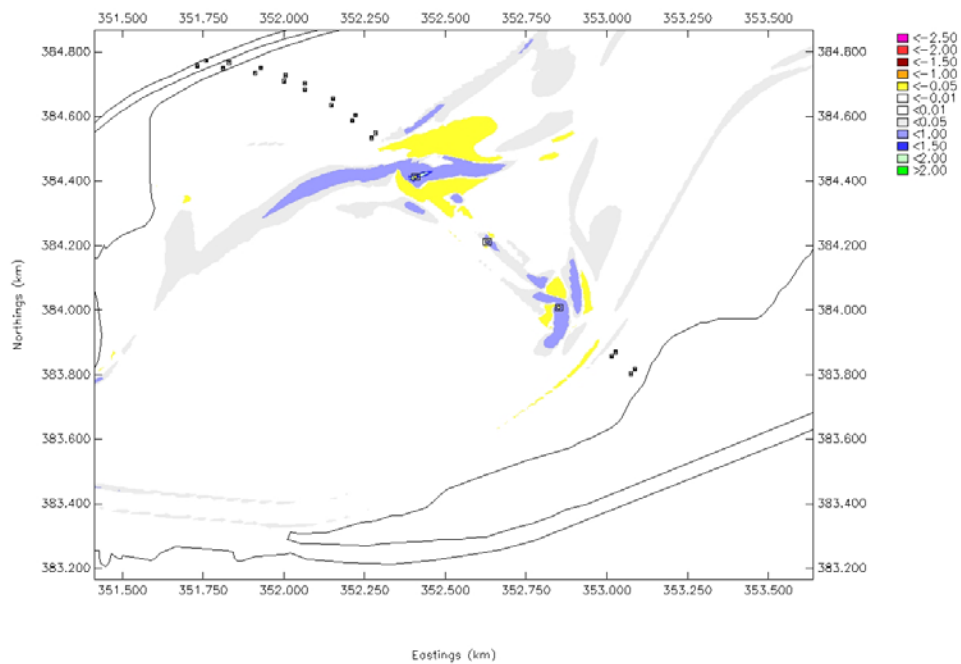


Figure 13b. Plot showing differences in sediment thickness between the scheme and the baseline case over a spring-neap period. Plotted using a coarser scale

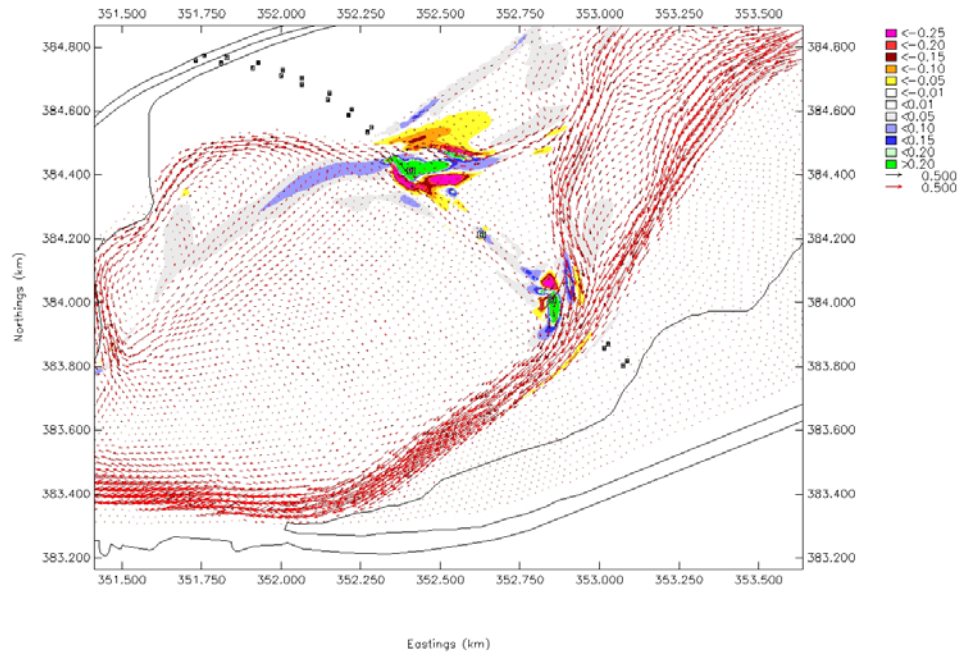


Figure 14a. Plot showing the tidal residuals for the baseline case and scheme

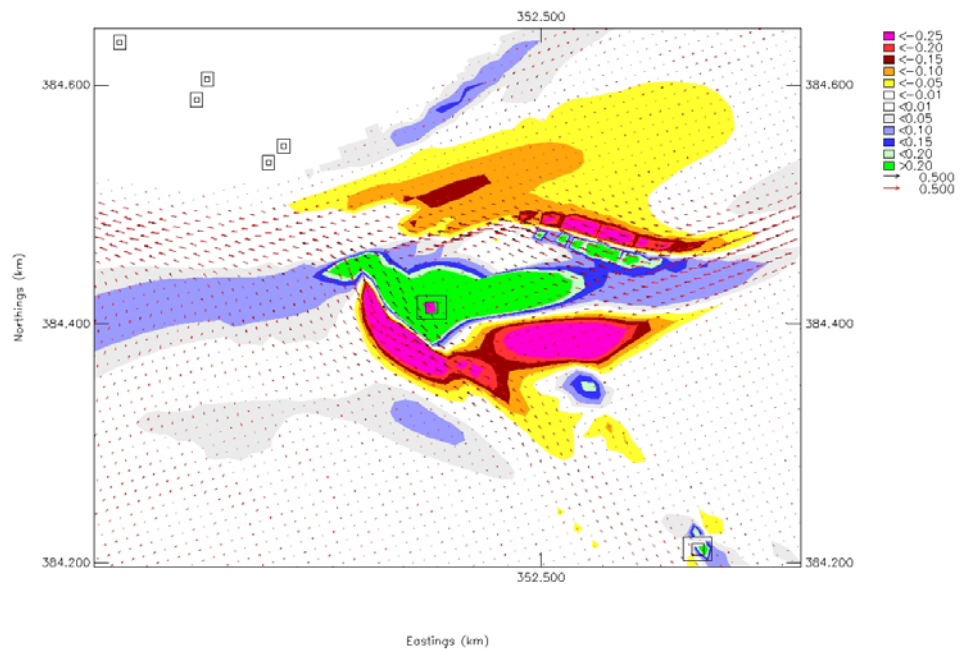


Figure 14b. Plot showing the tidal residuals for the baseline case and scheme in close up around the north bridge tower




ABP Marine Environmental Research Ltd
Suite B, Waterside House
Town Quay
Southampton
Hampshire SO14 2AQ

Tel: +44 (0)23 8071 1840
Fax: +44 (0)23 8071 1841
Email: enquiries@abpmer.co.uk

www.abpmer.co.uk





Gifford & Partners

Additional Modelling - Mersey Gateway

Technical Note C: Flat Bed Morphological Modelling

Date: December 2005

Project Ref: R/3411/4

Report No: R.1241c

mer
marine environmental research

Gifford & Partners

Additional Modelling - Mersey Gateway Technical Note C: Flat Bed Morphological Modelling

Date: December 2005

Project Ref: R/3411/4

Report No: R.1241c

© ABP Marine Environmental Research Ltd

Version	Details of Change	Authorised By	Date
1	Draft for Comment	J M Harris	9/12/2005
2	Final	J M Harris	20/12/2005

Document Authorisation		Signature	Date
Project Manager:	J M Harris	<i>John Harris</i>	<i>20/12/2005</i>
Quality Manager:	R H Swift	<i>Richard Swift</i>	<i>19/01/2006</i>
Project Director:	W S Cooper	<i>W. Cooper</i>	<i>10-1-06</i>

ABP Marine Environmental Research Ltd
Suite B, Waterside House
Town Quay
SOUTHAMPTON
Hampshire
SO14 2AQ



Tel: +44(0)23 8071 1840
Fax: +44(0)23 8071 1841
Web: www.abpmer.co.uk
Email: enquires@abpmer.co.uk



INVESTOR IN PEOPLE

Summary

This technical note describes the flat bed morphological simulations undertaken as part of the additional modelling studies carried out for Phase II of the Mersey Gateway Project. The principal aim of these tests was to simulate channel formation in the upper estuary with and without bridge towers in place and to observe differences in predicted channel formation.

This report is one of a series of five Technical Notes (R1241a to R.1241e):

- Technical Note A: Residual Modelling - Stage I;
- Technical Note B: Residual Modelling - Stage II;
- Technical Note C: Flat Bed Morphological Modelling;
- Technical Note D: Real Hydrograph Modelling; and
- Technical Note E: Phase Differences.

From all the tests undertaken the following key conclusions are drawn:

- For the 10m diameter structures the model results are very similar to those obtained with no structure in place (compare Figure 12f with Figure 3f). This implies that the impact of the proposed bridge scheme will be small and localised. In addition, the placing of structures of this size and number should not lead to fixing of the channel.
- The results from these model tests showed that the daily variability in channel form and position observed in nature cannot be readily reproduced in models of this type regardless of the forcing used.
- Sediment type does not appear to be a primary driver in the formation of the channels, although in combination with other drivers such as fluvial flow and tidal conditions there will be some influence in the smaller-scale channel dynamics.
- In general the model appears capable of reproducing the gross features of the upper estuary. This also implies that the general features of the system are dictated by the tidal flows.
- The sensitivity of the model to the value of the initial depth of sediment used in the simulation would suggest that the underlying geology is a key parameter in determining the form and position that channels take.

Additional Modelling - Mersey Gateway Technical Note C: Flat Bed Morphological Modelling

Contents

	Page
Summary	i
1. Introduction	1
2. Methodology	1
3. Results	2
4. Discussion	4
5. Conclusions	5
6. References	5

Tables

1. Baseline runs	2
2. Scheme runs	2

Figures

1.	Curvilinear model grid for the Mersey Estuary	7
2.	Initial starting bathymetry.....	7
3a.	Bathymetric change after 1 month for 150µm sediment, using a real tidal time-series driver and a constant mean annual fluvial flow	8
3b.	Bathymetric change after 2 months for 150µm sediment, using a real tidal time-series driver and a constant mean annual fluvial flow	8
3c.	Bathymetric change after 3 months for 150µm sediment, using a real tidal time-series driver and a constant mean annual fluvial flow	9
3d.	Bathymetric change after 4 months for 150µm sediment, using a real tidal time-series driver and a constant mean annual fluvial flow	9
3e.	Bathymetric change after 5 months for 150µm sediment, using a real tidal time-series driver and a constant mean annual fluvial flow	10
3f.	Bathymetric change after 6 months for 150µm sediment, using a real tidal time-series driver and a constant mean annual fluvial flow	10
4a.	Bathymetric change after 1 month for 100µm sediment, using a real tidal time-series driver and a constant mean annual fluvial flow	11
4b.	Bathymetric change after 2 months for 100µm sediment, using a real tidal time-series driver and a constant mean annual fluvial flow	11
4c.	Bathymetric change after 3 months for 100µm sediment, using a real tidal time-series driver and a constant mean annual fluvial flow	12
4d.	Bathymetric change after 4 months for 100µm sediment, using a real tidal time-series driver and a constant mean annual fluvial flow	12
4e.	Bathymetric change after 5 months for 100µm sediment, using a real tidal time-series driver and a constant mean annual fluvial flow	13
4f.	Bathymetric change after 6 months for 100µm sediment, using a real tidal time-series driver and a constant mean annual fluvial flow	13
5a.	Bathymetric change after 1 month for 64µm sediment, using a real tidal time-series driver and a constant mean annual fluvial flow	14
5b.	Bathymetric change after 2 months for 64µm sediment, using a real tidal time-series driver and a constant mean annual fluvial flow	14
5c.	Bathymetric change after 3 months for 64µm sediment, using a real tidal time-series driver and a constant mean annual fluvial flow	15
5d.	Bathymetric change after 4 months for 64µm sediment, using a real tidal time-series driver and a constant mean annual fluvial flow	15

5e.	Bathymetric change after 5 months for 64µm sediment, using a real tidal time-series driver and a constant mean annual fluvial flow	16
5f.	Bathymetric change after 6 months for 64µm sediment, using a real tidal time-series driver and a constant mean annual fluvial flow	16
6a.	Bathymetric change after 1 month for 300µm sediment, using a real tidal time-series driver and a constant mean annual fluvial flow	17
6b.	Bathymetric change after 2 months for 300µm sediment, using a real tidal time-series driver and a constant mean annual fluvial flow	17
6c.	Bathymetric change after 3 months for 300µm sediment, using a real tidal time-series driver and a constant mean annual fluvial flow	18
6d.	Bathymetric change after 4 months for 300µm sediment, using a real tidal time-series driver and a constant mean annual fluvial flow	18
6e.	Bathymetric change after 5 months for 300µm sediment, using a real tidal time-series driver and a constant mean annual fluvial flow	19
6f.	Bathymetric change after 6 months for 300µm sediment, using a real tidal time-series driver and a constant mean annual fluvial flow	19
7a.	Bathymetric change after 1 month for 150µm sediment, using harmonic tidal constituents and a constant mean annual fluvial flow	20
7b.	Bathymetric change after 2 months for 150µm sediment, using harmonic tidal constituents and a constant mean annual fluvial flow	20
7c.	Bathymetric change after 3 months for 150µm sediment, using harmonic tidal constituents and a constant mean annual fluvial flow	21
7d.	Bathymetric change after 4 months for 150µm sediment, using harmonic tidal constituents and a constant mean annual fluvial flow	21
7e.	Bathymetric change after 5 months for 150µm sediment, using harmonic tidal constituents and a constant mean annual fluvial flow	22
7f.	Bathymetric change after 6 months for 150µm sediment, using harmonic tidal constituents and a constant mean annual fluvial flow	22
8a.	Bathymetric change after 1 month for 150µm sediment, using harmonic tidal constituents and a daily mean fluvial flow	23
8c.	Bathymetric change after 2 months for 150µm sediment, using harmonic tidal constituents and a daily mean fluvial flow	23
8d.	Bathymetric change after 3 months for 150µm sediment, using harmonic tidal constituents and a daily mean fluvial flow	24
8e.	Bathymetric change after 4 months for 150µm sediment, using harmonic tidal constituents and a daily mean fluvial flow	24

9a.	Bathymetric change after 15 days for 300µm sediment, using a real tidal time-series driver, a constant mean annual fluvial flow and an initial 4m depth of sediment	25
9b.	Bathymetric change after 1 month for 300µm sediment, using a real tidal time-series driver, a constant mean annual fluvial flow and an initial 4m depth of sediment	25
9c.	Bathymetric change after 2 months for 300µm sediment, using a real tidal time-series driver, a constant mean annual fluvial flow and an initial 4m depth of sediment	26
9d.	Bathymetric change after 3 months for 300µm sediment, using a real tidal time-series driver, a constant mean annual fluvial flow and an initial 4m depth of sediment	26
10a.	Bathymetric change after 15 days for 300µm sediment, using a real tidal time-series driver, a constant mean annual fluvial flow an initial 4m depth of sediment and an hourly wind speed and direction	27
10b.	Bathymetric change after 1 month for 300µm sediment, using a real tidal time-series driver, a constant mean annual fluvial flow an initial 4m depth of sediment and an hourly wind speed and direction	27
10c.	Bathymetric change after 2 months for 300µm sediment, using a real tidal time-series driver, a constant mean annual fluvial flow an initial 4m depth of sediment and an hourly wind speed and direction	28
10d.	Bathymetric change after 3 months for 300µm sediment, using a real tidal time-series driver, a constant mean annual fluvial flow an initial 4m depth of sediment and an hourly wind speed and direction	28
11a.	Bathymetric change after 1 month with three 80m x 80m structures in place for 150µm sediment, using a real tidal time-series driver and a constant mean annual fluvial flow	29
11b.	Bathymetric change after 2 months with three 80m x 80m structures in place for 150µm sediment, using a real tidal time-series driver and a constant mean annual fluvial flow	29
11c.	Bathymetric change after 3 months with three 80m x 80m structures in place for 150µm sediment, using a real tidal time-series driver and a constant mean annual fluvial flow	30
11d.	Bathymetric change after 4 months with three 80m x 80m structures in place for 150µm sediment, using a real tidal time-series driver and a constant mean annual fluvial flow	30
11e.	Bathymetric change after 5 months with three 80m x 80m structures in place for 150µm sediment, using a real tidal time-series driver and a constant mean annual fluvial flow	31

11f.	Bathymetric change after 6 months with three 80m x 80m structures in place for 150µm sediment, using a real tidal time-series driver and a constant mean annual fluvial flow	31
12a.	Bathymetric change after 1 month with three 10m diameter structures in place (represented using added friction terms) for 150µm sediment, using a real tidal time-series driver and a constant mean annual fluvial flow.....	32
12b.	Bathymetric change after 2 months with three 10m diameter structures in place (represented using added friction terms) for 150µm sediment, using a real tidal time-series driver and a constant mean annual fluvial flow.....	32
12c.	Bathymetric change after 3 months with three 10m diameter structures in place (represented using added friction terms) for 150µm sediment, using a real tidal time-series driver and a constant mean annual fluvial flow.....	33
12d.	Bathymetric change after 4 months with three 10m diameter structures in place (represented using added friction terms) for 150µm sediment, using a real tidal time-series driver and a constant mean annual fluvial flow.....	33
12e.	Bathymetric change after 5 months with three 10m diameter structures in place (represented using added friction terms) for 150µm sediment, using a real tidal time-series driver and a constant mean annual fluvial flow.....	34
12f.	Bathymetric change after 1 month with three 10m diameter structures in place (represented using added friction terms) for 150µm sediment, using a real tidal time-series driver and a constant mean annual fluvial flow.....	34

1. Introduction

This technical note describes the flat bed morphological simulations undertaken as part of the additional modelling studies carried out for Phase II of the Mersey Gateway Project. The principal aim of these tests was to simulate channel formation in the upper estuary with and without bridge towers in place and to observe differences in predicted channel formation.

To undertake this modelling work a relatively coarse grid model has been used. This is primarily to allow longer time-scale simulations to be undertaken within a reasonable time span. Figure 1 shows the model grid used in the study.

The process of meandering of tidal channels is a relatively poorly studied subject despite the fact that meandering is a common feature of tidal environments. Solari *et al.* (2002) report that recent observational evidence suggests that meander wavelength scales with channel width, which would also imply that the process of meander formation must arise from the effect of secondary flows driven by some planimetric instability similar to that observed in rivers. In natural tidal basins channel meandering is a continuous process. If there is available space the meanders have a tendency to grow. During this process of growth the channel length increases and energy losses due to friction become more important (Dronkers, 2005).

2. Methodology

The bathymetric and LIDAR surveys undertaken in the Mersey for 2002 were used as the starting point for this modelling study. Upstream of Runcorn the bathymetry was flattened (excluding principal hard points such as quay walls) but maintaining the general channel slope along the length of this upstream section to the weir at Westy (Figure 2).

A series of model runs were undertaken for the 'baseline' case, that is the flattened bathymetry but with no bridge towers in place. The morphology was allowed to develop over a year. Different model drivers and combination of model drivers were tried to investigate the sensitivity of the model. The combination of drivers used in the baseline tests is shown in Table 1.

For the bridge tower scenario two tests were undertaken (see Table 2). One with the bridge towers represented as solid structures and the other represented as added friction. The initial run (run 1s) represents an extreme scenario as the three towers each occupy a single grid cell in the model making them of the order of 80m in diameter. An 8 times amplification of their actual proposed size. The second test (run 2s) puts the structures in at their actual size, but uses added friction terms to represent them.

Table 1. Baseline runs

Run No.	Sediment Type	Tidal Boundary	Fluvial Flow	Wind	Initial Sediment Depth (m)
1	Sand - 150µm	Harmonic constituents	Constant mean annual	None	1
2	Sand - 150µm	Harmonic constituents	Mean daily	None	1
3	Sand - 150µm	Real time-series	Constant mean annual	None	1
4	Sand - 150µm	Real time-series	Mean daily	None	1
5	Sand - 100µm	Real time-series	Constant mean annual	None	1
6	Sand - 64µm	Real time-series	Constant mean annual	None	1
7	Sand - 300µm	Real time-series	Constant mean annual	None	1
8	Sand - 300µm	Real time-series	Constant mean annual	None	4
9	Sand - 300µm	Real time-series	Constant mean annual	Real (hourly)	4

Table 2. Scheme runs

Run No.	Sediment Type	Tidal Boundary	Fluvial Flow	Wind	Initial Sediment Depth (m)
1s	Sand - 150µm	Real time-series	Constant mean annual	None	1
2s	Sand - 150µm	Real time-series	Constant mean annual	None	1

3. Results

The morphological model proved to be unstable for different model drivers and combination of drivers. This made comparison difficult for some of the scenarios tested. In general the model appears capable of reproducing the gross features of the upper estuary, but not the daily variations. Even using a range of non-linear driving conditions the model appears to want to develop a form of equilibrium channel the longitudinal shape of which is dictated to a large extent by the lateral boundaries making up the upper estuary.

Figures 3-6 show the variation in channel formation over several months for 150 μ m, 100 μ m, 64 μ m and 300 μ m sediment sizes, respectively. Overall, the difference in sediment size has little effect on the formation and position of the channels. The only difference is in the time required to form them. There are subtle differences between the morphology formed using the various sediments, but in general the patterns are identical. This would suggest that the sediment type is not a primary driver in the formation of the channels, although in combination with other drivers such as fluvial flow and tidal conditions there will be some influence in the smaller-scale channel dynamics.

Figure 7 shows the variation in channel formation over a 6 months period for 150 μ m sediment under a harmonically driven tidal boundary and a constant annual mean fluvial flow. Over the length of the simulation, the model shows the development of a single main channel. Initially a channel is formed in the location of the existing north channel observed in the real bathymetry. However, this channel does not develop and is eventually cut off. As was observed in the previous sediment runs, the model appears to develop an equilibrium form relatively quickly. There is no significant difference between the channel formed under these driving conditions and that formed using a real tidal time-series and shown in Figure 3.

Figure 8 shows the results for the model driven using harmonic boundary conditions and real mean daily flows over a 4 months period. The model proved to be unstable due primarily to the varying daily discharge. However, as previously the model shows the development of a single main channel and there is no significant difference between the channel formed under these driving conditions and that formed in the previous scenarios and shown in Figures 3 and 7.

Running the model with both real tidal conditions and real mean daily flows led to instabilities in the results limiting the data obtained to about a month of output. Therefore, these results have not been presented.

Figure 9 shows the results of a simulation using 300 μ m sediment, a real tidal time-series at the seaward boundary and a constant mean annual discharge at the upstream boundary. In addition, the initial depth of sediment was set at 4m. This compares with a 1m initial depth of sediment used in the other base scenarios. The ability to erode the sediment to a deeper depth gives a different set of channel profiles (compare with Figure 6). There is still a main single channel formed, however, initially channels are also formed along the south and north sides of the estuary. Towards Runcorn, the main channel is deeper and narrower than that formed previously. Interestingly, the formation of the channels towards the sides of the estuary shows some similarity to the existing situation. The imposition of a real hourly wind speed and direction on the model set up has no major impact on the model results (Figure 10).

Figures 11 and 12 show the results for the two tower scenario runs. Figure 11 has the towers represented as solid structures within the model grid thereby making them 8

times larger than the actual bridge scheme, whilst in Figure 12 the results show the model results for 10m diameter structures represented using added friction. An initial conclusion of these results is that the size of the structures placed in the system is important. After an identical simulation period the results for the 80m x 80m structures still show some impact within the channel. However, for the 10m diameter structures the model results are very similar to those obtained with no structure in place (compare Figure 12f with Figure 3f). From this it suggests that bridge piers of the width and number proposed under the current design, the likely impact will be small and localised.

It should also be noted though, that despite using a number of different random drivers (real tides, including atmospheric forcing, real discharges and real winds) in different combinations the morphological model continued to display a tendency to move to an equilibrium form that did not vary perceptibly over the time-scale of the simulation. This implies that the daily variability in channel form and position observed in nature cannot be readily reproduced in models of this type. Therefore, it would be of little benefit to run such models over a longer time-scale as the model is relatively insensitive to typical variations in forcing that occur in nature.

4. Discussion

A series of model runs were undertaken for a flattened bathymetry upstream of Runcorn to test the sensitivity of the morphological model to different forcing mechanisms. These were primarily undertaken for the 'baseline' case, which represented the upper estuary with no bridge structures in place. The results of these model tests showed that the daily variability in channel form and position observed in nature cannot be readily reproduced in models of this type.

However, the model showed the ability to reproduce the gross form of the upper estuary including the ability to form channels along the north and south sides of the estuary. The sensitivity of the model to the value of the initial depth of sediment used in the simulation would suggest that the underlying geology is a key parameter in determining the form and position that channels take. It is not possible to represent this aspect in the model to that level of detail. In addition, it would require detailed vertical profiles of the soil properties throughout the estuary as a whole.

The model wants to move towards an equilibrium form based on the forcing conditions and sediment properties applied. Once this profile has developed very little change occurs. Using typical forcing mechanisms, such as varying the wind speed and fluvial flow used in the model has little impact as stated above.

Imposing bridge structures within the initial flat bed bathymetry shows that the larger the impact on flow cross-sectional area the greater the impact on channel morphology.

In addition, for the 10m diameter structures, the channel forms independently of them with the simulation showing similar results with and without the towers in place.

5. Conclusions

Therefore, from all the tests undertaken the following key conclusions are drawn:

- For the 10m diameter structures the model results are very similar to those obtained with no structure in place (compare Figure 12f with Figure 3f). This implies that the impact of the proposed bridge scheme will be small and localised. In addition, the placing of structures of this size and number should not lead to fixing of the channel.
- The results from these model tests showed that the daily variability in channel form and position observed in nature cannot be readily reproduced in models of this type regardless of the forcing used.
- Sediment type does not appear to be a primary driver in the formation of the channels, although in combination with other drivers such as fluvial flow and tidal conditions there will be some influence in the smaller-scale channel dynamics.
- In general the model appears capable of reproducing the gross features of the upper estuary. This also implies that the general features of the system are dictated by the tidal flows.
- The sensitivity of the model to the value of the initial depth of sediment used in the simulation would suggest that the underlying geology is a key parameter in determining the form and position that channels take.

6. References

Dronkers, J. (2005). *Dynamics of Coastal Systems*. Advances Series on Ocean Engng., Vol. 25, World Scientific, 519pp.

Solari, L., Seminara, G., Lanzoni, S., Marani, M. and Rinaldo, A. (2002). Sand bars in tidal channels Part 2. Tidal meanders. *J. Fluid Mech.*, Vol. 451, pp. 203-238.

Figures

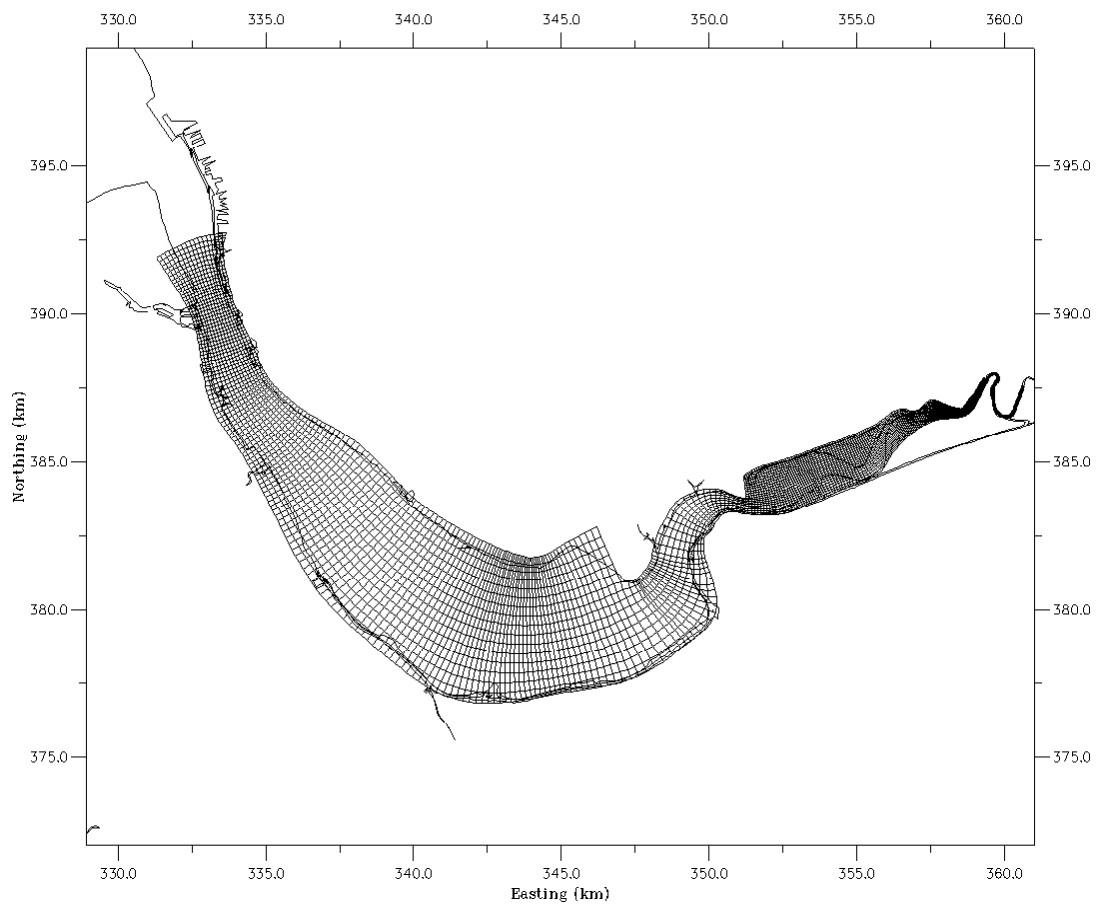


Figure 1. Curvilinear model grid for the Mersey Estuary

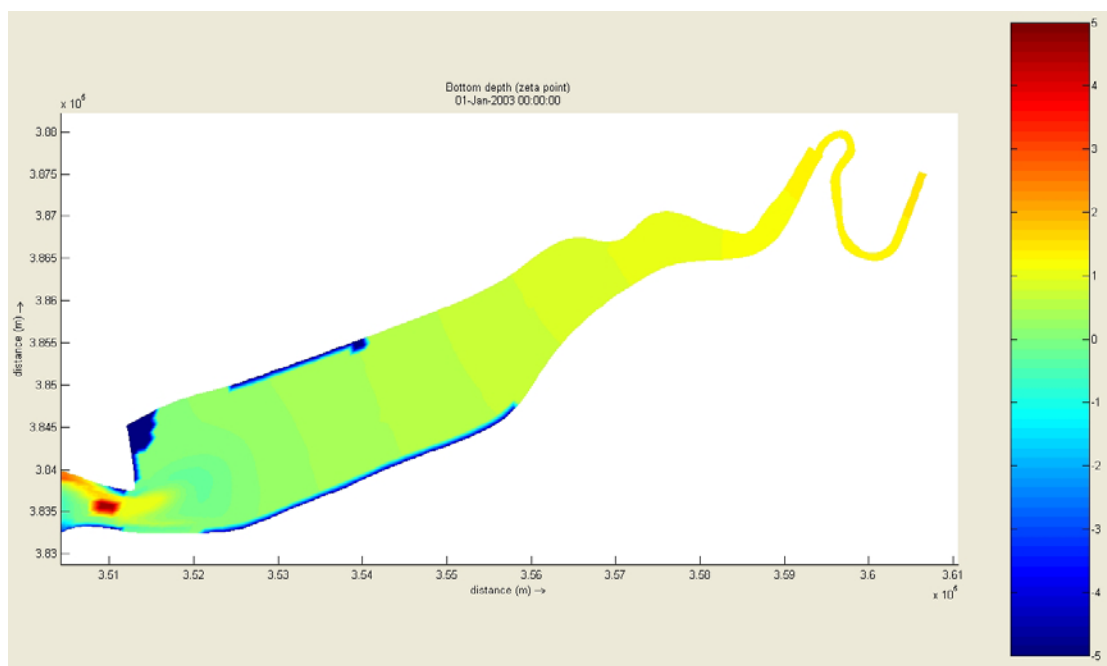


Figure 2. Initial starting bathymetry

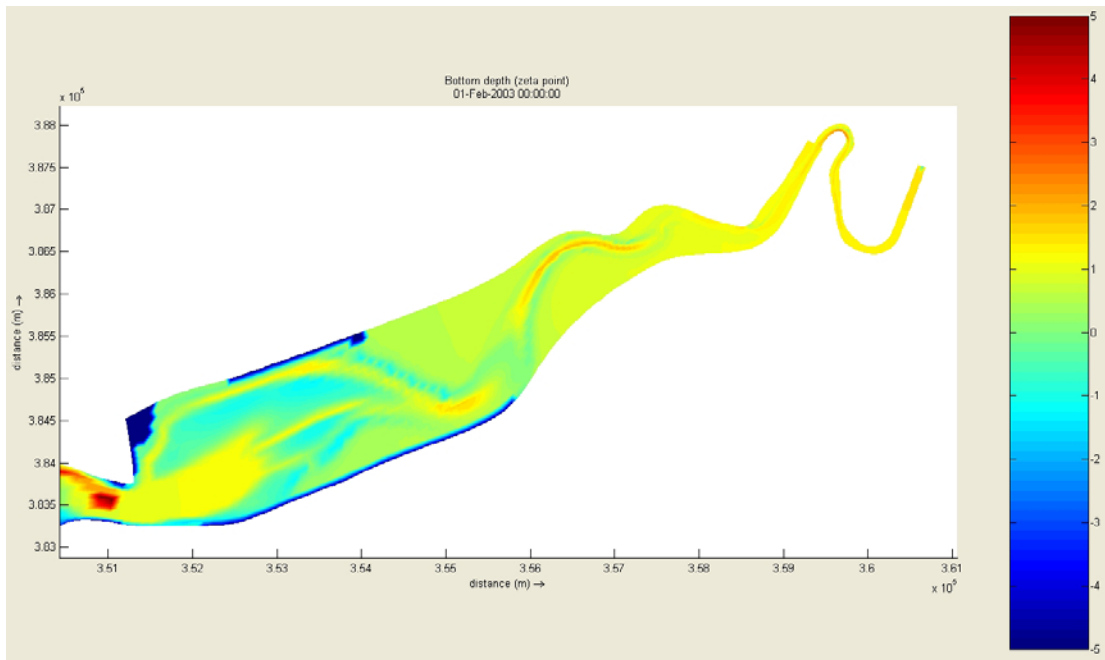


Figure 3a. Bathymetric change after 1 month for 150µm sediment, using a real tidal time-series driver and a constant mean annual fluvial flow

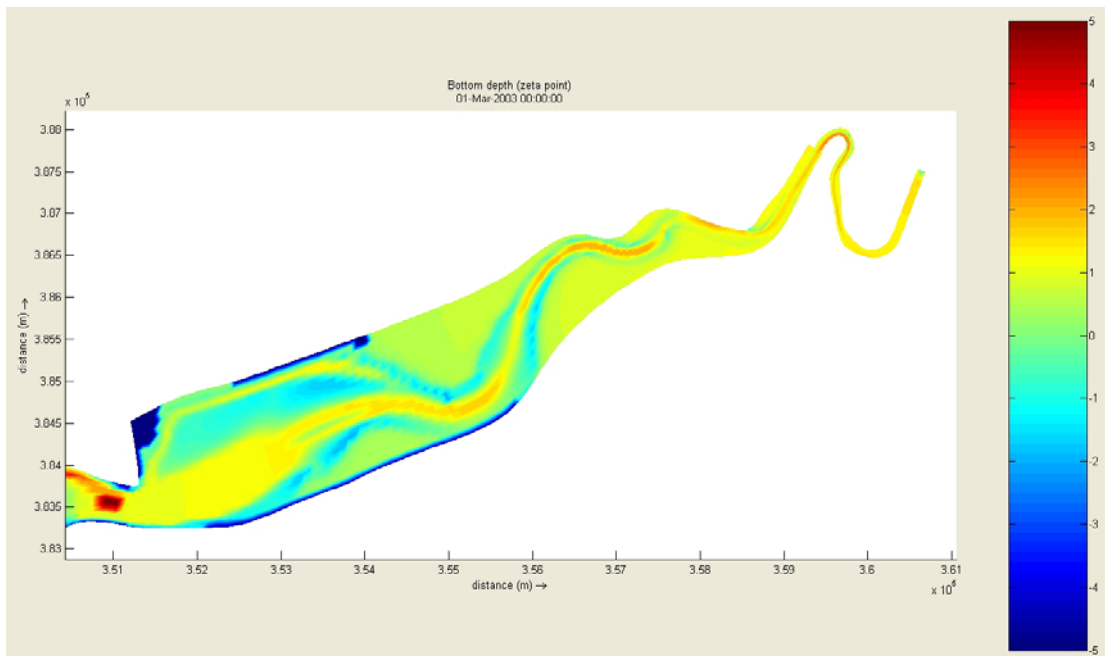


Figure 3b. Bathymetric change after 2 months for 150µm sediment, using a real tidal time-series driver and a constant mean annual fluvial flow

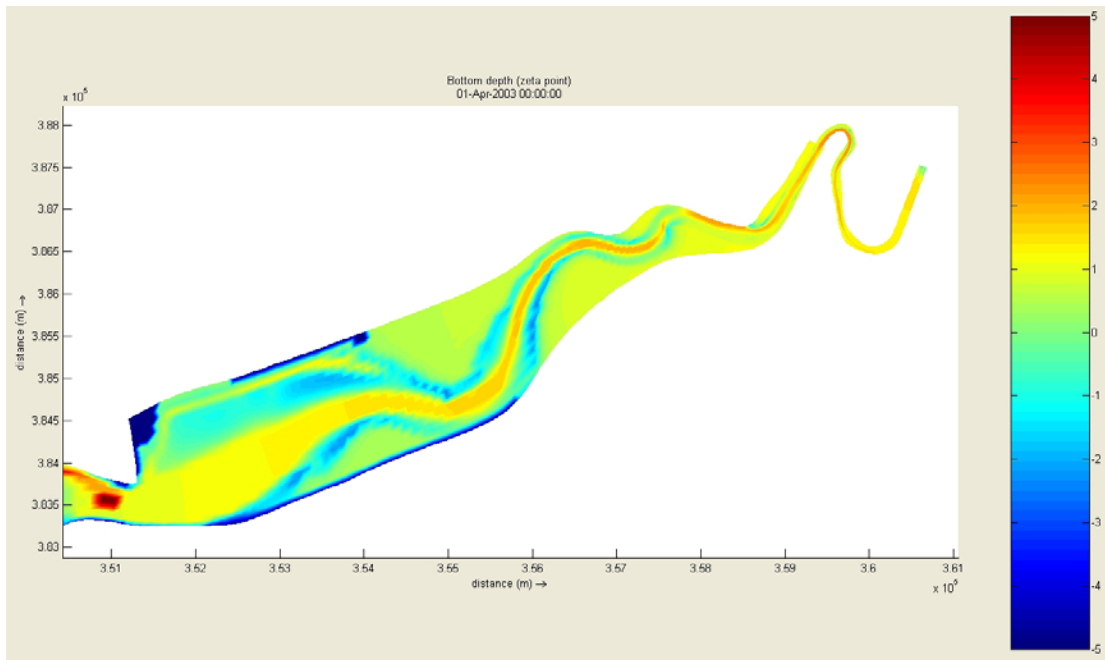


Figure 3c. Bathymetric change after 3 months for 150µm sediment, using a real tidal time-series driver and a constant mean annual fluvial flow

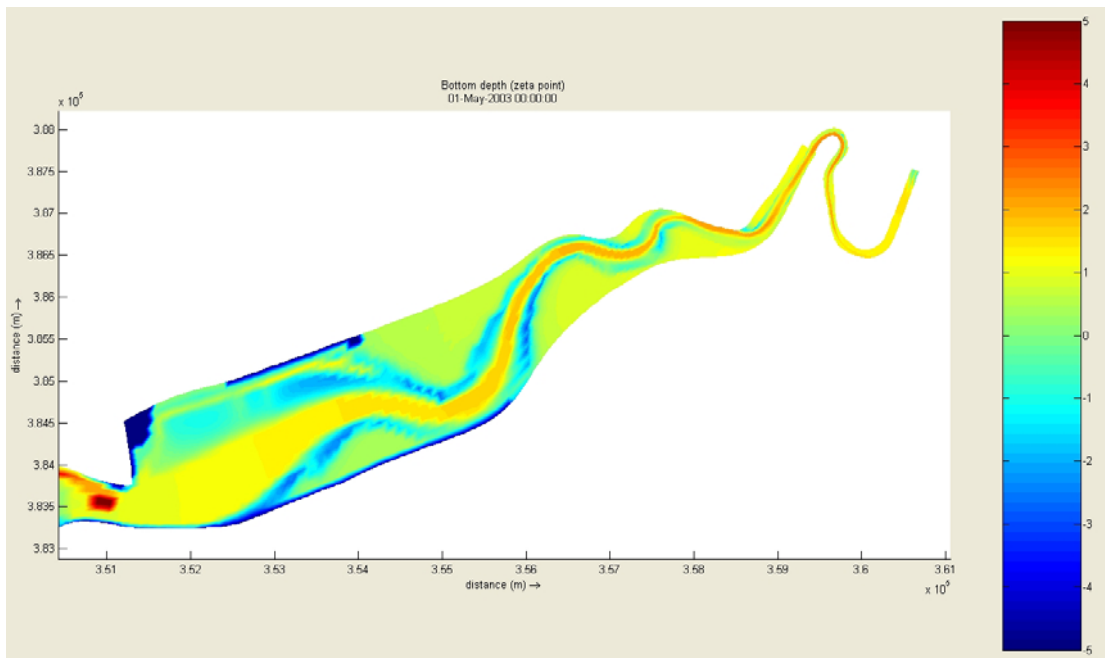


Figure 3d. Bathymetric change after 4 months for 150µm sediment, using a real tidal time-series driver and a constant mean annual fluvial flow

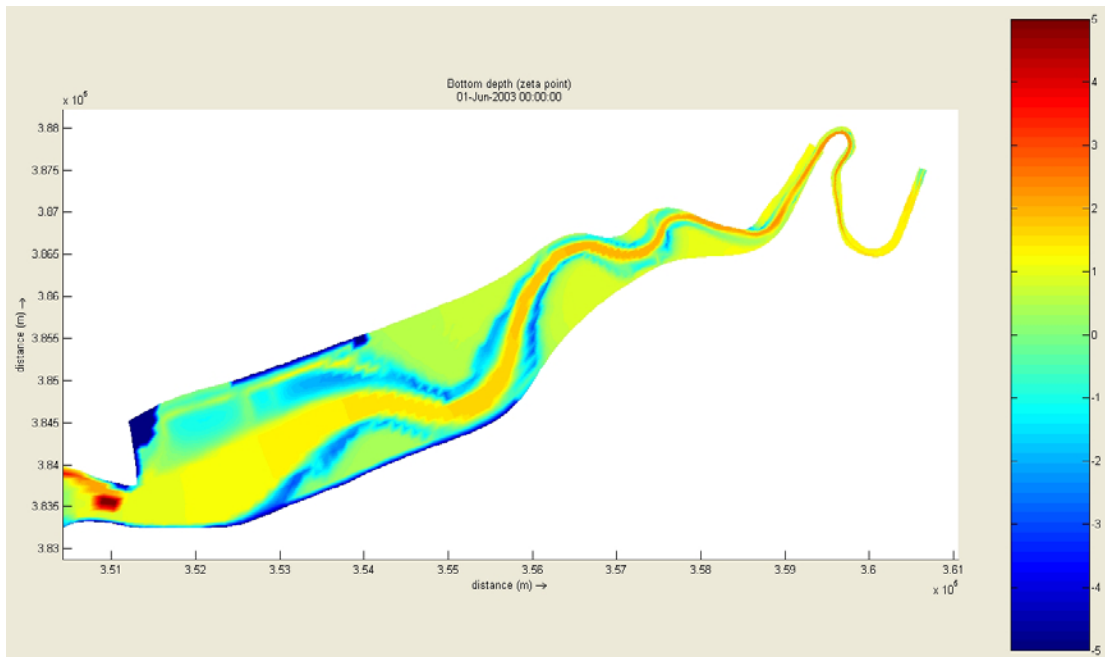


Figure 3e. Bathymetric change after 5 months for 150µm sediment, using a real tidal time-series driver and a constant mean annual fluvial flow

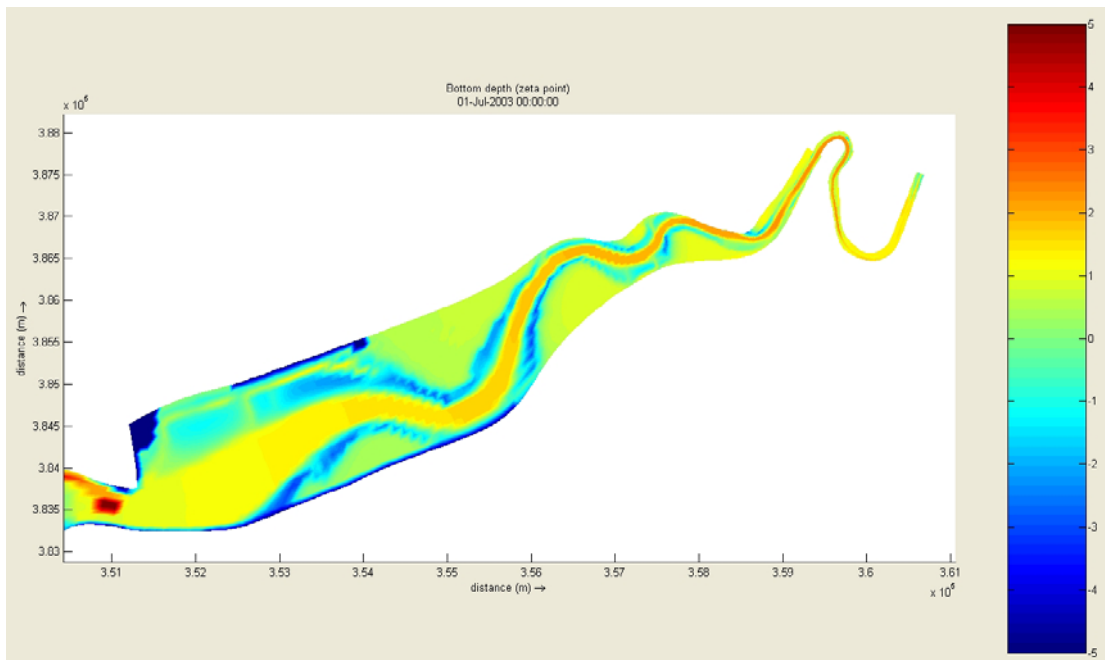


Figure 3f. Bathymetric change after 6 months for 150µm sediment, using a real tidal time-series driver and a constant mean annual fluvial flow

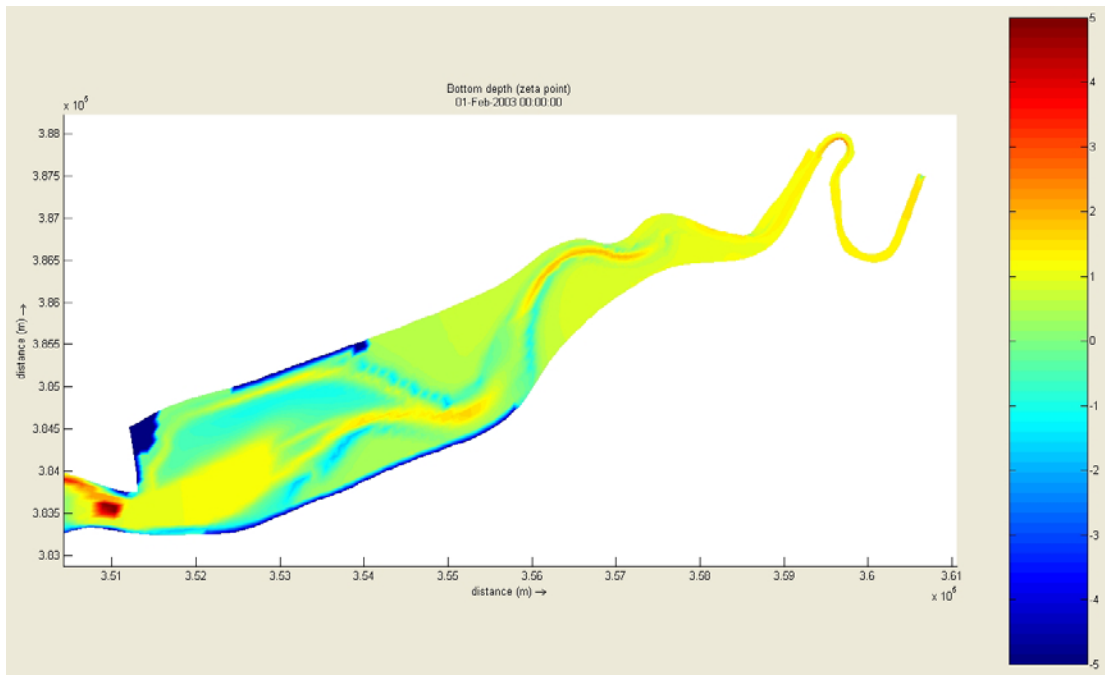


Figure 4a. Bathymetric change after 1 month for 100µm sediment, using a real tidal time-series driver and a constant mean annual fluvial flow

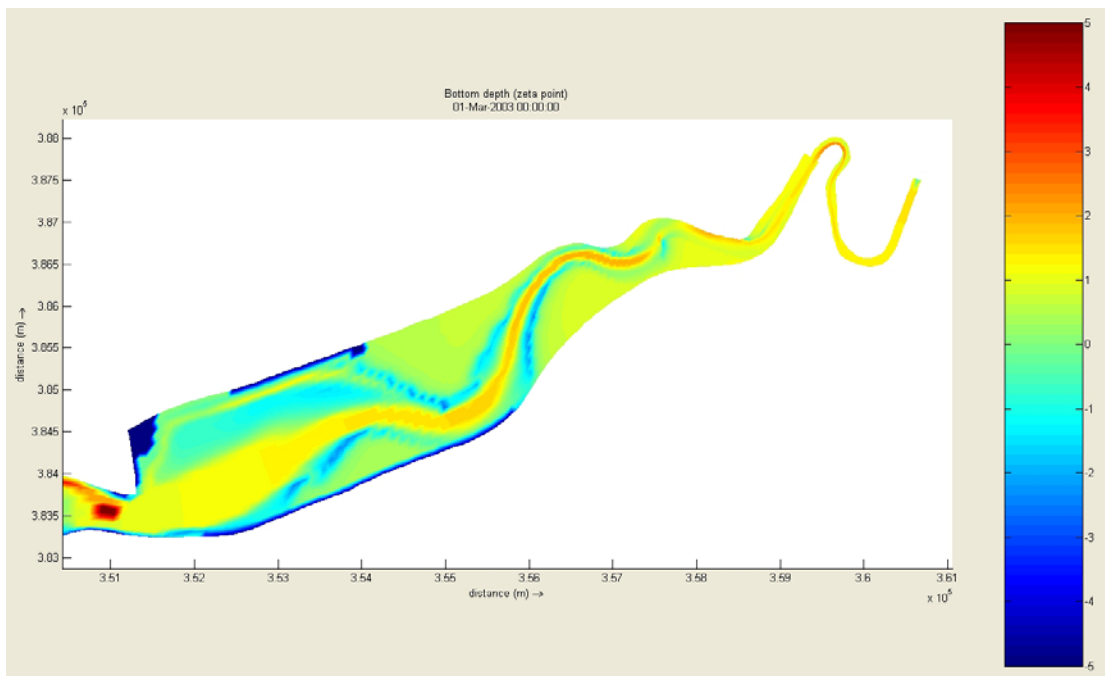


Figure 4b. Bathymetric change after 2 months for 100µm sediment, using a real tidal time-series driver and a constant mean annual fluvial flow

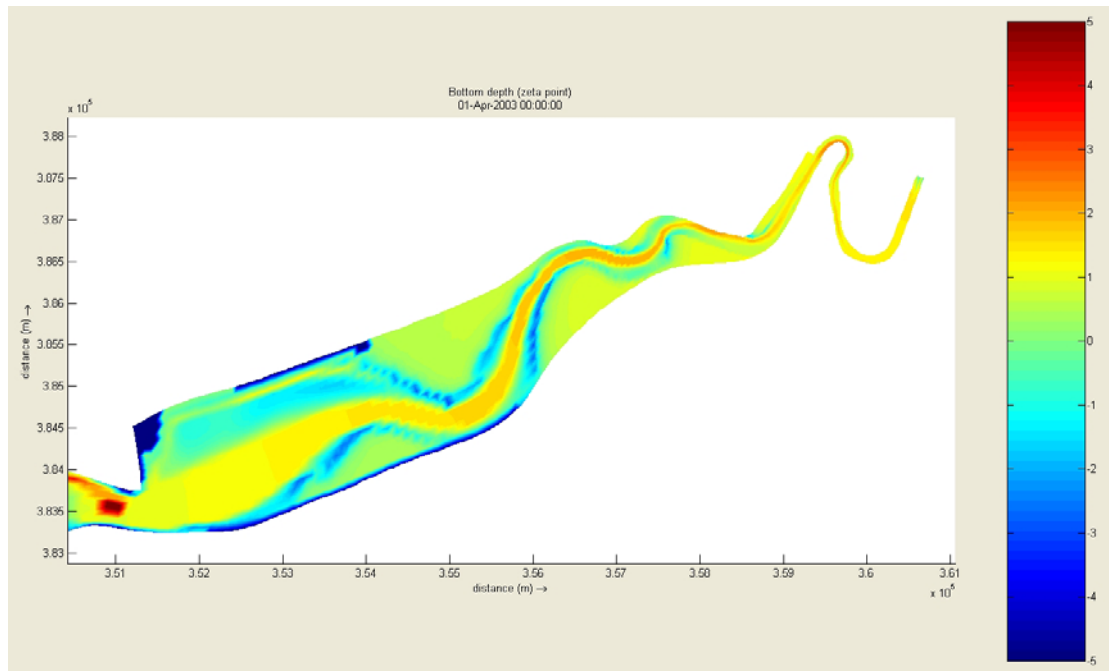


Figure 4c. Bathymetric change after 3 months for 100µm sediment, using a real tidal time-series driver and a constant mean annual fluvial flow

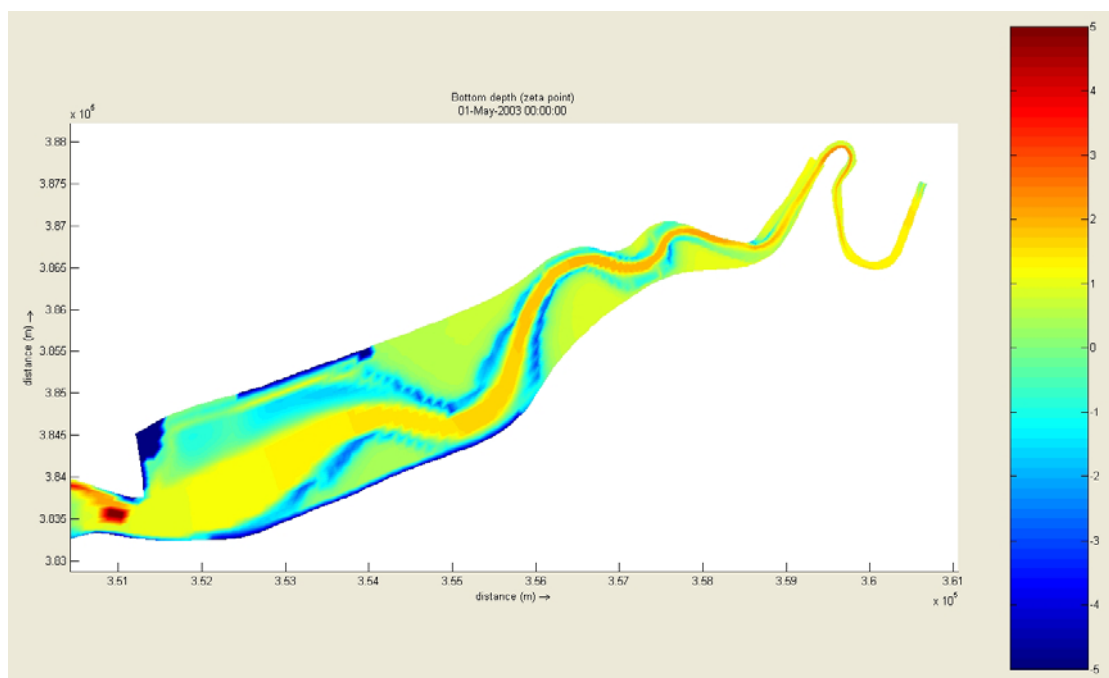


Figure 4d. Bathymetric change after 4 months for 100µm sediment, using a real tidal time-series driver and a constant mean annual fluvial flow

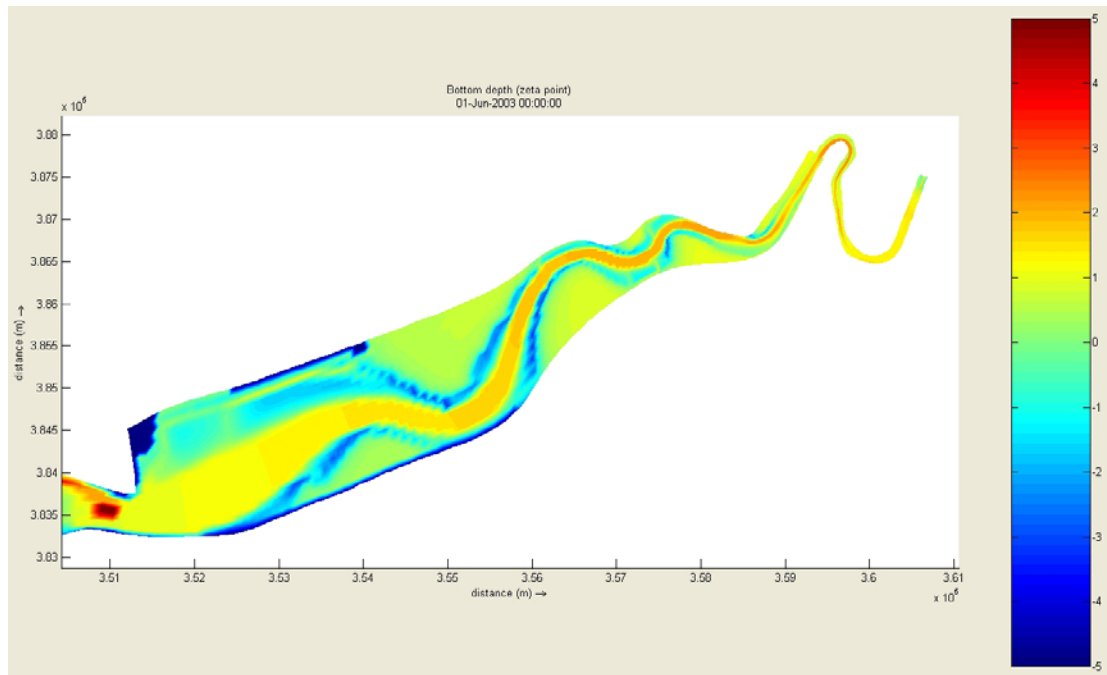


Figure 4e. Bathymetric change after 5 months for 100µm sediment, using a real tidal time-series driver and a constant mean annual fluvial flow

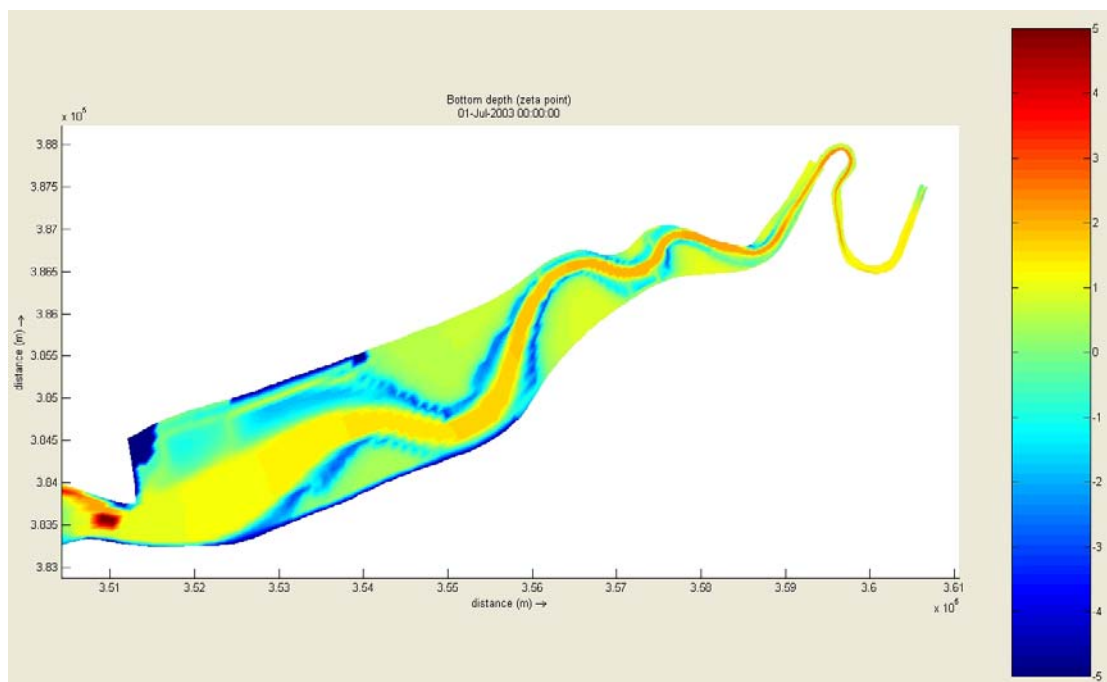


Figure 4f. Bathymetric change after 6 months for 100µm sediment, using a real tidal time-series driver and a constant mean annual fluvial flow

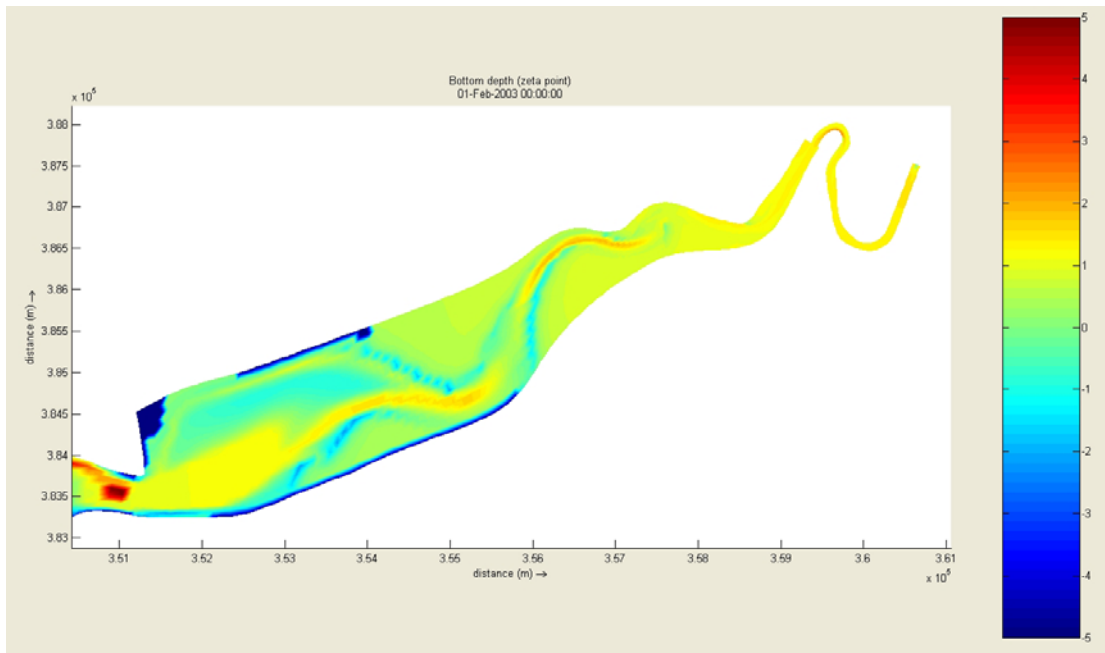


Figure 5a. Bathymetric change after 1 month for 64µm sediment, using a real tidal time-series driver and a constant mean annual fluvial flow

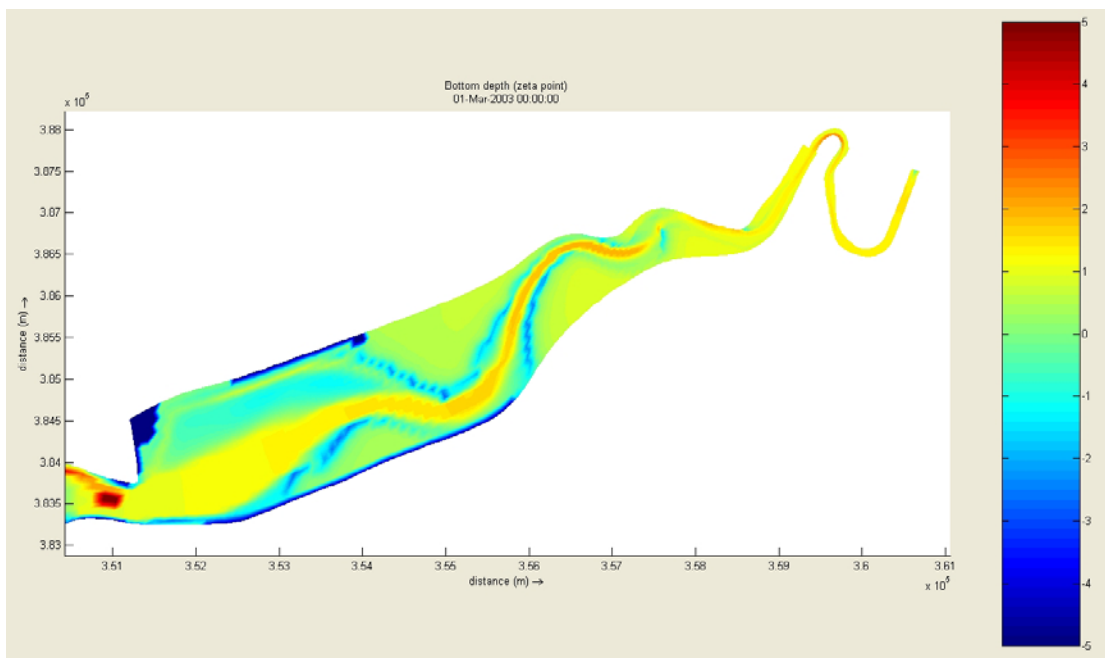


Figure 5b. Bathymetric change after 2 months for 64µm sediment, using a real tidal time-series driver and a constant mean annual fluvial flow

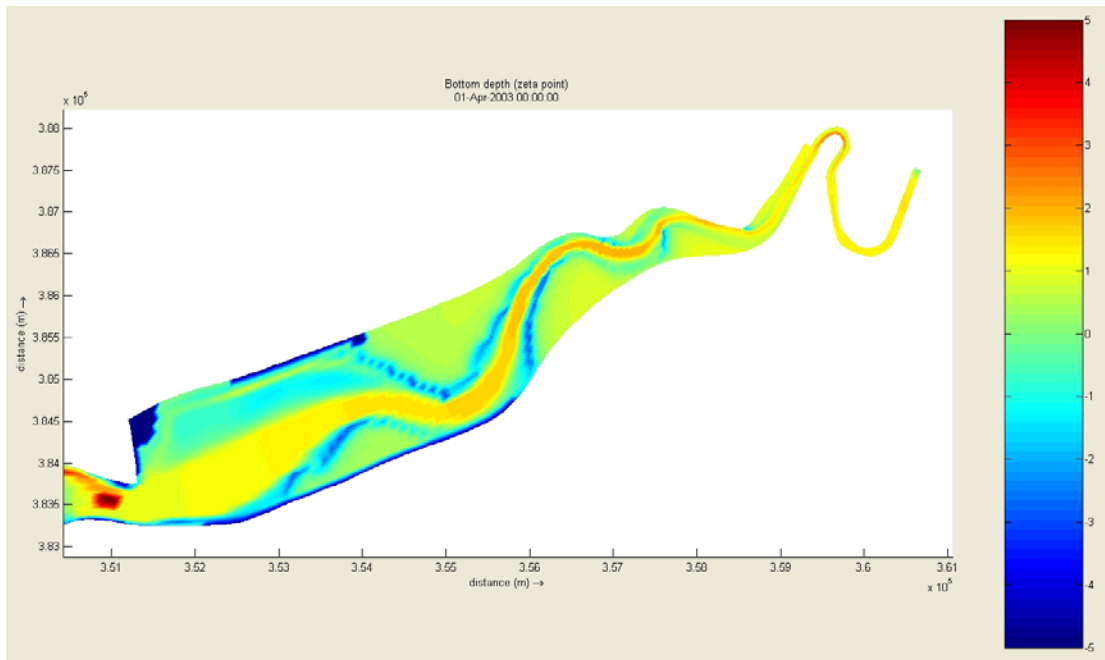


Figure 5c. Bathymetric change after 3 months for 64µm sediment, using a real tidal time-series driver and a constant mean annual fluvial flow

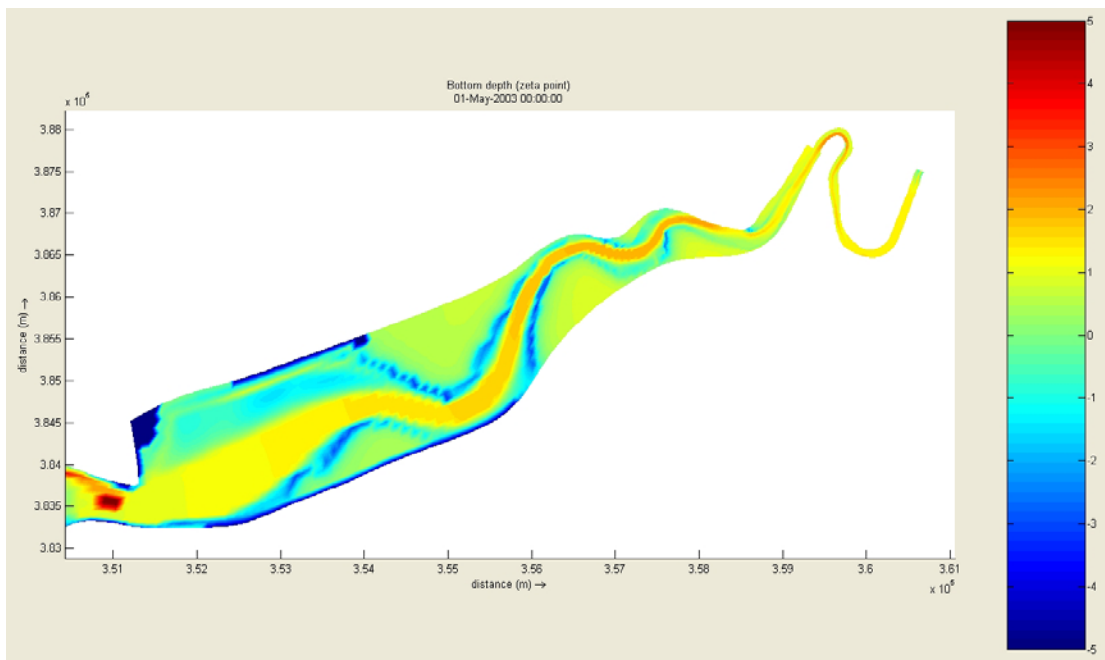


Figure 5d. Bathymetric change after 4 months for 64µm sediment, using a real tidal time-series driver and a constant mean annual fluvial flow

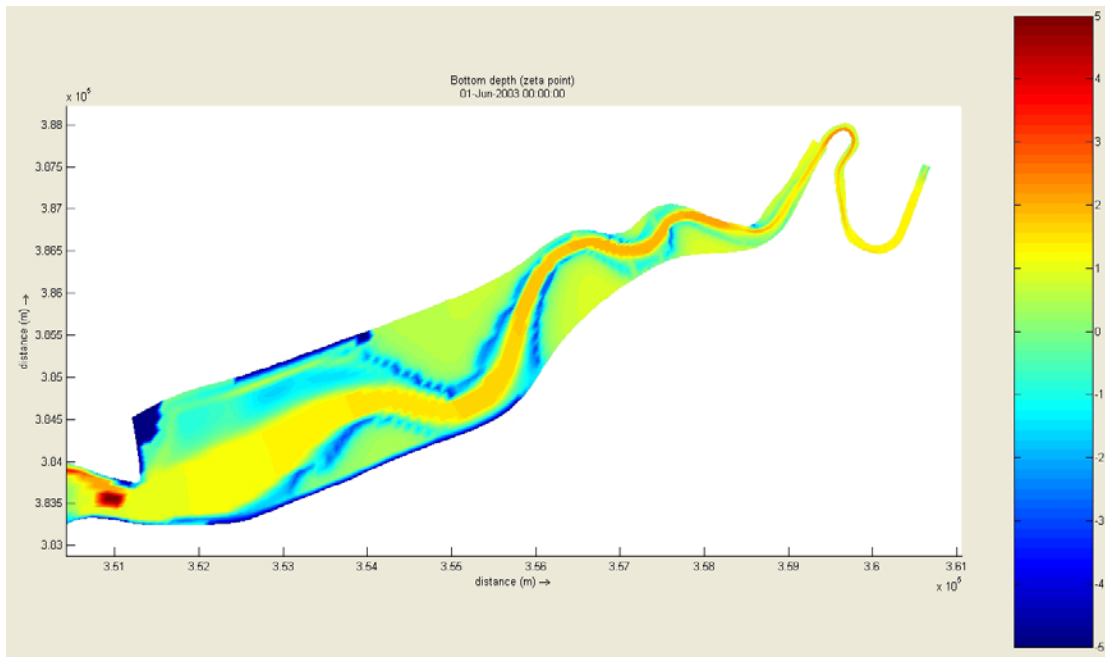


Figure 5e. Bathymetric change after 5 months for 64µm sediment, using a real tidal time-series driver and a constant mean annual fluvial flow

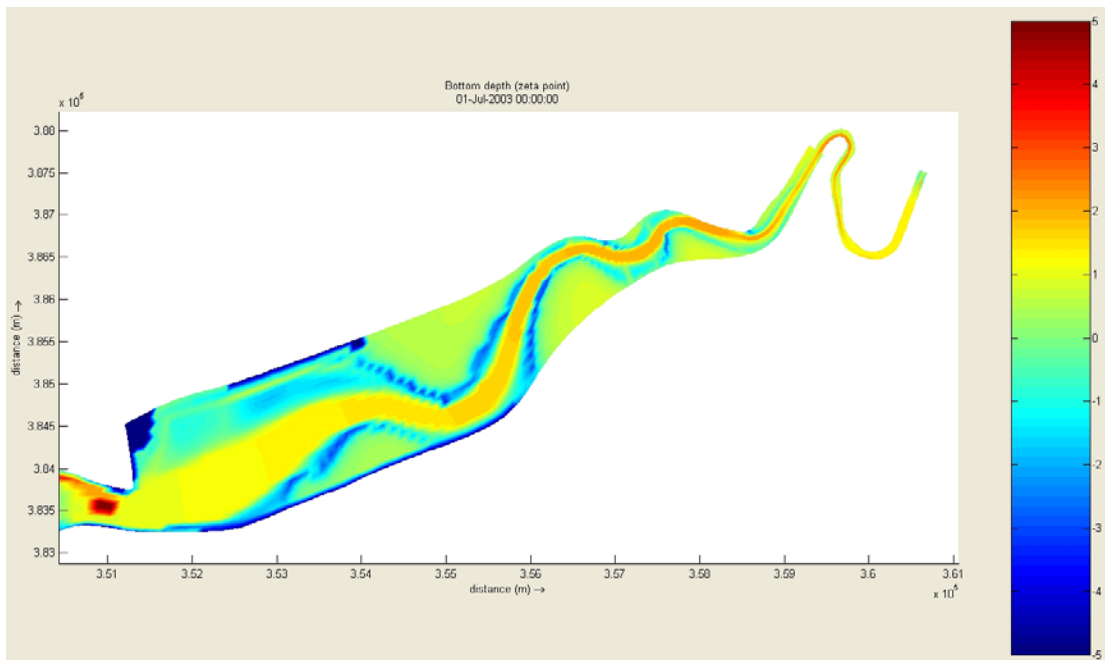


Figure 5f. Bathymetric change after 6 months for 64µm sediment, using a real tidal time-series driver and a constant mean annual fluvial flow

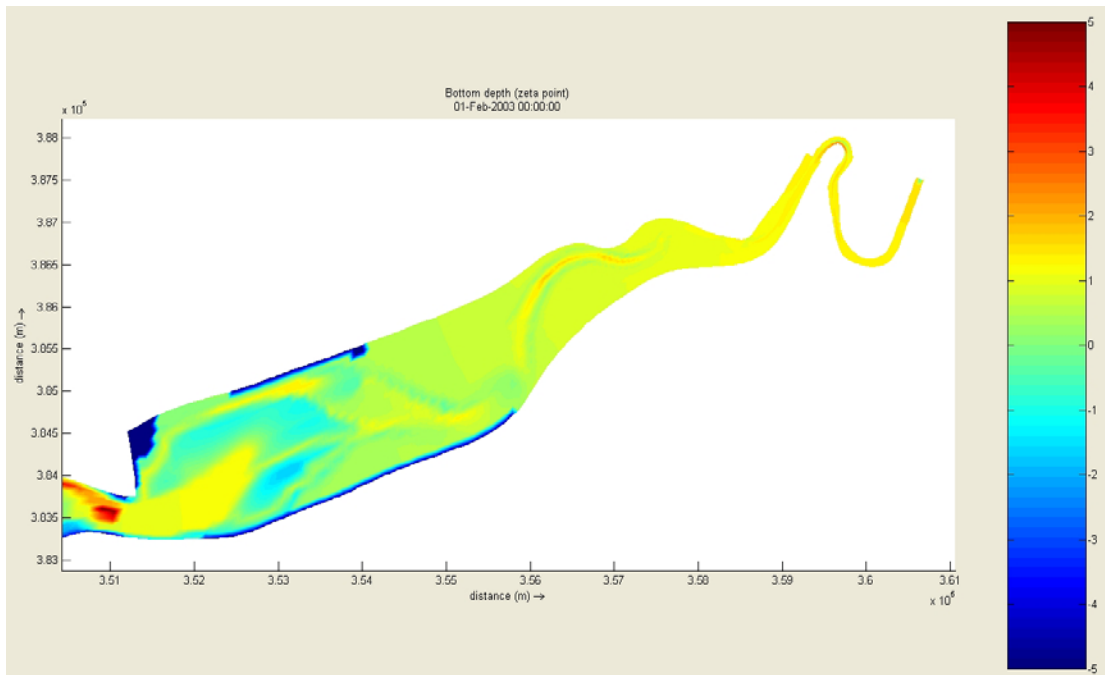


Figure 6a. Bathymetric change after 1 month for 300µm sediment, using a real tidal time-series driver and a constant mean annual fluvial flow

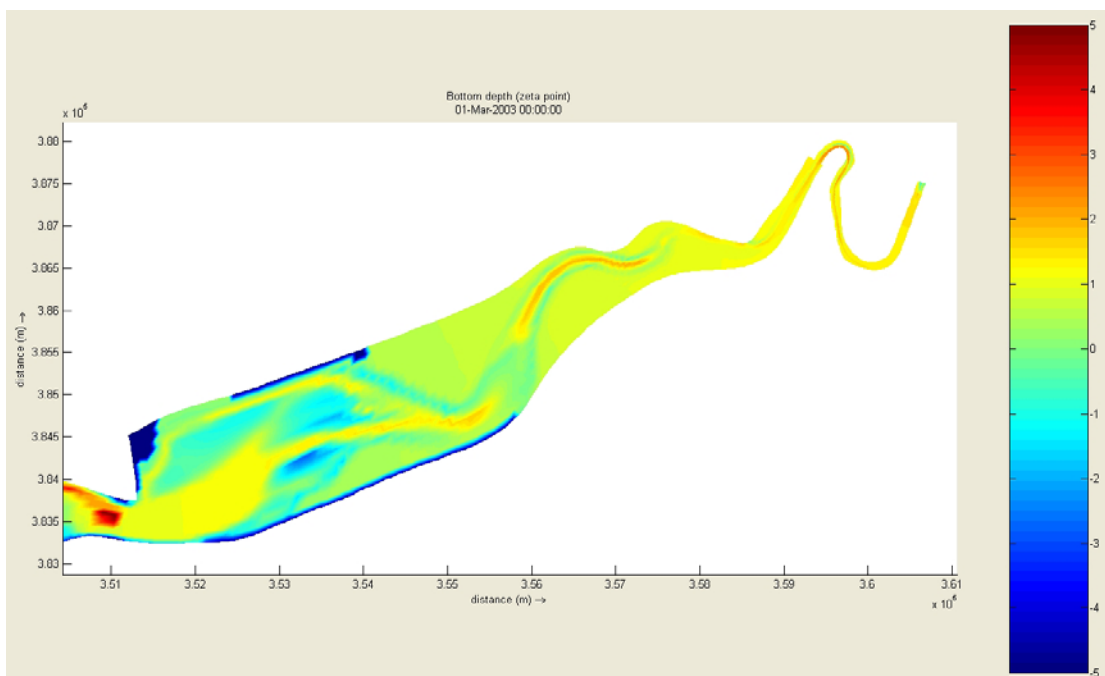


Figure 6b. Bathymetric change after 2 months for 300µm sediment, using a real tidal time-series driver and a constant mean annual fluvial flow

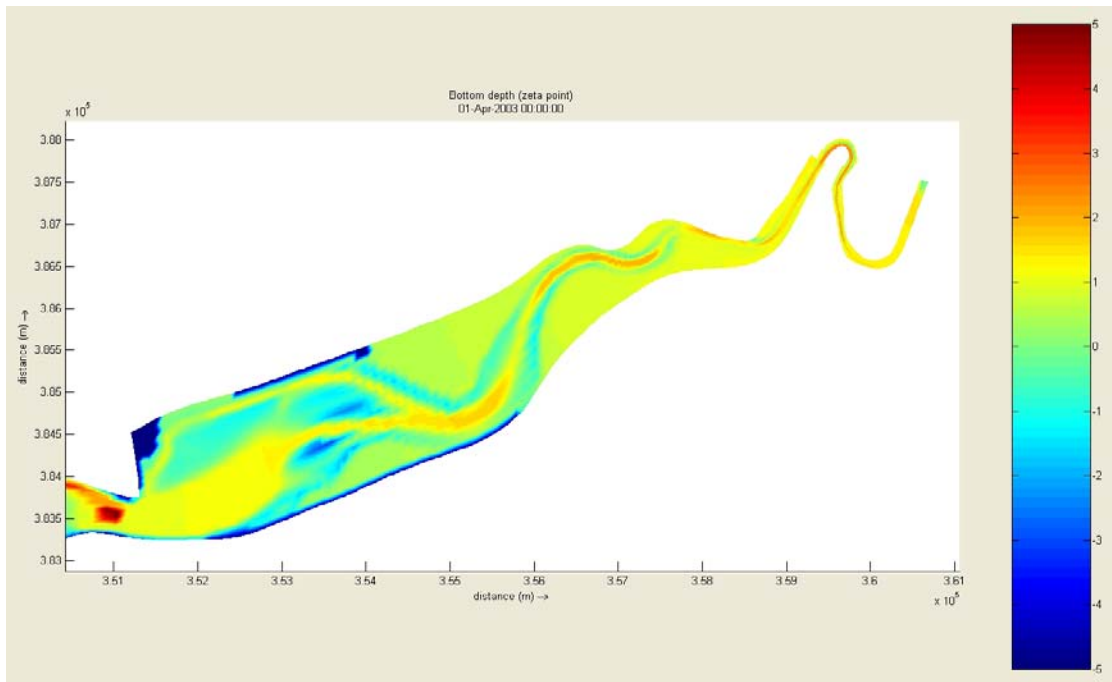


Figure 6c. Bathymetric change after 3 months for 300µm sediment, using a real tidal time-series driver and a constant mean annual fluvial flow

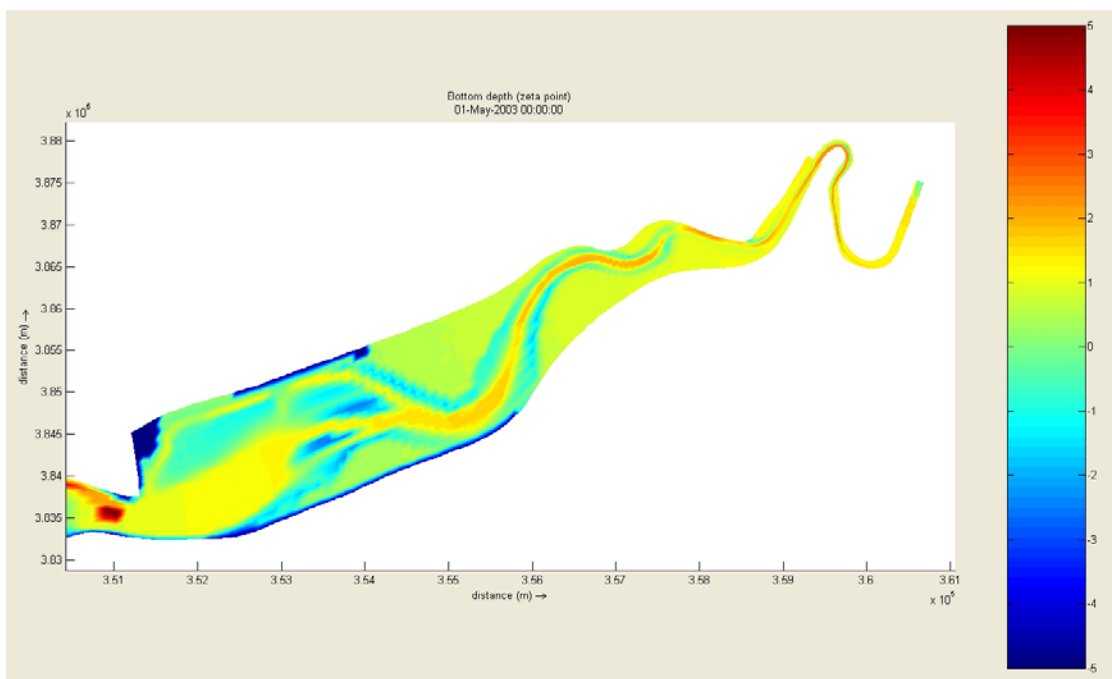


Figure 6d. Bathymetric change after 4 months for 300µm sediment, using a real tidal time-series driver and a constant mean annual fluvial flow

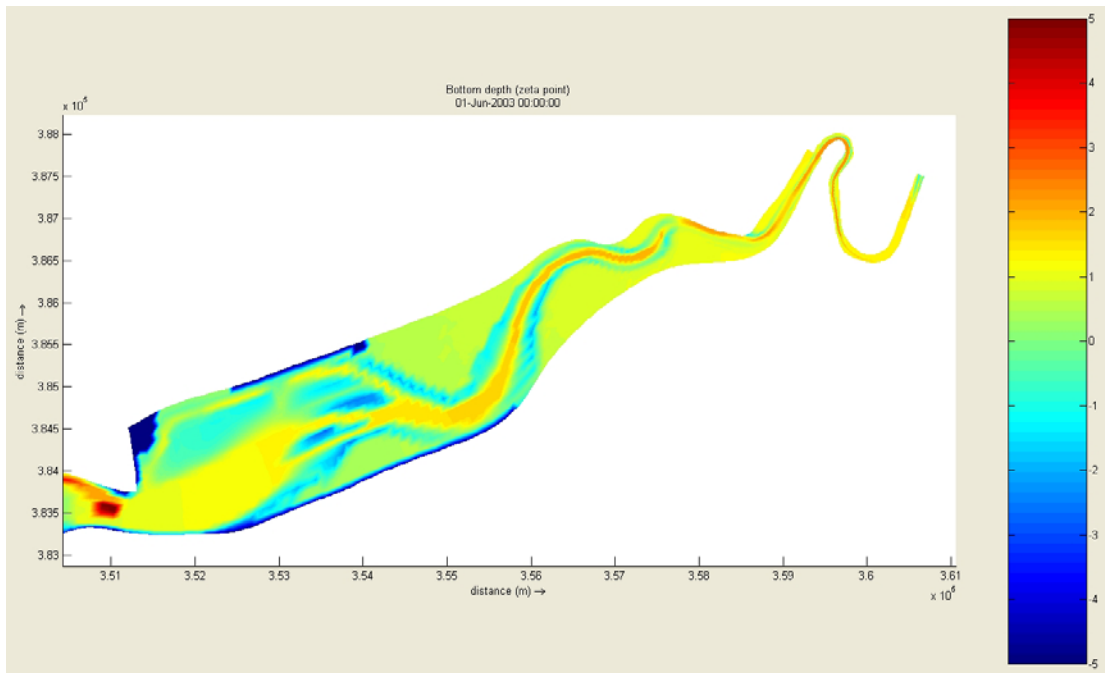


Figure 6e. Bathymetric change after 5 months for 300µm sediment, using a real tidal time-series driver and a constant mean annual fluvial flow

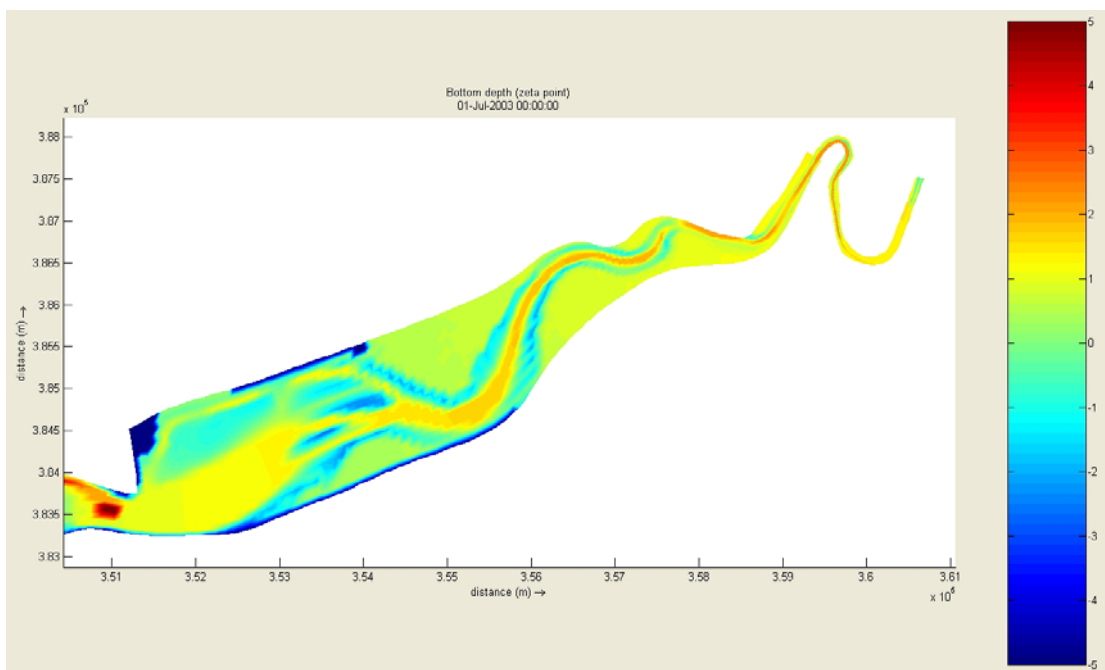


Figure 6f. Bathymetric change after 6 months for 300µm sediment, using a real tidal time-series driver and a constant mean annual fluvial flow

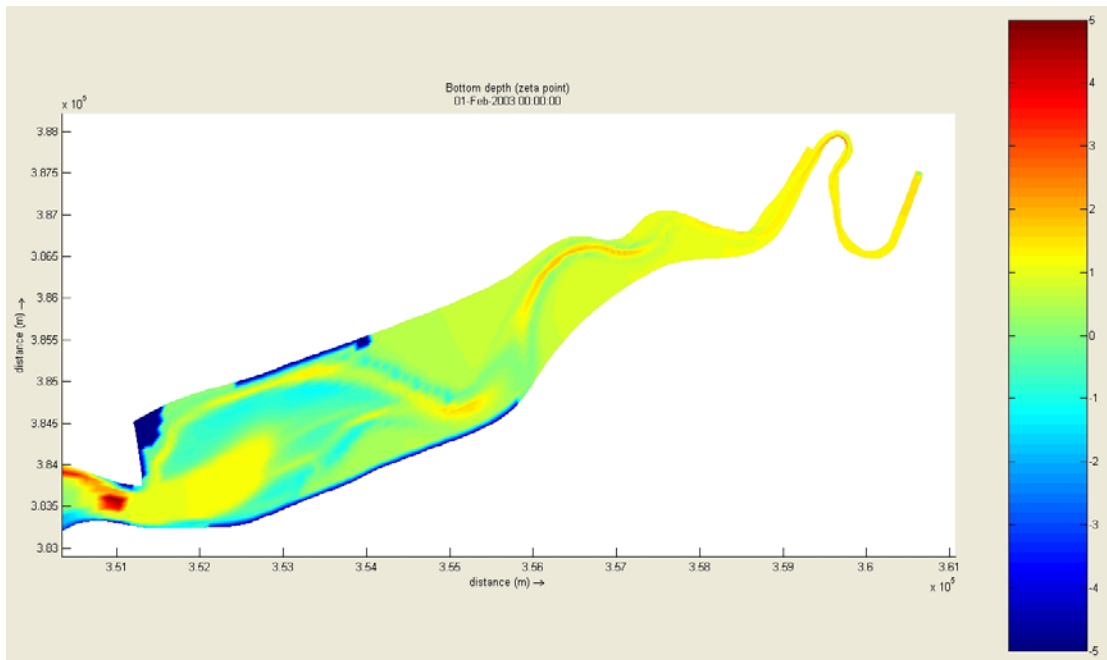


Figure 7a. Bathymetric change after 1 month for 150µm sediment, using harmonic tidal constituents and a constant mean annual fluvial flow

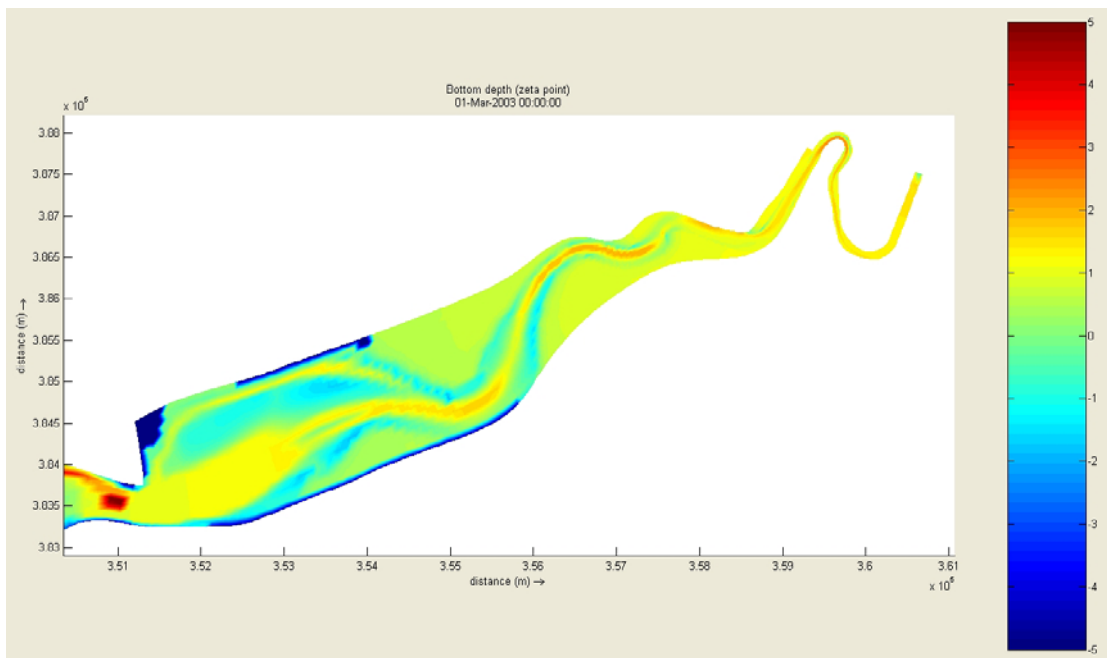


Figure 7b. Bathymetric change after 2 months for 150µm sediment, using harmonic tidal constituents and a constant mean annual fluvial flow

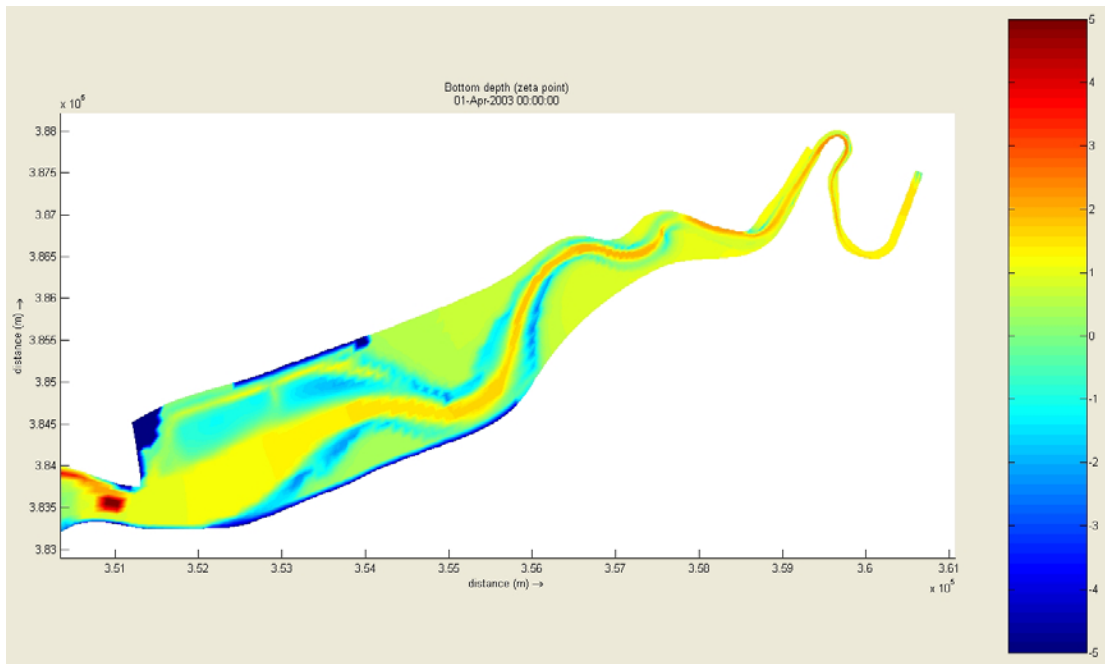


Figure 7c. Bathymetric change after 3 months for 150µm sediment, using harmonic tidal constituents and a constant mean annual fluvial flow

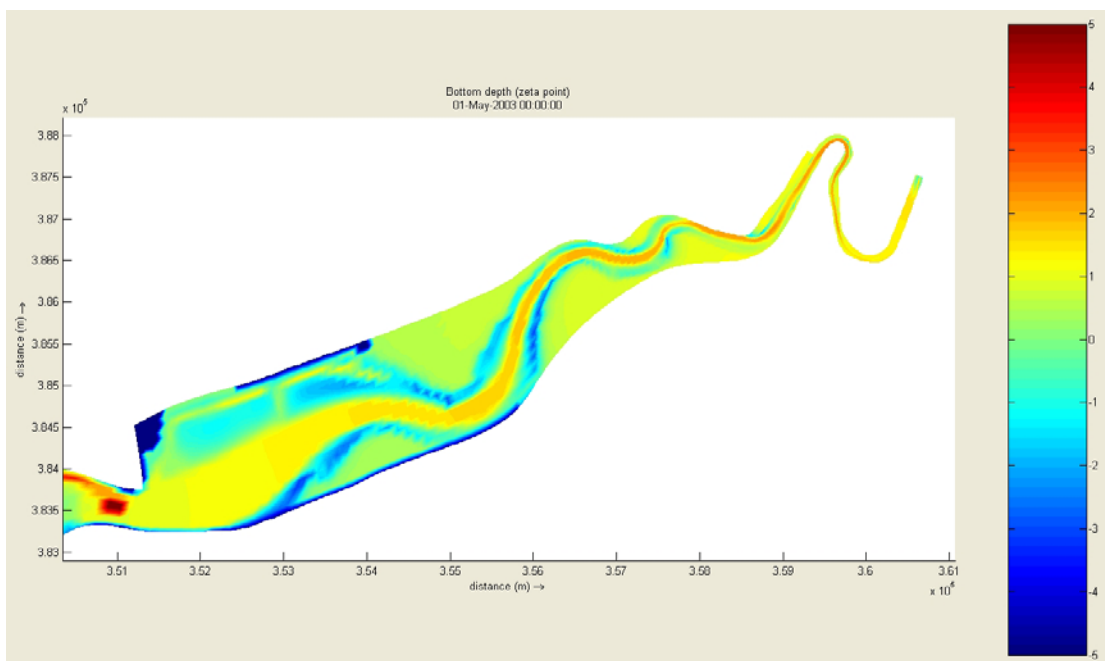


Figure 7d. Bathymetric change after 4 months for 150µm sediment, using harmonic tidal constituents and a constant mean annual fluvial flow

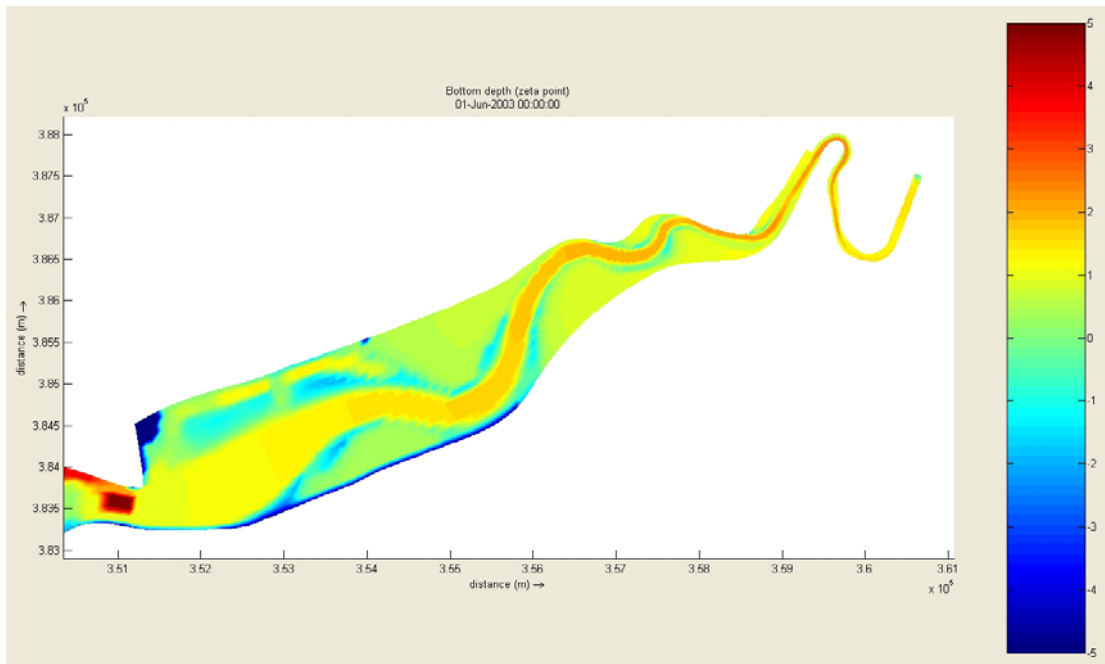


Figure 7e. Bathymetric change after 5 months for 150µm sediment, using harmonic tidal constituents and a constant mean annual fluvial flow

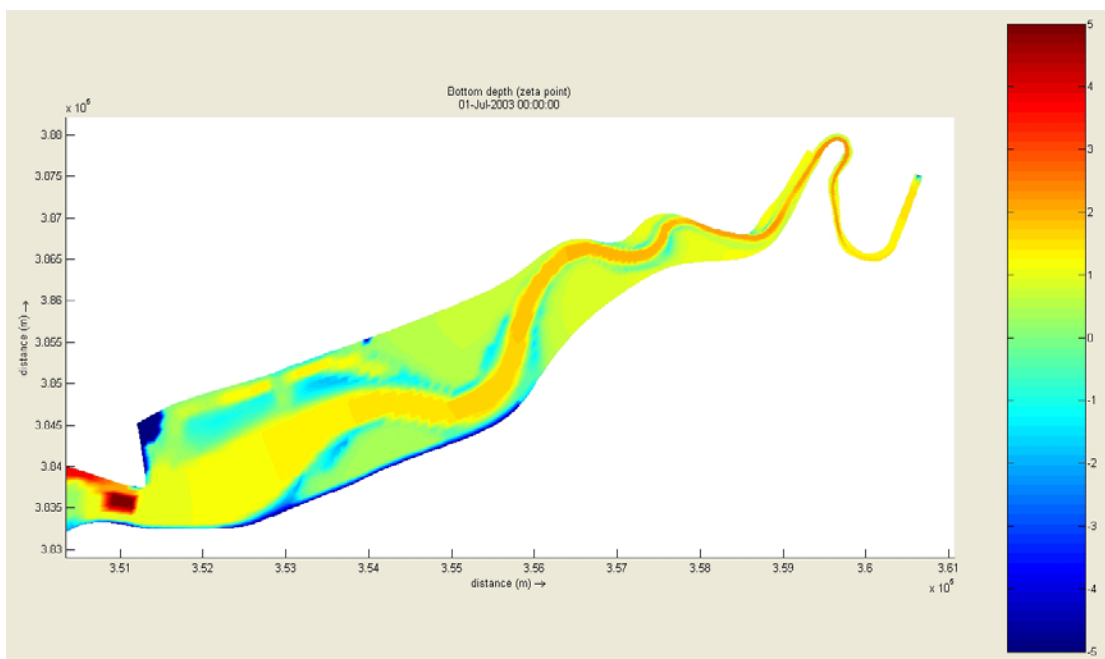


Figure 7f. Bathymetric change after 6 months for 150µm sediment, using harmonic tidal constituents and a constant mean annual fluvial flow

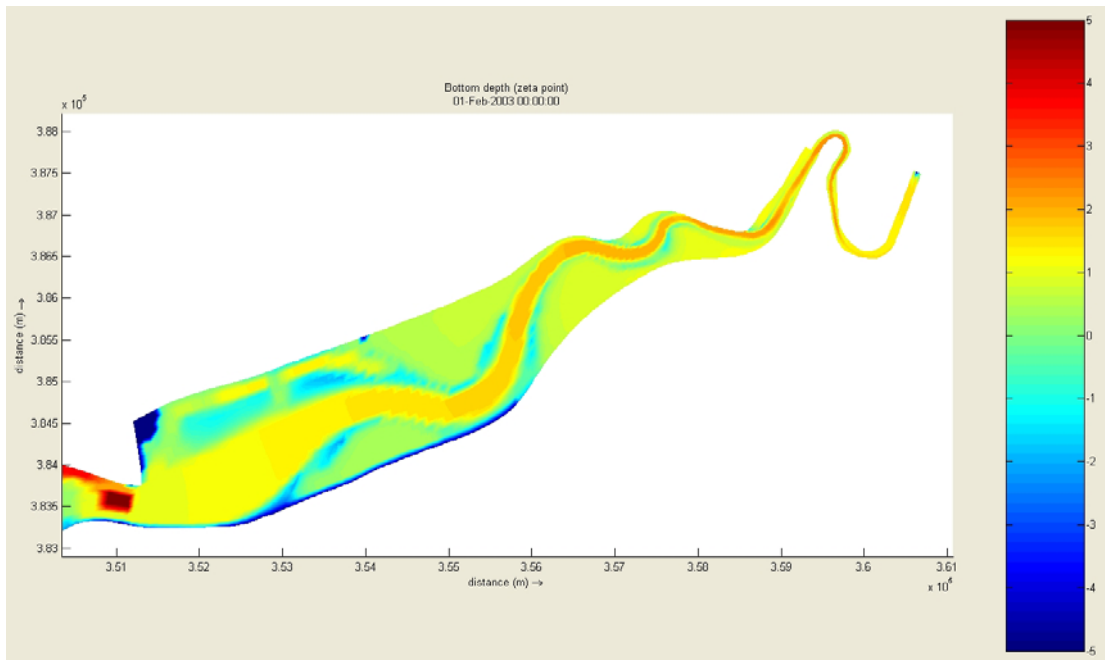


Figure 8a. Bathymetric change after 1 month for 150µm sediment, using harmonic tidal constituents and a daily mean fluvial flow

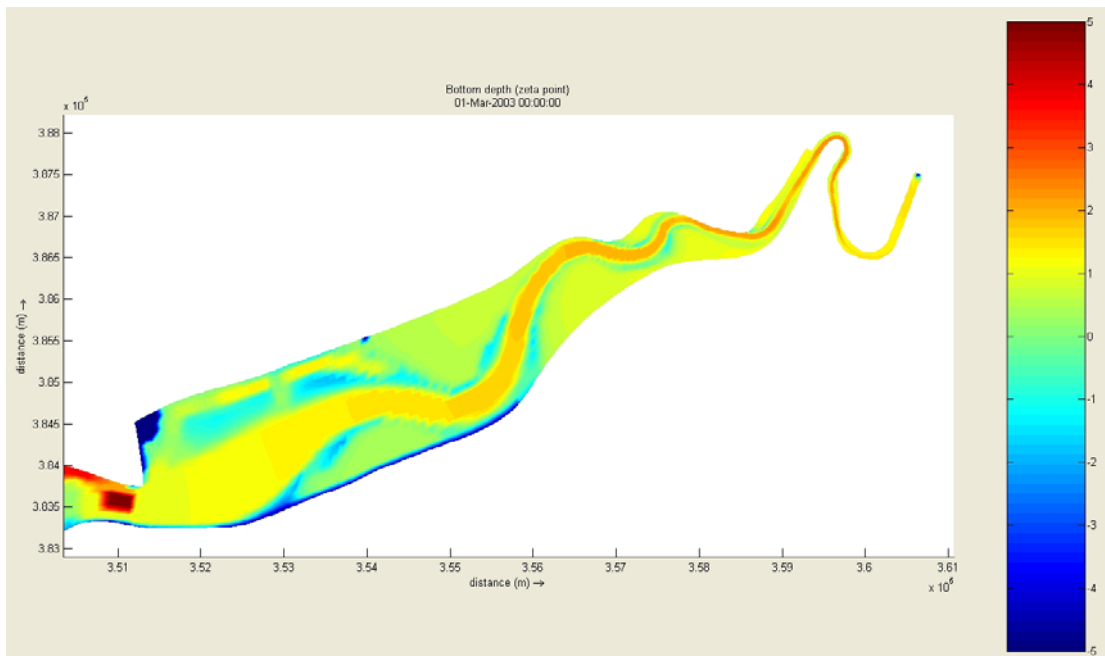


Figure 8c. Bathymetric change after 2 months for 150µm sediment, using harmonic tidal constituents and a daily mean fluvial flow

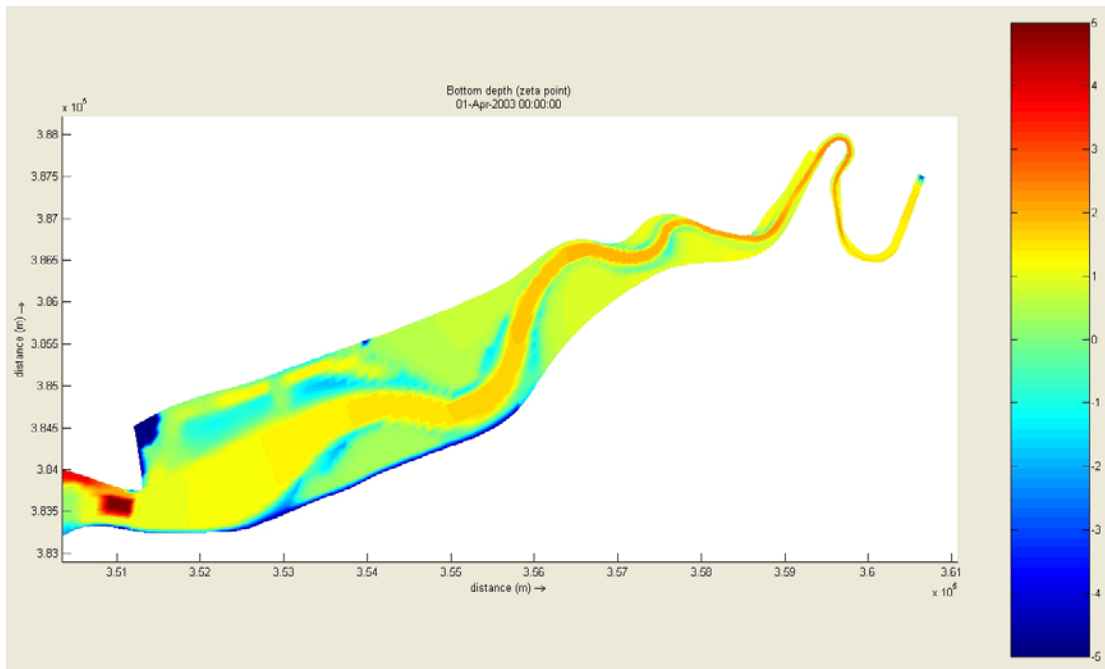


Figure 8d. Bathymetric change after 3 months for 150µm sediment, using harmonic tidal constituents and a daily mean fluvial flow

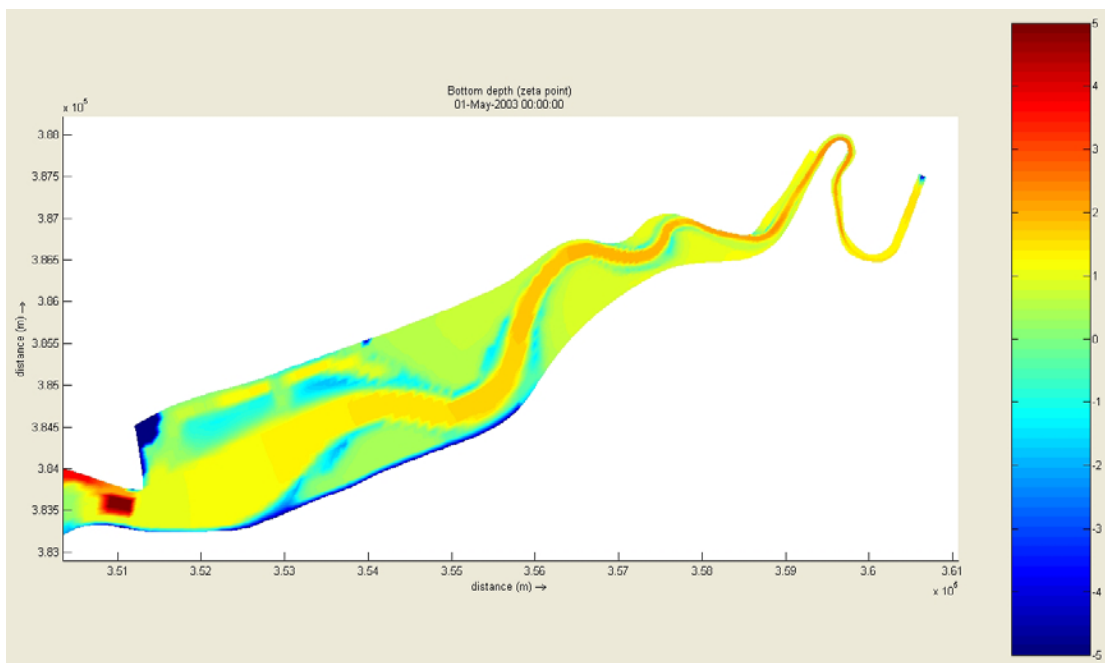


Figure 8e. Bathymetric change after 4 months for 150µm sediment, using harmonic tidal constituents and a daily mean fluvial flow

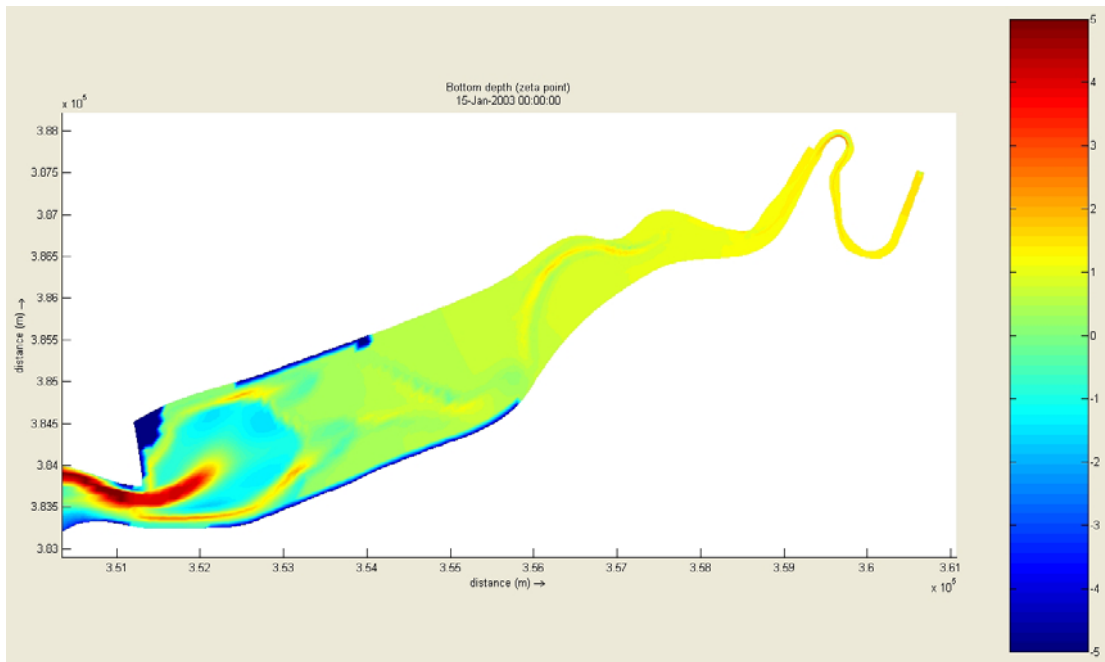


Figure 9a. Bathymetric change after 15 days for 300µm sediment, using a real tidal time-series driver, a constant mean annual fluvial flow and an initial 4m depth of sediment

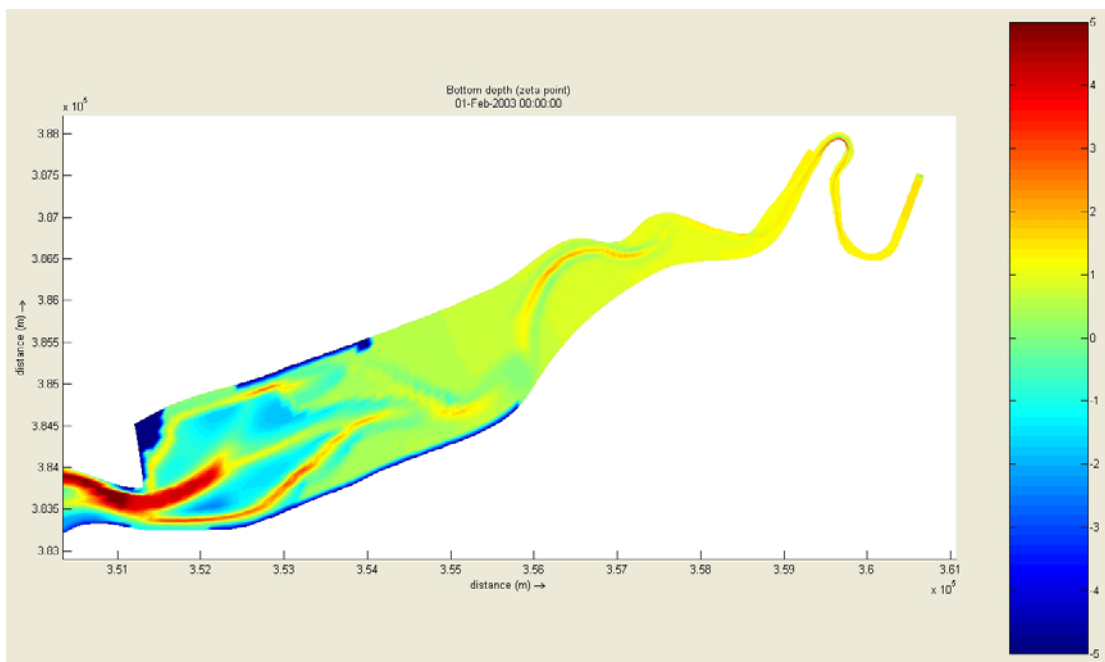


Figure 9b. Bathymetric change after 1 month for 300µm sediment, using a real tidal time-series driver, a constant mean annual fluvial flow and an initial 4m depth of sediment

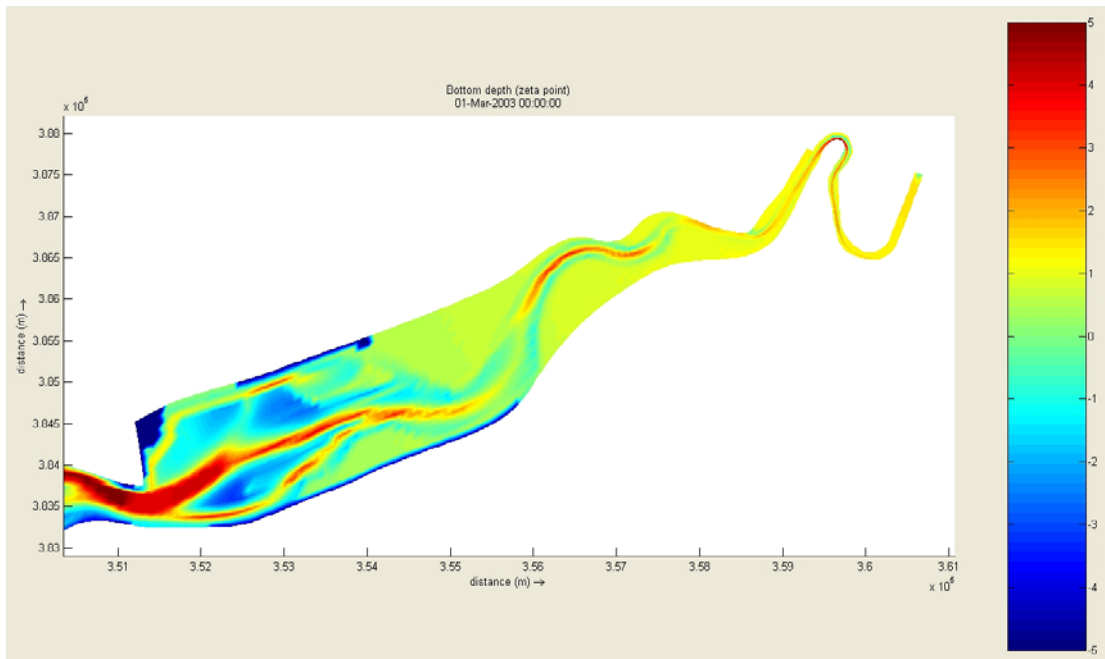


Figure 9c. Bathymetric change after 2 months for 300µm sediment, using a real tidal time-series driver, a constant mean annual fluvial flow and an initial 4m depth of sediment

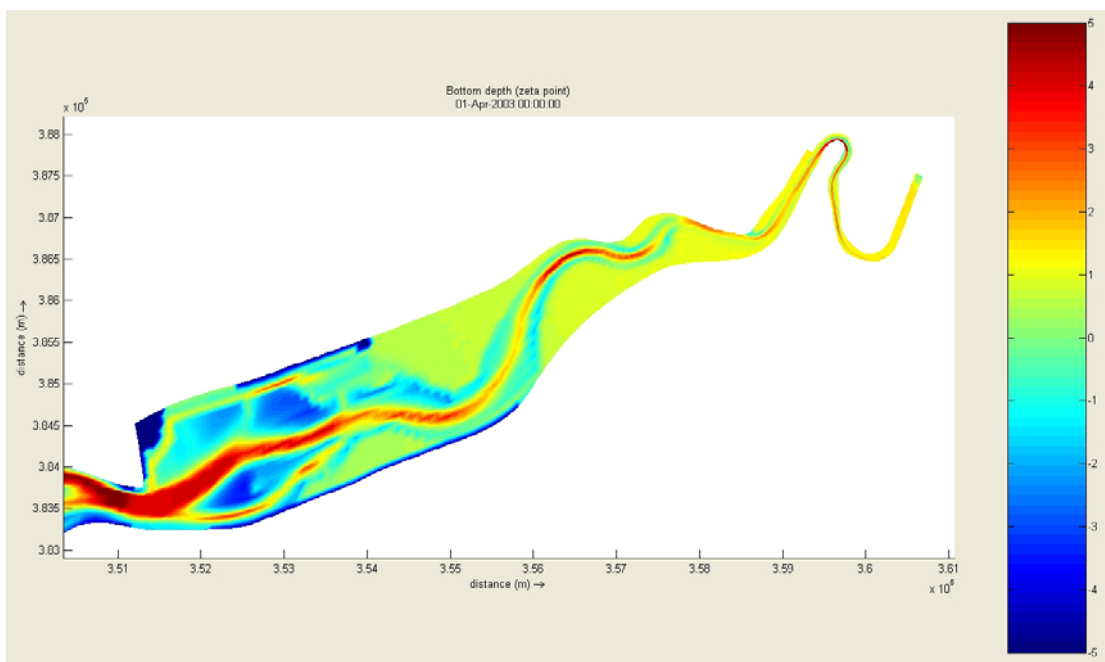


Figure 9d. Bathymetric change after 3 months for 300µm sediment, using a real tidal time-series driver, a constant mean annual fluvial flow and an initial 4m depth of sediment

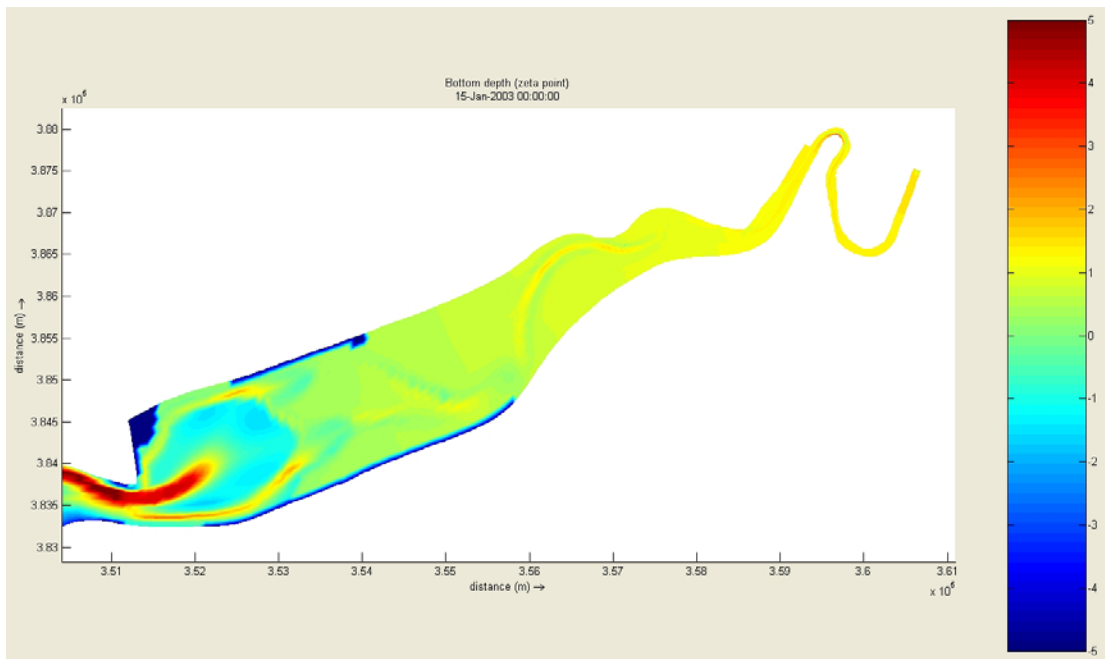


Figure 10a. Bathymetric change after 15 days for 300µm sediment, using a real tidal time-series driver, a constant mean annual fluvial flow an initial 4m depth of sediment and an hourly wind speed and direction

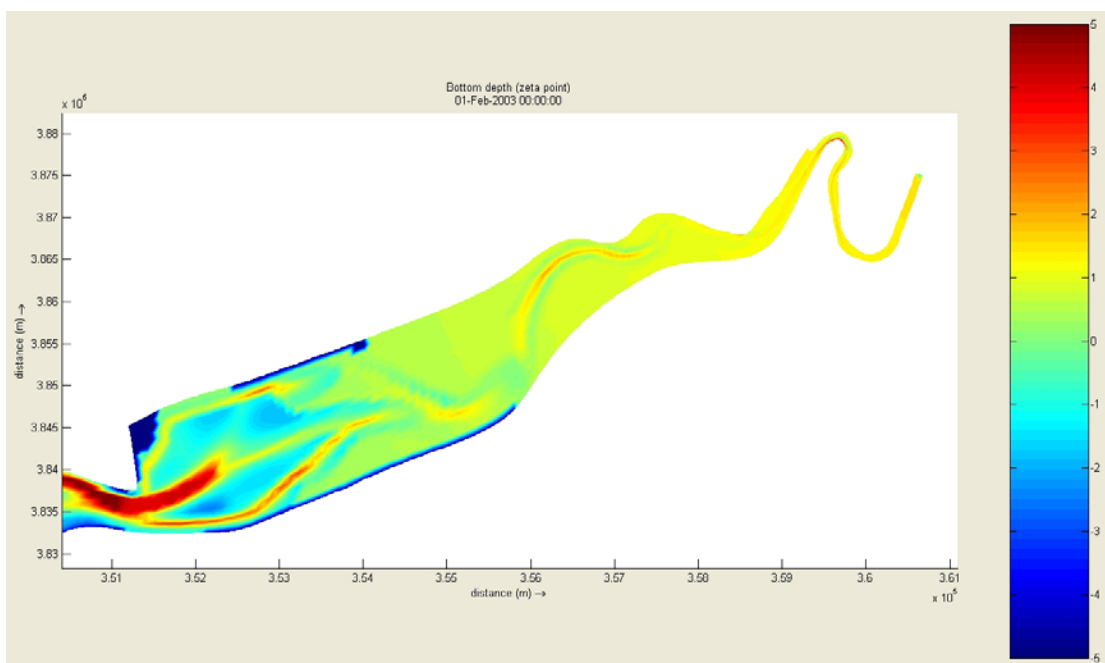


Figure 10b. Bathymetric change after 1 month for 300µm sediment, using a real tidal time-series driver, a constant mean annual fluvial flow an initial 4m depth of sediment and an hourly wind speed and direction

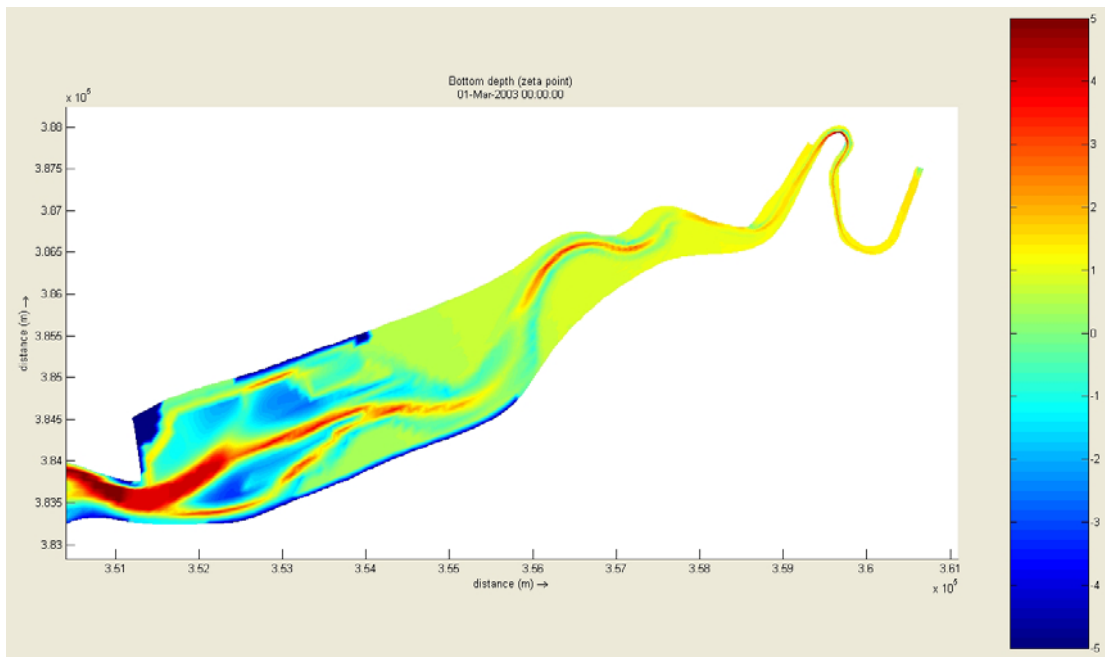


Figure 10c. Bathymetric change after 2 months for 300µm sediment, using a real tidal time-series driver, a constant mean annual fluvial flow an initial 4m depth of sediment and an hourly wind speed and direction

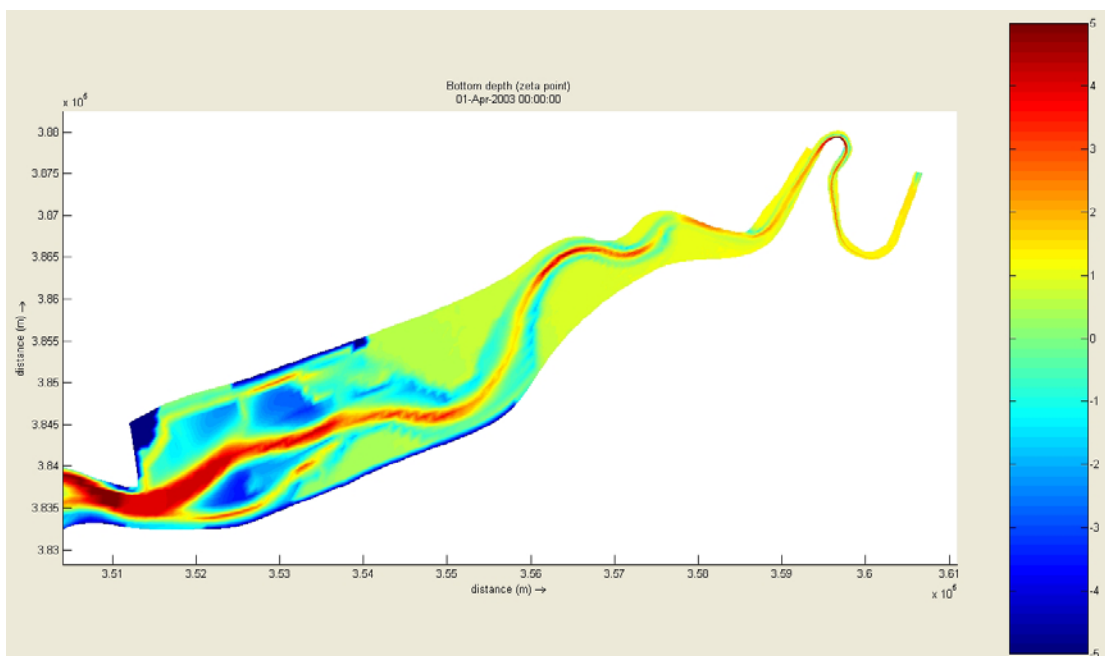


Figure 10d. Bathymetric change after 3 months for 300µm sediment, using a real tidal time-series driver, a constant mean annual fluvial flow an initial 4m depth of sediment and an hourly wind speed and direction

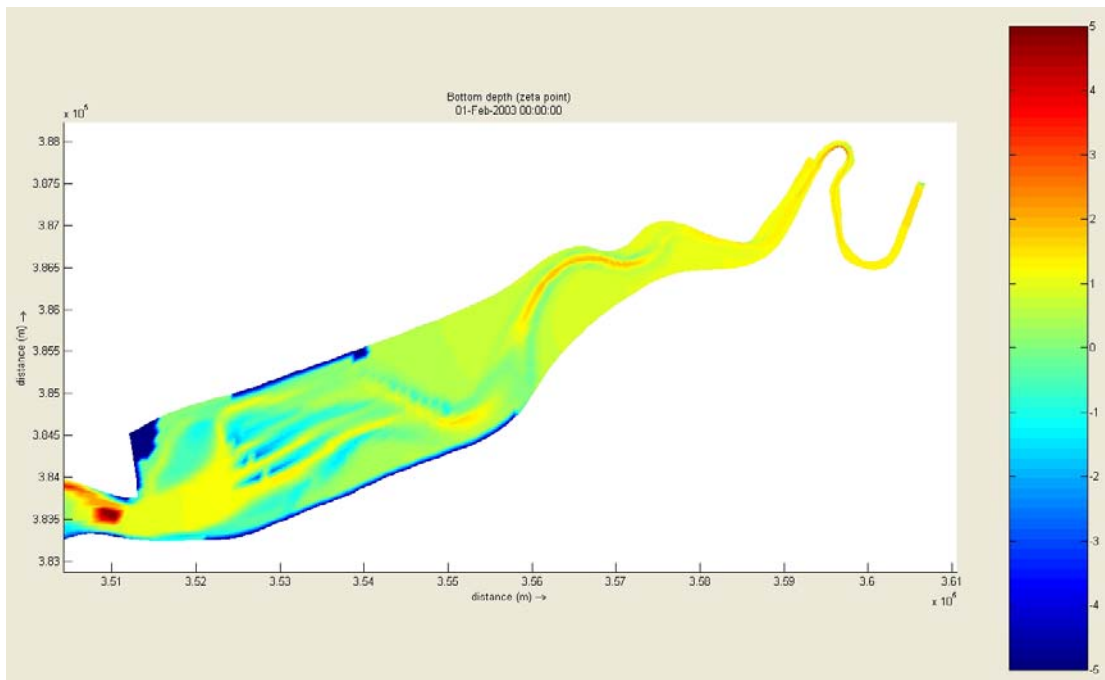


Figure 11a. Bathymetric change after 1 month with three 80m x 80m structures in place for 150µm sediment, using a real tidal time-series driver and a constant mean annual fluvial flow

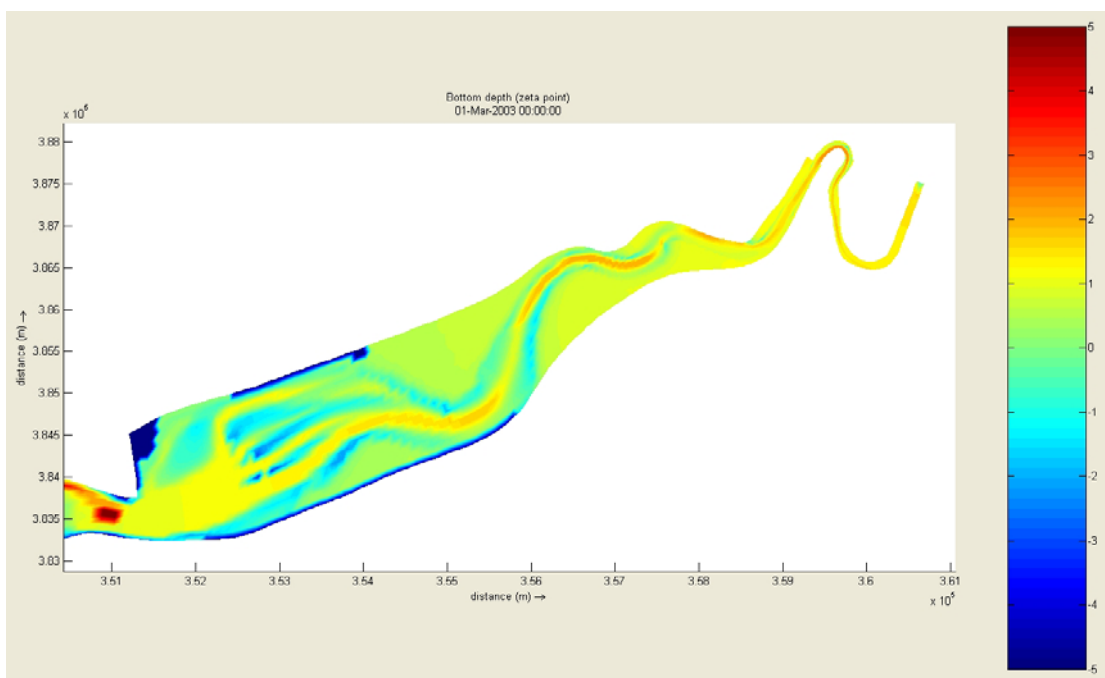


Figure 11b. Bathymetric change after 2 months with three 80m x 80m structures in place for 150µm sediment, using a real tidal time-series driver and a constant mean annual fluvial flow

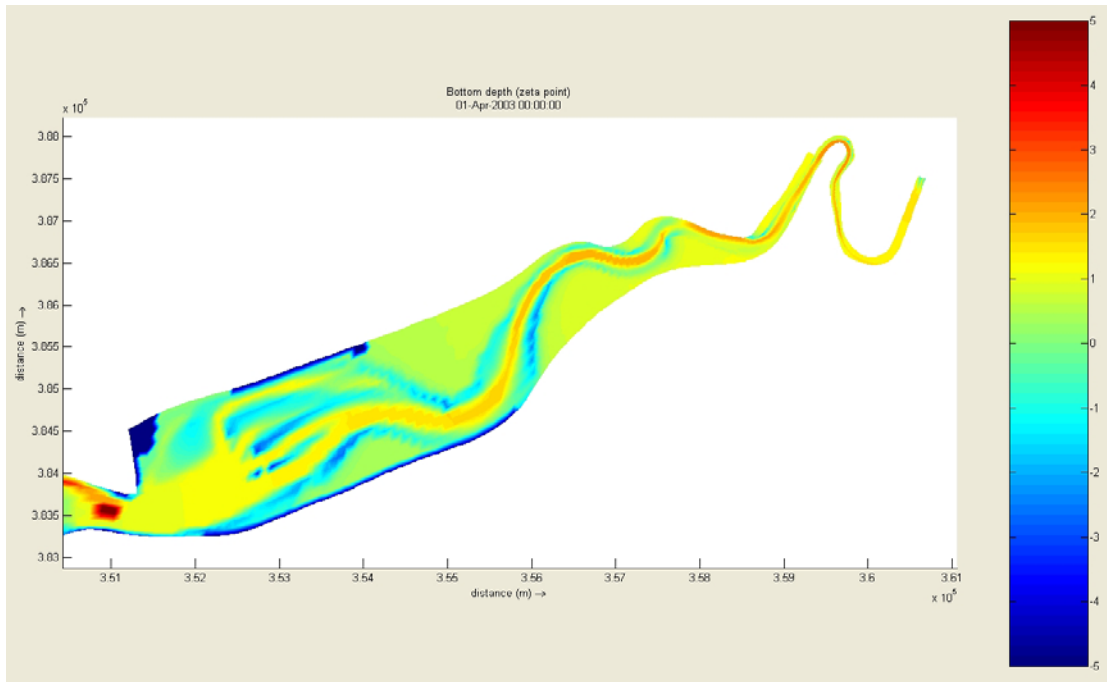


Figure 11c. Bathymetric change after 3 months with three 80m x 80m structures in place for 150µm sediment, using a real tidal time-series driver and a constant mean annual fluvial flow

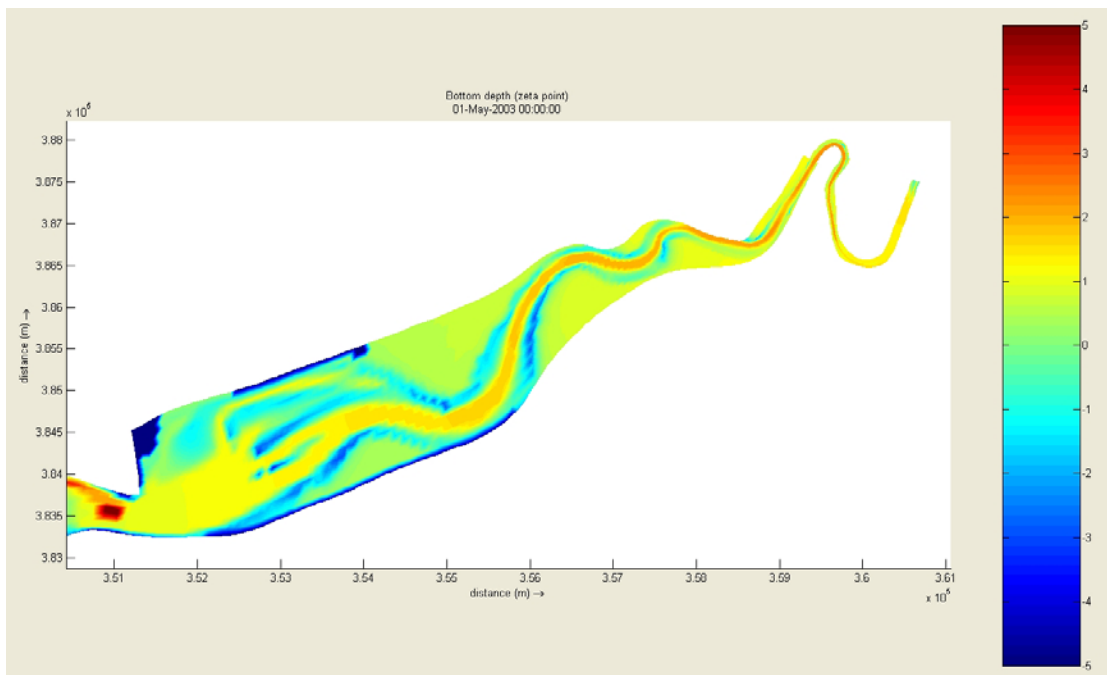


Figure 11d. Bathymetric change after 4 months with three 80m x 80m structures in place for 150µm sediment, using a real tidal time-series driver and a constant mean annual fluvial flow

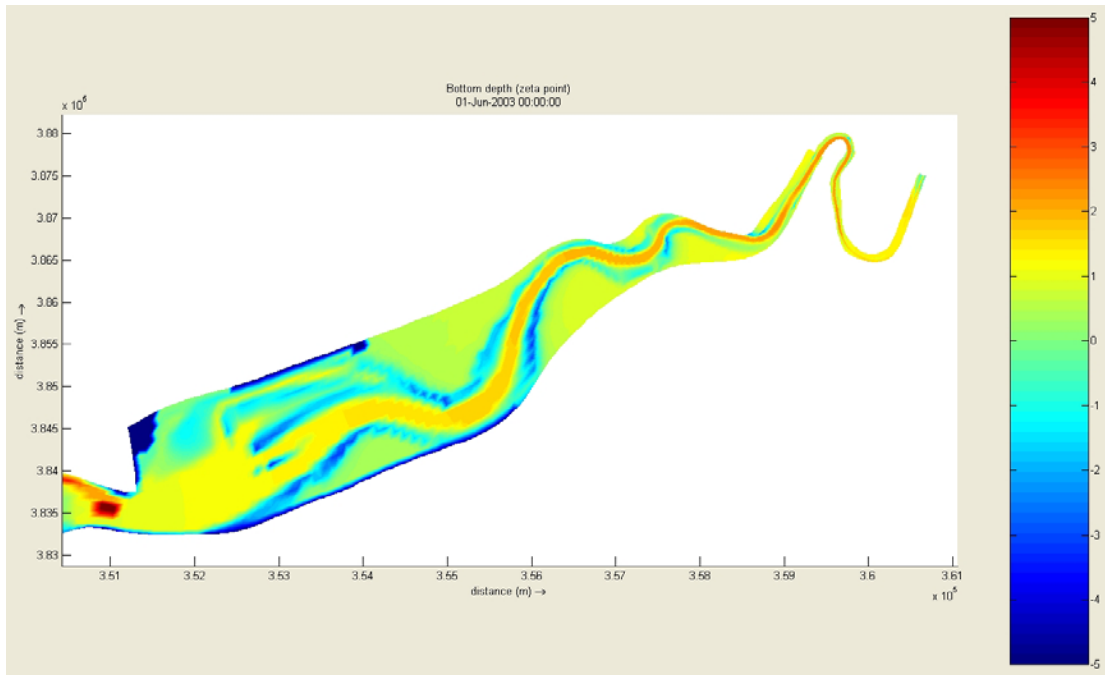


Figure 11e. Bathymetric change after 5 months with three 80m x 80m structures in place for 150µm sediment, using a real tidal time-series driver and a constant mean annual fluvial flow

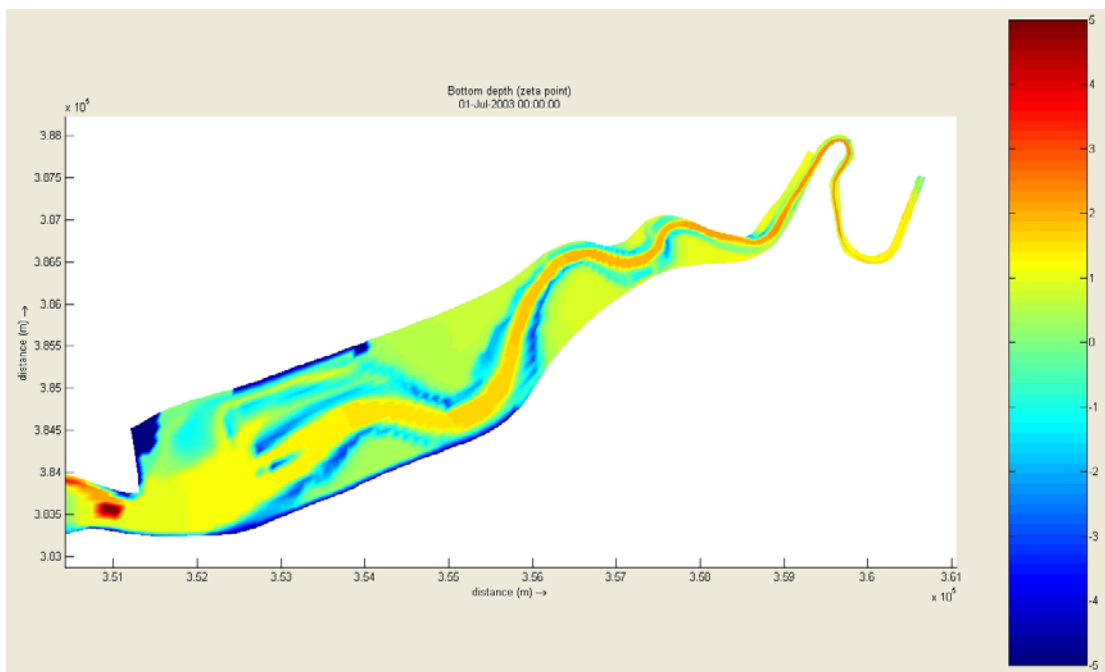


Figure 11f. Bathymetric change after 6 months with three 80m x 80m structures in place for 150µm sediment, using a real tidal time-series driver and a constant mean annual fluvial flow

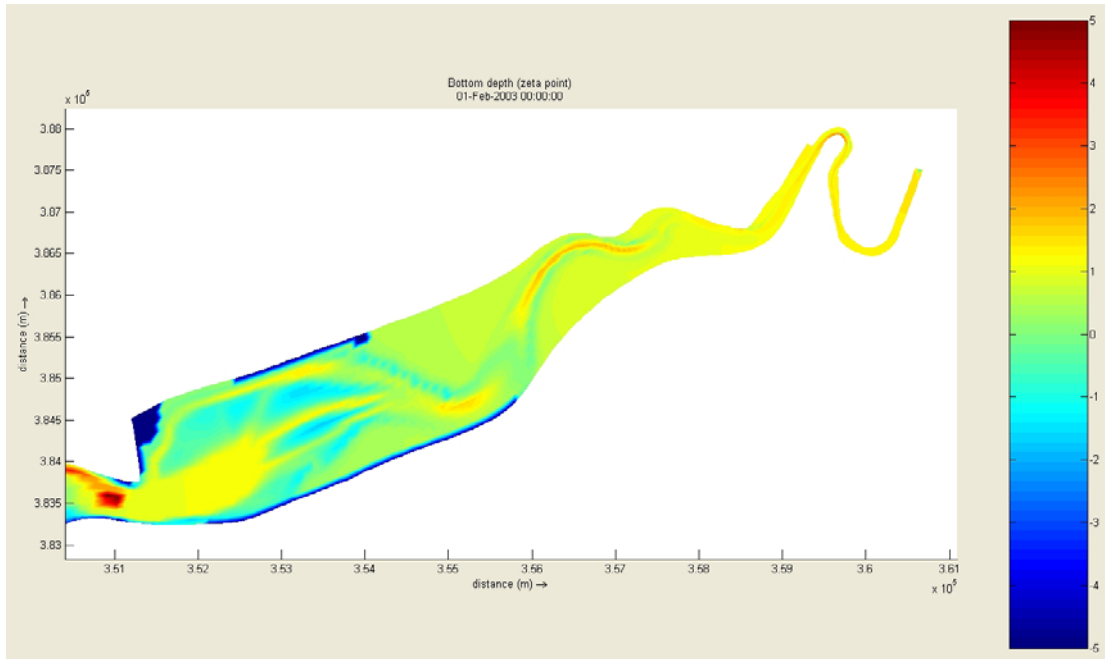


Figure 12a. Bathymetric change after 1 month with three 10m diameter structures in place (represented using added friction terms) for 150 μ m sediment, using a real tidal time-series driver and a constant mean annual fluvial flow

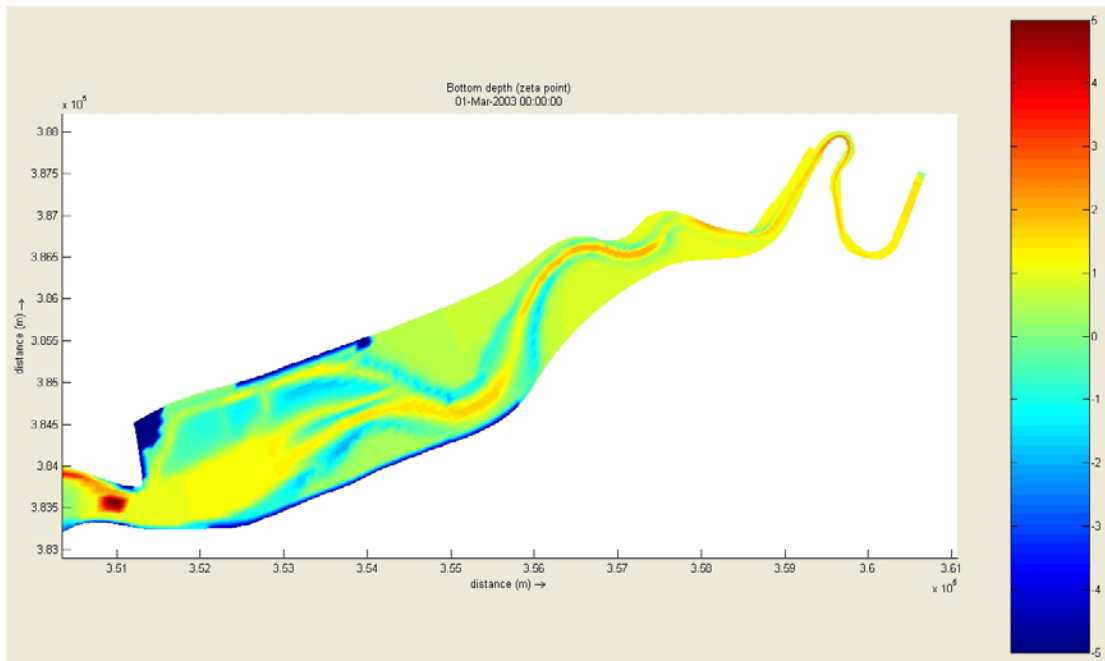


Figure 12b. Bathymetric change after 2 months with three 10m diameter structures in place (represented using added friction terms) for 150 μ m sediment, using a real tidal time-series driver and a constant mean annual fluvial flow

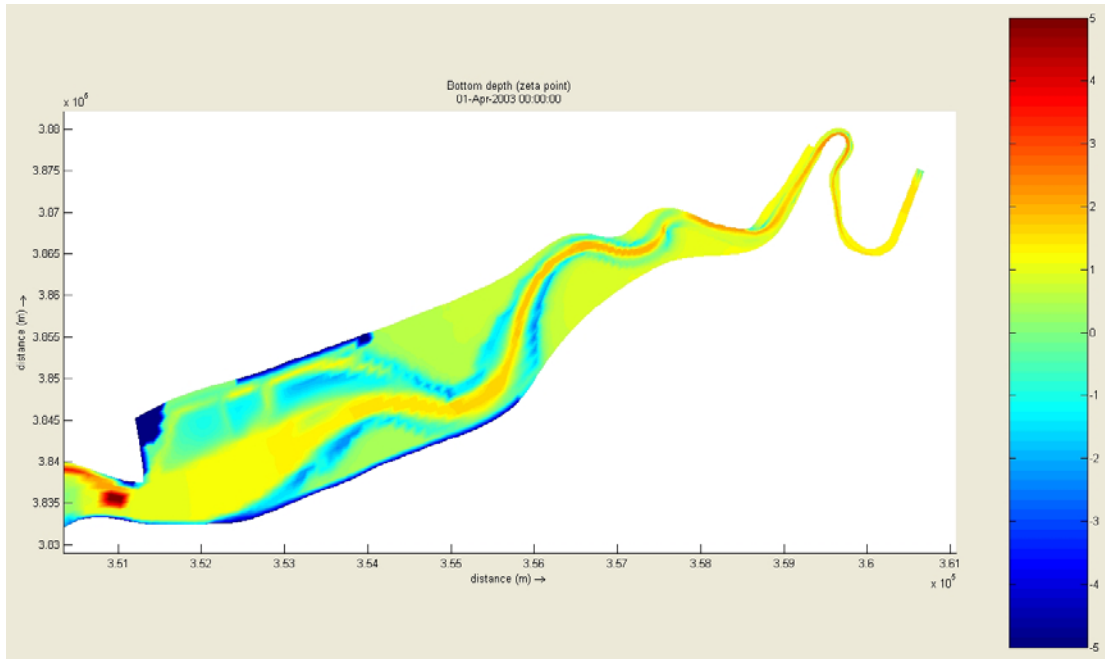


Figure 12c. Bathymetric change after 3 months with three 10m diameter structures in place (represented using added friction terms) for 150 μ m sediment, using a real tidal time-series driver and a constant mean annual fluvial flow

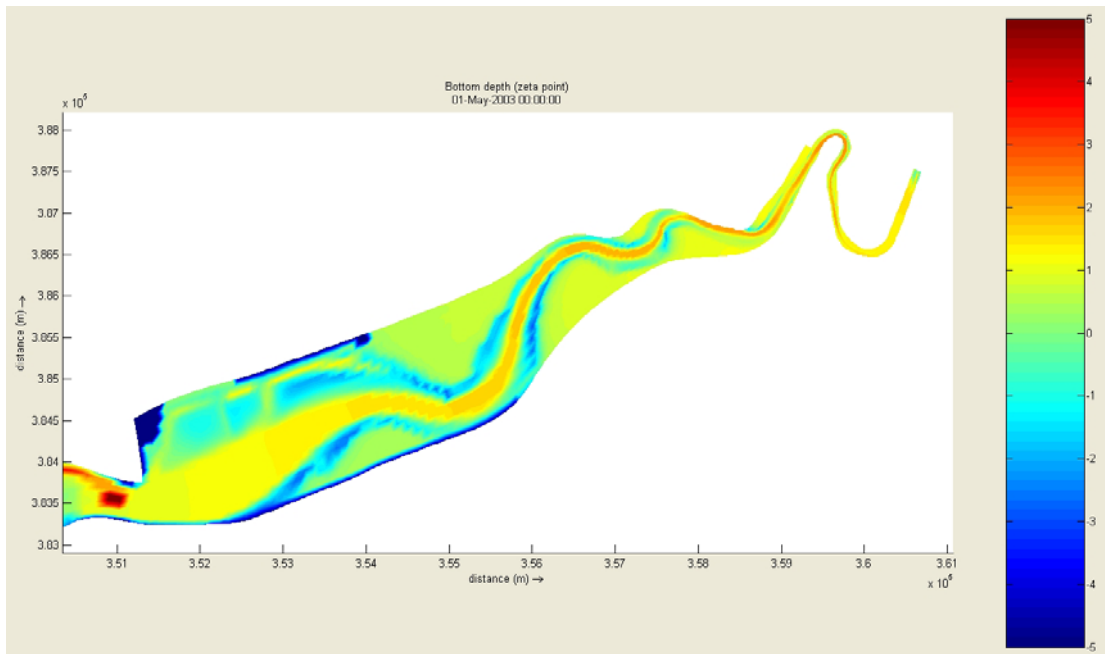


Figure 12d. Bathymetric change after 4 months with three 10m diameter structures in place (represented using added friction terms) for 150 μ m sediment, using a real tidal time-series driver and a constant mean annual fluvial flow

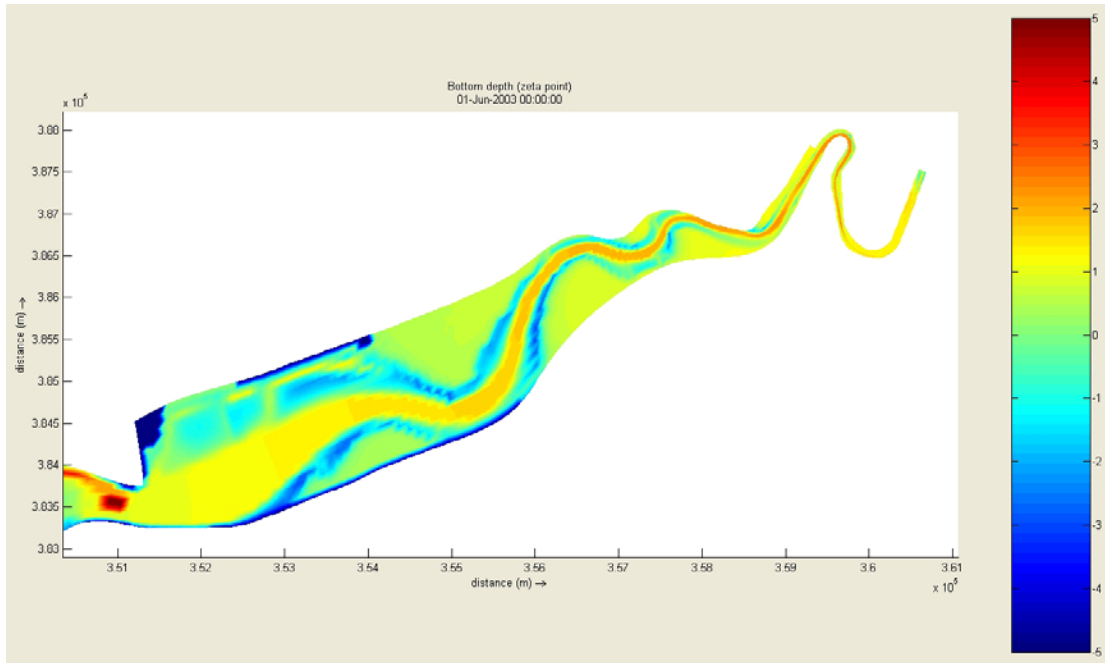


Figure 12e. Bathymetric change after 5 months with three 10m diameter structures in place (represented using added friction terms) for 150 μ m sediment, using a real tidal time-series driver and a constant mean annual fluvial flow

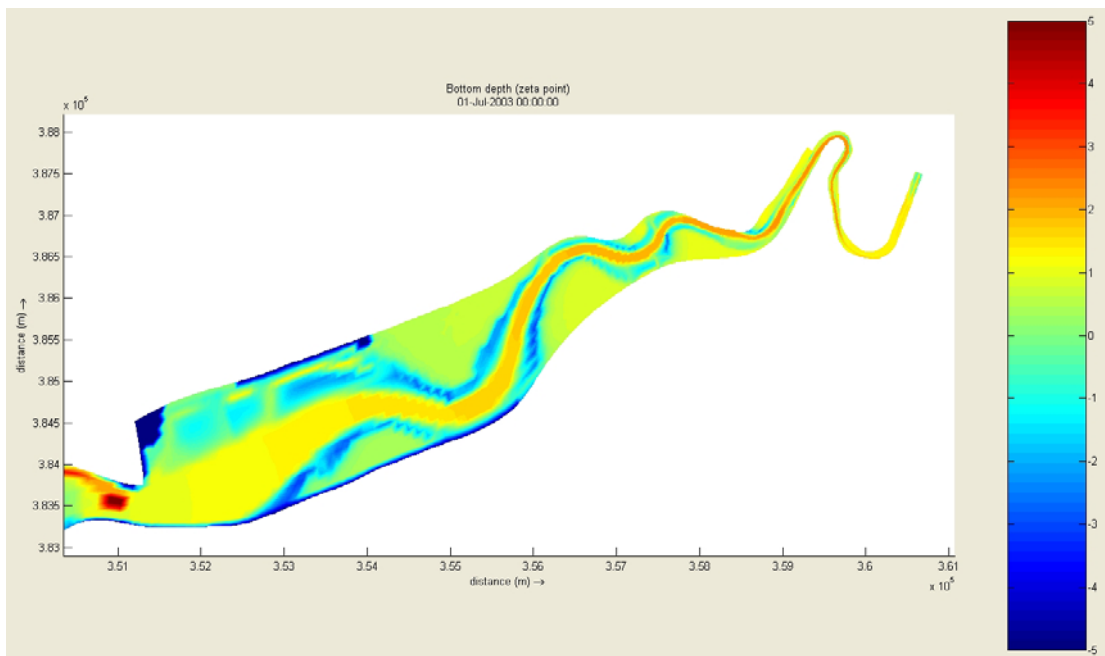


Figure 12f. Bathymetric change after 1 month with three 10m diameter structures in place (represented using added friction terms) for 150 μ m sediment, using a real tidal time-series driver and a constant mean annual fluvial flow



ABP Marine Environmental Research Ltd
Suite B, Waterside House
Town Quay
Southampton
Hampshire SO14 2AQ

Tel: +44 (0)23 8071 1840
Fax: +44 (0)23 8071 1841
Email: enquiries@abpmer.co.uk

www.abpmer.co.uk



Gifford & Partners

Additional Modelling - Mersey Gateway

Technical Note D: Real Hydrograph Modelling

Date: December 2005

Project Ref: R/3411/4

Report No: R.1241d



Gifford & Partners

Additional Modelling - Mersey Gateway Technical Note D: Real Hydrograph Modelling

Date: December 2005

Project Ref: R/3411/4

Report No: R.1241d

© ABP Marine Environmental Research Ltd

Version	Details of Change	Authorised By	Date
1	Draft for Comment	J M Harris	9/12/2005
2	Final	J M Harris	20/12/2005

Document Authorisation		Signature	Date
Project Manager:	J M Harris	<i>J M Harris</i>	20/12/2005
Quality Manager:	R H Swift	<i>Richard Swift</i>	19/01/2006
Project Director:	W S Cooper	<i>W S Cooper</i>	10-1-06

ABP Marine Environmental Research Ltd
Suite B, Waterside House
Town Quay
SOUTHAMPTON
Hampshire
SO14 2AQ



Tel: +44(0)23 8071 1840
Fax: +44(0)23 8071 1841
Web: www.abpmer.co.uk
Email: enquires@abpmer.co.uk



INVESTOR IN PEOPLE

Summary

This technical note describes the morphological simulations undertaken as part of the additional modelling studies carried out for Phase II of the Mersey Gateway Project. The principal aim of these tests was to assess the difference applying a real hydrograph and real tidal data would have on the modelling results for the 3 Tower revised scheme with and without bridge towers in place and to observe differences in predicted channel formation.

This report is one of a series of five Technical Notes (R1241a to R.1241e):

- Technical Note A: Residual Modelling - Stage I;
- Technical Note B: Residual Modelling - Stage II;
- Technical Note C: Flat Bed Morphological Modelling;
- Technical Note D: Real Hydrograph Modelling; and
- Technical Note E: Phase Differences.

Two morphological simulations were undertaken using a three domain model run with a real tidal signal (including harmonic and atmospheric components) and a mean daily discharge. The simulations were undertaken for a baseline and scheme (3 Tower revised). From these additional model tests the key conclusions are:

- There is remarkable agreement between the simulations run with the real tidal and fluvial data, and the corresponding simulations run with tidal constituents and a mean annual discharge. There are differences over the intertidal banks, but this is not unsurprising as both the tidal signal, which contains a non-linear surge component, and the fluvial flow, which includes larger discharge events particularly in the winter period and smaller events in the summer period will have a greater impact on the morphology.
- The extent of change is no greater than that observed in previous simulations and this together with the magnitude of change would suggest that running the model with both a real tidal signal and a varying freshwater discharge has no major impact on the model results.

Additional Modelling - Mersey Gateway Technical Note D: Real Hydrograph Modelling

Contents

	Page
Summary	i
1. Introduction	1
2. Methodology	1
3. Results	2
4. Conclusions	2
5. References	3

Figures

1. Morphological curvilinear model grids for the Mersey Estuary Phase II modelling study	5
2. Difference in morphology (m) between baseline scenarios run with real tidal and fluvial forcing and tidal constituents and a mean annual discharge, respectively, after 1 year	6
3. Morphological change (m) after 1 year. Route 3A Medium Span - 3 Tower Revised Alignment Scenario. Simulations run with real tidal and fluvial forcing	6
4. Morphological change (m) after 1 year. Route 3A Medium Span - 3 Tower Revised Alignment Scenario. Simulations run with tidal constituents and a mean annual discharge	7

1. Introduction

This technical note describes the morphological simulations undertaken as part of the additional modelling studies carried out for Phase II of the Mersey Gateway Project. The principal aim of these tests was to assess the difference applying a real hydrograph and real tidal data would have on the modelling results for the 3 Tower revised scheme with and without bridge towers in place and to observe differences in predicted channel formation.

The modelling work applied the three domain model used in the morphological modelling reported in ABPmer (2005). Figure 1 shows the model grid used in the study. The morphological model of the Mersey Estuary is based on a three domain calibrated Delft3D-FLOW hydrodynamic model of the Mersey Estuary and reported in ABPmer (2005). All hydrodynamic parameters are identical to those applied in the more detailed five domain model used to assess hydrodynamic change. The initial bathymetry and sediment distribution map was set up using data provided by the Environment Agency, the British Geological Survey, The University of Southampton, Gifford & Partners and ABPmer.

The computational grid of the hydrodynamic model consisted of 8 layers through the vertical. The turbulence closure model used was a $k-\epsilon$ turbulence model. Due to the addition of the sediment fraction and morphological updating the computational time-step was reduced to 0.3 min for stability purposes.

The model utilizes the domain decomposition module of Delft3D allowing a model grid to be sub-divided into several smaller model domains (sub-domains). The sub-division is based on the horizontal and vertical model resolution required for adequately simulating the key physical processes under consideration. Domain decomposition allows for local grid refinement in both the horizontal and vertical directions. 3 grids were chosen with a constant vertical resolution. The middle grid had the finest horizontal resolution of typically 20-30m. The coarse resolution of the outer and inner grids enabled the model to simulate longer time-scales than would otherwise be the case (see ABPmer, 2005).

The dominant sediment type was chosen based on particle size analysis from the field survey and borehole data. A sand fraction with a d_{50} grain size of 150 μm was applied in the morphological modelling (see also ABPmer, 2003).

2. Methodology

The model set up was kept the same as those runs reported in ABPmer (2005) except that the tidal constituent boundary applied at Gladstone was replaced with a real tidal signal (including harmonic and atmospheric components) and the mean annual fluvial

discharge applied at Howley weir was replaced with a mean daily discharge. The model was then run for a period representative of 1 year to allow comparison with the results reported previously in ABPmer (2005).

3. Results

Figure 2 shows a comparison of the baseline model results for the middle grid run with the real tidal and fluvial data against the corresponding model results run with tidal constituents and a mean annual discharge. The results from the morphological model show a significant difference between the two simulations though this is not unsurprising due to the difference in tidal and fluvial forcing. Of more interest is the difference between the baseline case and the scheme run with the real tidal and fluvial data, the results of which are shown for all three grids in Figure 3. Comparing this with Figure 4, which shows a similar comparison but for the simulation run with tidal constituents and a mean annual discharge, there is remarkable agreement between the two simulations.

Comparing the two simulations for the 3 Tower revised scheme the general pattern of morphological change is similar. However, there are differences over the intertidal banks, but this is expected as both the tidal signal, which contains a non-linear surge component, and the fluvial flow, which includes larger discharge events particularly in the winter period and smaller events in the summer period will have a greater impact on the morphology. The extent of change is no greater than that observed in previous simulations (see ABPmer 2005) and this together with the magnitude of change would suggest that running the model with both a real tidal signal and a varying freshwater discharge has no major impact on the model results.

The approach adopted prior to this simulation was to remove the variability in the fluvial flow and non-linear components present in the measured tidal signature. This was done so that the separate contributions of the various forcing mechanisms could be investigated. However, it was also important to look at the effect of combining real tidal conditions with real river discharges to see what the difference would be, but only once a preferred scheme was selected.

4. Conclusions

Two morphological simulations were undertaken using a three domain model run with a real tidal signal (including harmonic and atmospheric components) and a mean daily discharge. The simulations were undertaken for a baseline and scheme (3 Tower revised). From these additional model tests the key conclusions are:

- There is remarkable agreement between the simulations run with the real tidal and fluvial data, and the corresponding simulations run with tidal constituents and a mean annual discharge. There are differences over the intertidal banks, but this is expected as both the tidal signal, which contains a non-linear surge component, and the fluvial flow, which includes larger discharge events particularly in the winter period and smaller events in the summer period will have a greater impact on the morphology.
- The extent of change is no greater than that observed in previous simulations and this together with the magnitude of change would suggest that running the model with both a real tidal signal and a varying freshwater discharge has no major impact on the model results.

5. References

ABPmer (2003). *New Mersey Crossing*. ABP Marine Environmental Research Ltd, Report No. R.1007.

ABPmer (2005). *New Mersey Crossing - Phase II Modelling Study*. ABP Marine Environmental Research Ltd, Report No. R.1151.

Figures

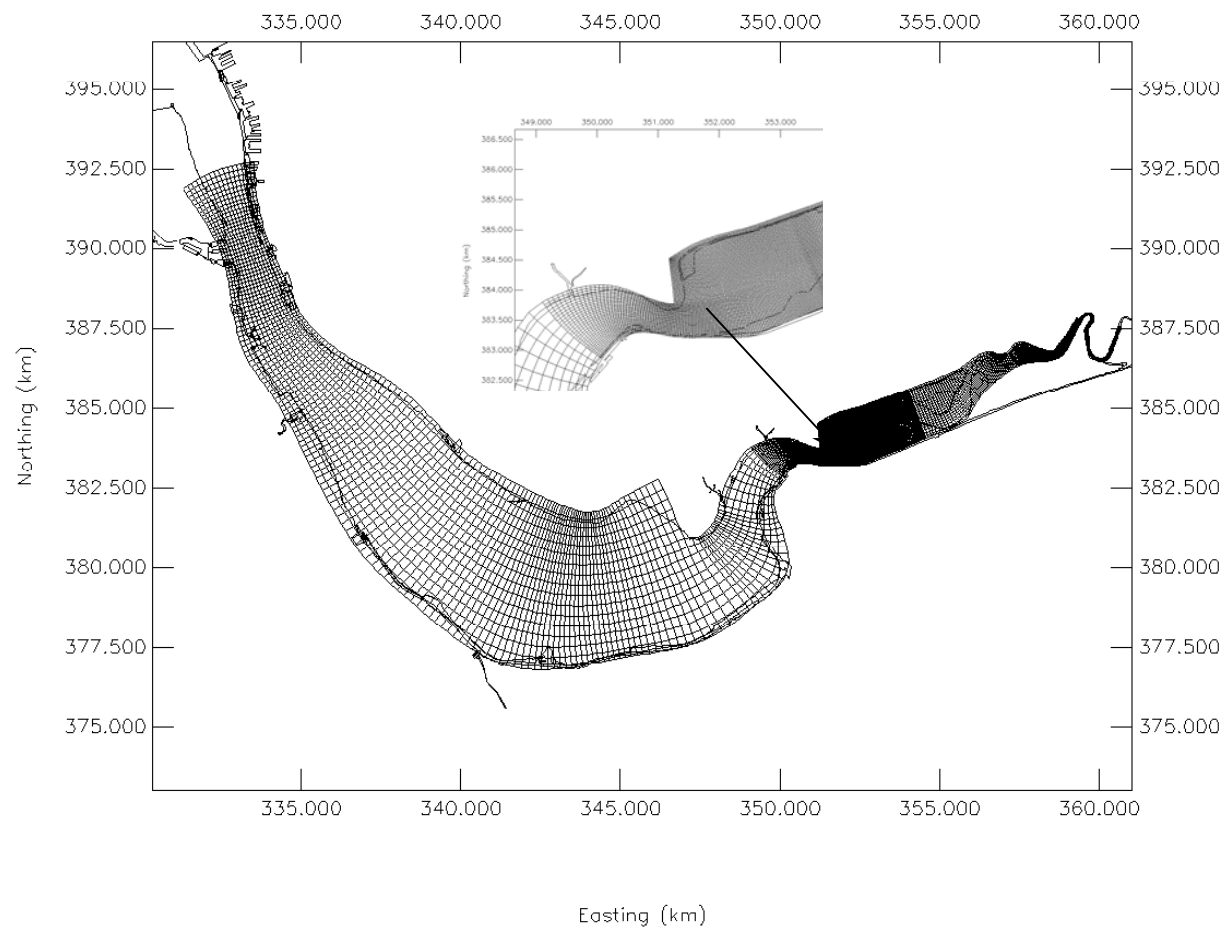


Figure 1. Morphological curvilinear model grids for the Mersey Estuary Phase II modelling study
Inset shows grid resolution in area of proposed crossing

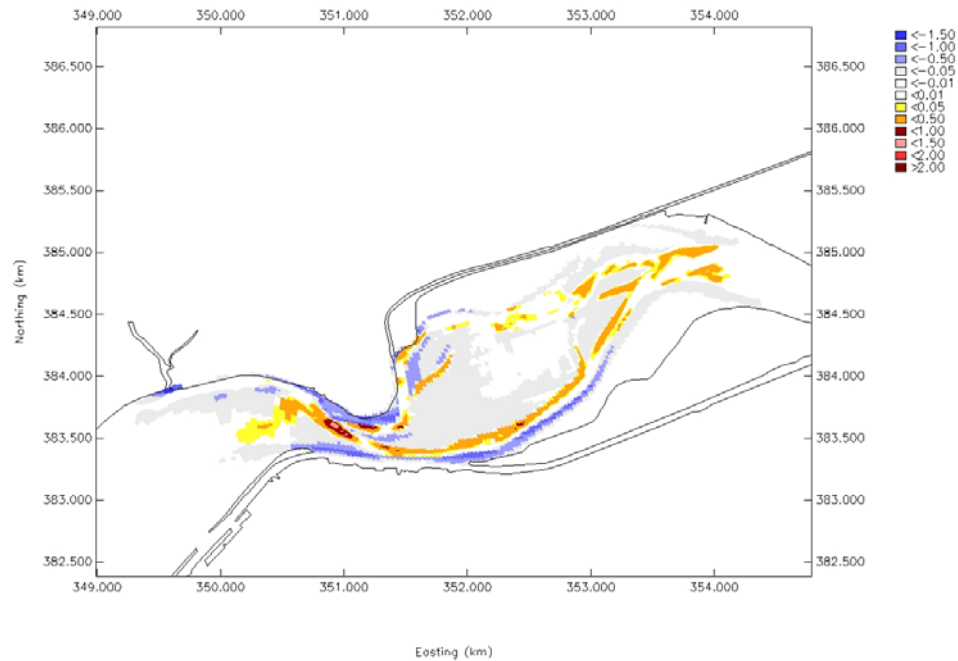


Figure 2. Difference in morphology (m) between baseline scenarios run with real tidal and fluvial forcing and tidal constituents and a mean annual discharge, respectively, after 1 year

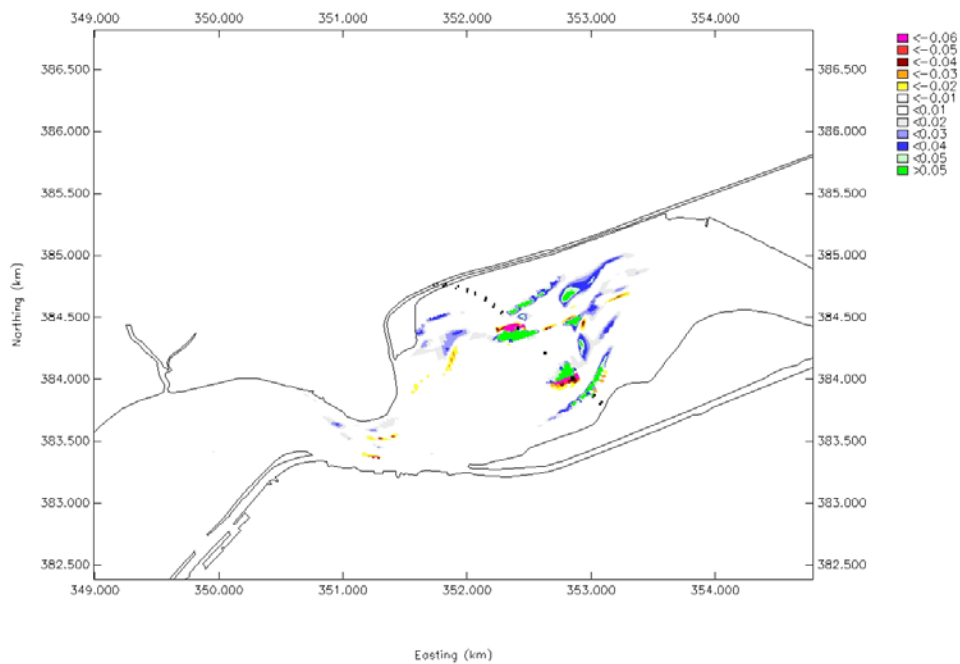


Figure 3. Morphological change (m) after 1 year. Route 3A Medium Span - 3 Tower Revised Alignment Scenario. Simulations run with real tidal and fluvial forcing

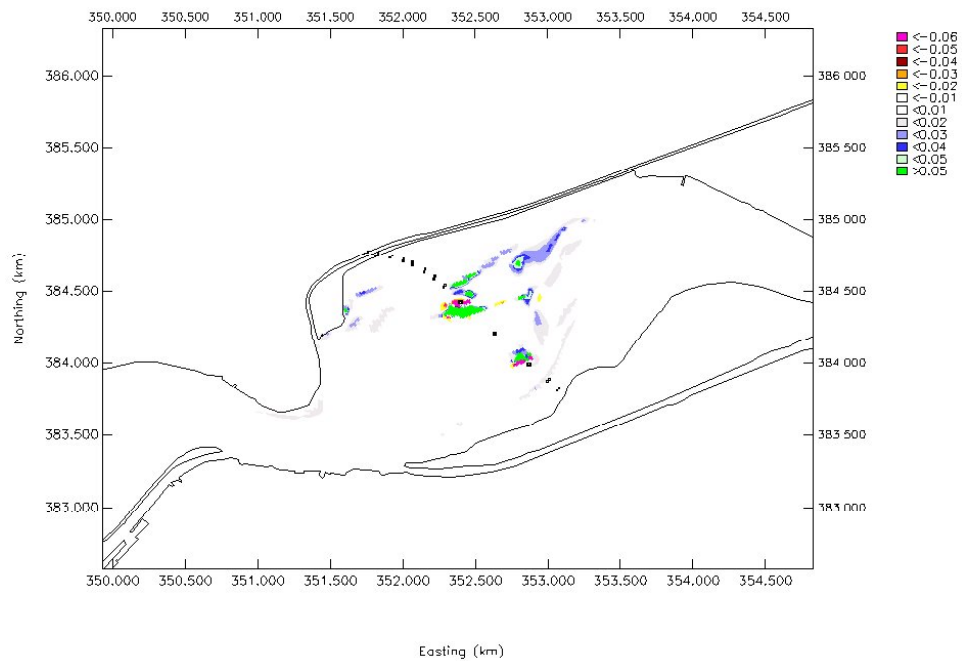


Figure 4. Morphological change (m) after 1 year. Route 3A Medium Span - 3 Tower Revised Alignment Scenario. Simulations run with tidal constituents and a mean annual discharge



ABP Marine Environmental Research Ltd
Suite B, Waterside House
Town Quay
Southampton
Hampshire SO14 2AQ

Tel: +44 (0)23 8071 1840
Fax: +44 (0)23 8071 1841
Email: enquiries@abpmer.co.uk

www.abpmer.co.uk



Gifford & Partners

Additional Modelling - Mersey Gateway

Technical Note E: Phase Differences

Date: December 2005

Project Ref: R/3411/4

Report No: R.1241e



Gifford & Partners

Additional Modelling - Mersey Gateway Technical Note E: Phase Differences

Date: December 2005

Project Ref: R/3411/4

Report No: R.1241e

© ABP Marine Environmental Research Ltd

Version	Details of Change	Authorised By	Date
1	Draft for Comment	J M Harris	9/12/2005
2	Final	J M Harris	20/12/2005

Document Authorisation		Signature	Date
Project Manager:	J M Harris	<i>John Harris</i>	<i>20/12/2005</i>
Quality Manager:	R H Swift	<i>Richard Swift</i>	<i>14/01/2006</i>
Project Director:	W S Cooper	<i>W S Cooper</i>	<i>10-1-6</i>

ABP Marine Environmental Research Ltd
Suite B, Waterside House
Town Quay
SOUTHAMPTON
Hampshire
SO14 2AQ



Tel: +44(0)23 8071 1840
Fax: +44(0)23 8071 1841
Web: www.abpmer.co.uk
Email: enquires@abpmer.co.uk



INVESTOR IN PEOPLE

Summary

This technical note describes the phase difference effects observed in the results of the modelling studies carried out for Phase II of the Mersey Gateway Project.

This report is one of a series of five Technical Notes (R1241a to R.1241e):

- Technical Note A: Residual Modelling - Stage I;
- Technical Note B: Residual Modelling - Stage II;
- Technical Note C: Flat Bed Morphological Modelling;
- Technical Note D: Real Hydrograph Modelling; and
- Technical Note E: Phase Differences.

Within the modelling study reference is made through out the reports to differences in phase and thus corresponding differences in magnitude between the baseline case and the scheme scenario. This Technical Note sets out and explains these effects in more detail.

Additional Modelling - Mersey Gateway Technical Note E: Phase Differences

Contents

	Page
Summary	i
1. Phase Difference	1

Figures

1a. Plot showing water levels at a single model observation point for the baseline and Route 3A 3 Tower revised scenarios	3
1b. Plot showing close up of water levels at a single observation point for the baseline and Route 3A 3 Tower revised scenarios.....	3
2a. Plot showing speed at the model observation point for the baseline and Route 3A 3 Tower revised scenarios	4
2b. Plot showing a close up of speed at the model observation point for the baseline and Route 3A 3 Tower revised scenarios	4

1. Phase Difference

Within the modelling study reference is made throughout the reports to differences in phase and thus corresponding differences in magnitude between the baseline case and the scheme scenario. For example:

“Figure C3B shows small differences in speed along the front of the tidal wave as it propagates onto the intertidal banks. This is considered to be due to a slight phase change between the baseline case and scheme caused by the interaction of the strong incoming tide and the weak ebbing tide.”

To demonstrate this effect water level and speed time-series have been plotted for a single observation point in close proximity to the proposed revised 3 Tower scheme for both the scheme and the baseline case.

Figure 1a shows the water level time-series for a single model observation point for the baseline and the scheme. Figure 1b shows a close up of the water level showing the phase shift and resulting change in magnitude in water levels. In the figures the red line represents the baseline “existing” conditions whilst the black line represents the water levels as a result of the scheme. In this instance the change in magnitude is small, of the order of 0.02m. In addition, from Figure 1a it is clear that there is no perceptible change in tidal range at the observation point and hence the overall magnitude of the tide at that point remains the same in the scheme as in the baseline case.

Figure 2a shows the corresponding surface speed at the same observation point as for the water levels for both the baseline and the scheme. In Figure 2b a close up of the speed over a short period of time can be seen. This corresponds to the same period of time selected in the water level time-series. Again, in Figure 2a, whilst the peak flood speed at the point of interest remains unchanged in the period of interest there is a change in timing. Therefore, at the same point in time there is a clear difference in magnitude. In this instance, the change is a decrease in speed of the order of 0.25m/s. Thus, when viewed as a contour plot of spatial change this would represent a large difference in speed between the baseline and the scheme. However, clearly the actual change represents only a change in the timing not in the overall magnitude of speed occurring at that location.

It is important to recognise these effects in the model results and differentiate between these and actual changes in magnitude. A similar effect will be observed in the bed shear stress results as these are a function of the velocity.

Figures

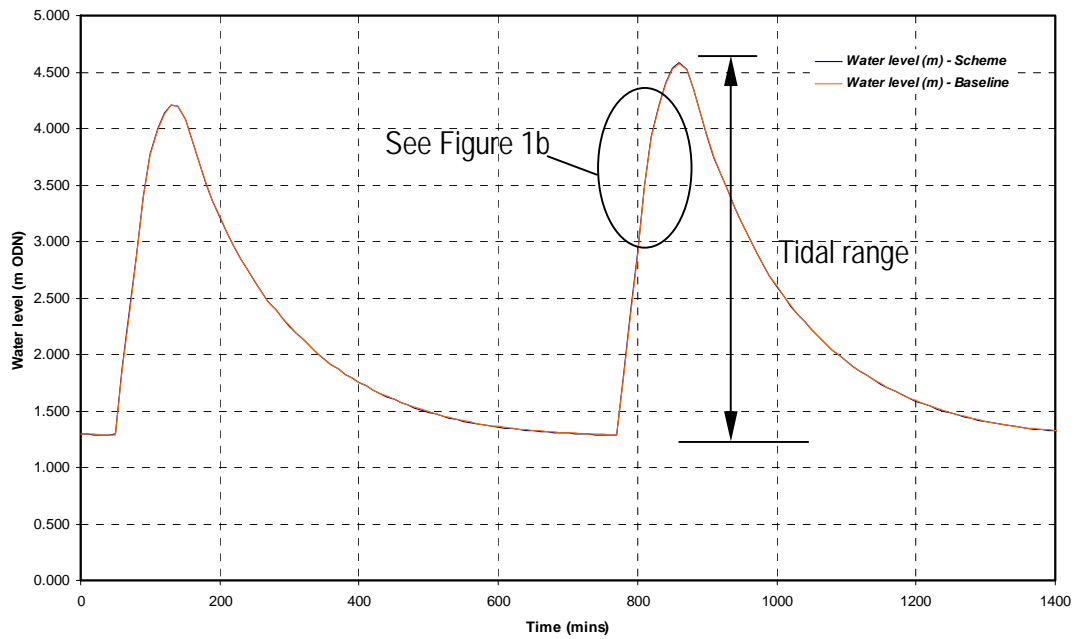


Figure 1a. Plot showing water levels at a single model observation point for the baseline and Route 3A 3 Tower revised scenarios

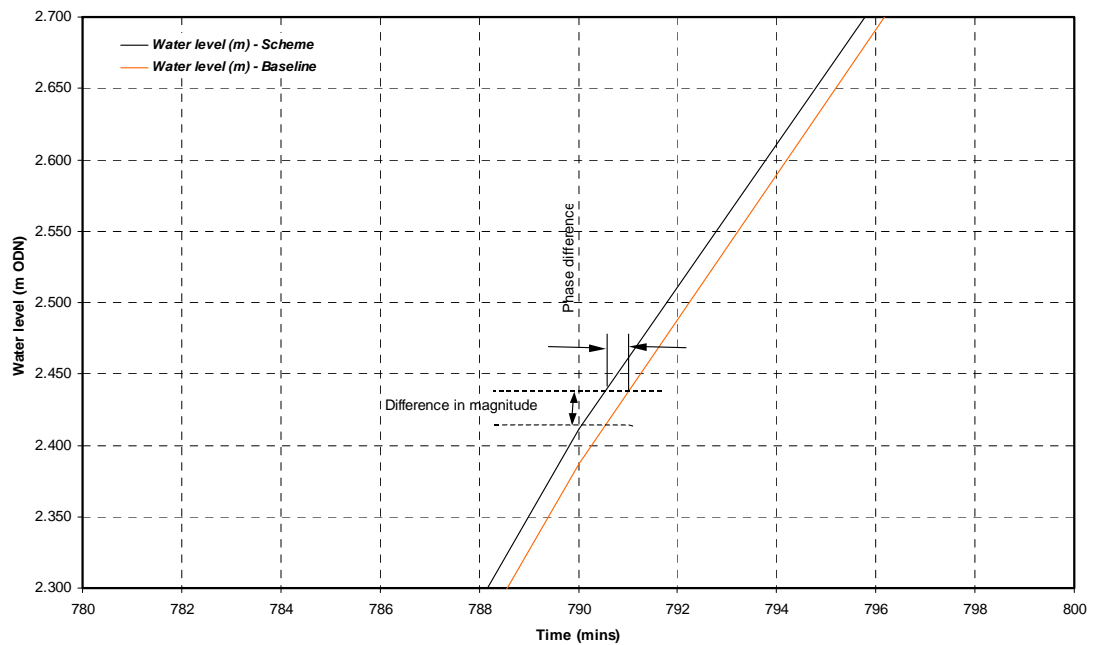


Figure 1b. Plot showing close up of water levels at a single observation point for the baseline and Route 3A 3 Tower revised scenarios

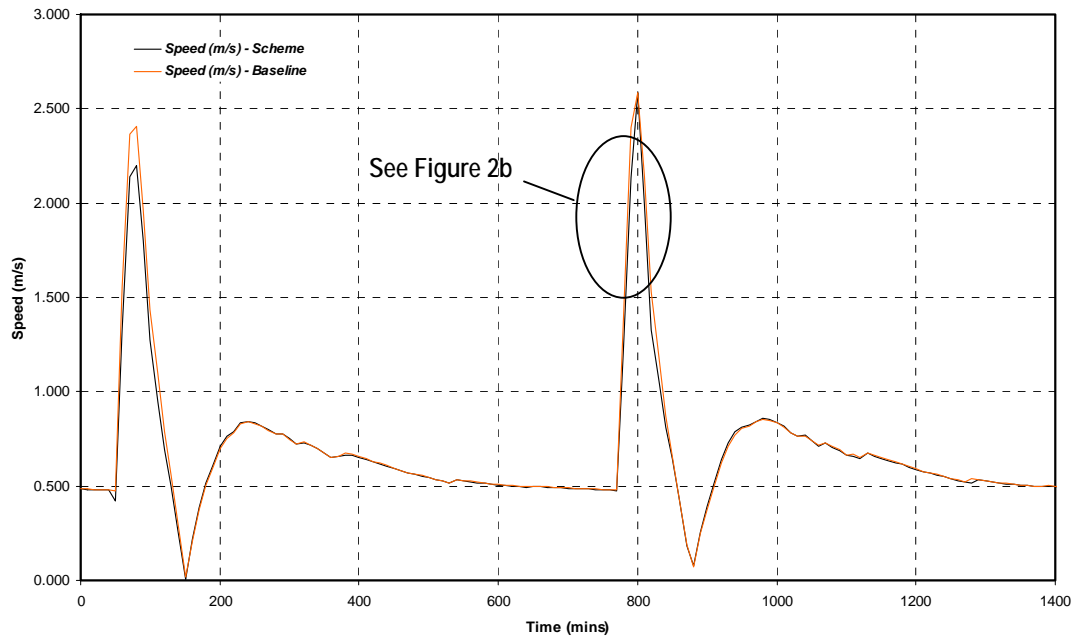


Figure 2a. Plot showing speed at the model observation point for the baseline and Route 3A 3 Tower revised scenarios

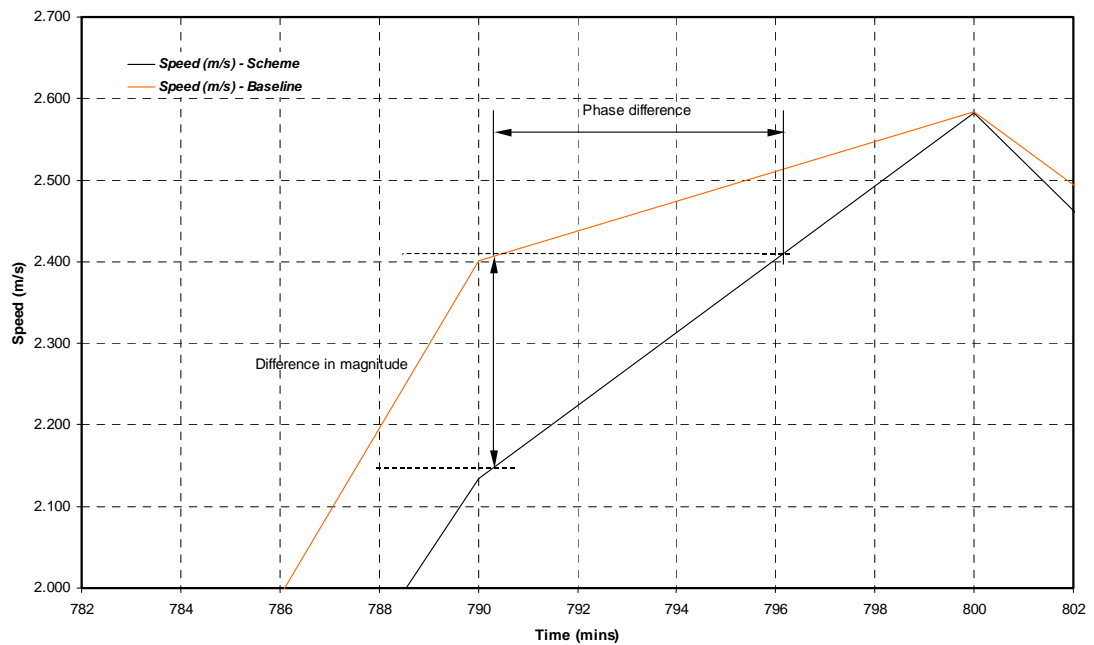


Figure 2b. Plot showing a close up of speed at the model observation point for the baseline and Route 3A 3 Tower revised scenarios



ABP Marine Environmental Research Ltd
Suite B, Waterside House
Town Quay
Southampton
Hampshire SO14 2AQ

Tel: +44 (0)23 8071 1840
Fax: +44 (0)23 8071 1841
Email: enquiries@abpmer.co.uk

www.abpmer.co.uk

